Link Prediction in the Stochastic Block Model with Outliers

Solenne Gaucher, Olga Klopp, Geneviève Robin

Link Prediction in the Stochastic Block Model with Outliers

Solenne Gaucher [*1], Olga Klopp [†2,3], and Geneviève Robin [‡4,5]

[1]Laboratoire de Mathématiques d'Orsay, Univ. Paris-Sud, CNRS, Université Paris-Saclay.
[2]ESSEC Business School
[3]CREST, ENSAE
[4]MATHERIALS, INRIA
[5]École des Ponts ParisTech

November 29, 2019

Abstract

The Stochastic Block Model is a popular model for network analysis in the presence of community structure. However, in numerous examples, the assumptions underlying this classical model are put in default by the behaviour of a small number of outlier nodes such as hubs, nodes with mixed membership profiles, or corrupted nodes. In addition, real-life networks are likely to be incomplete, due to non-response or machine failures. We introduce a new algorithm to estimate the connection probabilities in a network, which is robust to both outlier nodes and missing observations. Under fairly general assumptions, this method detects the outliers, and achieves the best known error for the estimation of connection probabilities with polynomial computation cost. In addition, we prove sub-linear convergence of our algorithm. We provide a simulation study which demonstrates the good behaviour of the method in terms of outliers selection and prediction of the missing links.

Keywords : robust network estimation, outlier detection, missing observations, link prediction

1 Introduction

Networks are a powerful tool used to analyze complex systems: agents are represented as nodes, and pairwise interactions between agents are recorded as edges between these nodes. Examples of fields of applications include biology, where networks may be used to describe protein-protein interactions; ecology, where they may represent food webs [13] or spatial distributions in crop diversity networks [46]; ethnology, where networks summarize relationships or trades between individuals or communities [40, 36]; sociology, where the recent development of online social networks offers unprecedented possibilities while fostering new challenges [47]. Real-life networks are often modeled as realizations of random graphs or, equivalently, as noisy versions of more structured networks. In this setting, recovering the "noiseless" version of the graph, i.e. estimating the underlying probabilities of interactions between agents, is a key problem that has recently gained considerable attention (see, e.g., [30, 15, 14, 17, 50]).

Most methods for recovering structural properties of a network rely on assumptions on the distribution of the underlying random graph. However, in numerous examples, these assumptions are put in default by the behaviour of a small number of individuals, which strongly departs from the behaviour of the majority of agents, introducing outlier profiles. For example, in graphs obtained from survey data, some individuals may be reluctant to participate and for this reason provide false answers; other individuals may even be paid to provide erroneous answers in order to distort the public opinion on a subject [3]. In other cases, edges can be erroneously recorded due to defaults of measurement instruments, human errors, or fraudulent

[*]solenne.gaucher@ensae.fr
[†]kloppolga@math.cnrs.fr
[‡]genevieve.robin@inria.fr

behaviours. Controlling the bias induced by these deviations from the model is an important task. Similarly, it is known that widely used models such as the stochastic block model (SBM) or the latent position model provide a bad fit to many real-life networks. Indeed, these networks often present a small fraction of nodes with high connectivity (hubs), which are not predicted by these models. The presence of such hubs in a data set can lead to erroneous conclusions regarding the structure of the graphs [10, 27].

In this work, we propose a new algorithm for estimating connection probabilities in networks that is robust against arbitrary outlier nodes. Following Hawkins [23], we define an outlier as "an observation that deviates so much from other observations as to arouse suspicion that it was generated by a different mechanism". To the best of our knowledge, the problem of robust estimation of network structure in the presence of outliers has been first studied in [10]. In this paper, the authors aim to recover community structure when the majority of the nodes follow an assortative stochastic block model in the presence of arbitrary outlier nodes. Note that our problem is different, as we would like to estimate the connection probabilities between nodes, and our assumptions on the random graph are more general. Moreover, the algorithm described in [10] does not allow to detect outliers. We argue that detecting individuals with anomalous connectivity is of interest in itself, providing us with meaningful hindsight on possible corruptions of the data-collecting mechanism or on fraudulent behaviours of users. For example, hubs are often linking different clusters and can be thought of as outliers. Their detection can help us gain a better understanding of the structure of the network, and finds applications in marketing [12] and epidemiology [48], among others. When analyzing the World Wide Web graph, recovering these hubs may help to identify spam pages [20]. Outlier detection has many other applications in security, finance, and health-care. Bearing these applications in mind, we design an algorithm able to identify outliers, when their connectivity pattern differs sufficiently from the remaining nodes.

Our work also focuses on the missing observations scenario and link prediction. In practice, many real-life networks are polluted by missing data [19, 21]. Indeed, complete exploration of all pairwise interactions between agents can be expensive, time consuming, and requires significant effort. In social sciences, graphs constructed from survey data are likely to be incomplete, due to non-response or drop-out of participants. Protein-protein interactions networks provide a blatant example of incompleteness, as the existence of each interaction must be tested experimentally, and most of these interactions have yet to be tested [51]. Finally, the size of some data sets coming, for example, from online social networks or genome sequencing makes the use of the full dataset computationally inefficient. Some researchers have proposed to study the properties of these networks based on a sample of their edges [6]. Unfortunately, the absence of information on the existence of edges between agents may distort the results of network analysis and corrupt the estimators [34]. When dealing with a partially observed network, being able to predict the existence of non-observed edges is of practical interest [7]. In the context of online social networks, it can be used to suggest new relations to users. In biology, testing for the existence of interactions between agents can be time-consuming and difficult. Prior estimations on the probability of the existence of non-observed edges enable researchers to test for the most likely interactions, thus recovering the structure of the network while avoiding a costly and time-consuming complete exploration of the edges.

The problem of connection probabilities estimation under the missing observation scenario and its application to link prediction has known a quite recent development. In [14], the authors study the least square estimator for the stochastic block model assuming observations missing uniformly at random, and show that it is minimax optimal. In [17], the authors show that the maximum likelihood estimator is minimax optimal in the same setting, while being adaptive to more general sampling schemes. These two estimators are too costly to compute to be used in practice (there exists computationally efficient approximations for the maximum likelihood). In [53], the authors consider the setting where non-existing edges can be erroneously recorded as observed (or existing edges recorded as not observed), both errors occuring at a fixed rate. More recently, [43] proposed an algorithm to estimate the edge probabilities when overlapping sub-graphs are observed. [49] considered the case where the edges are egocentrically sampled (that is all edges adjacent to certain nodes are sampled). Both papers present convincing numerical experiments, but lack theoretical guarantees.

In the present work, we introduce a new algorithm for outliers detection and for estimation of the connection probabilities which is robust to corruptions and missing observations. For this algorithm, we provide both statistical and computational guarantees. In particular, we prove that under fairly general assumptions our algorithm achieves exact selection of the outliers (Theorem 3) and we prove an upper bound on the estimation error of connection probabilities between inliers (Theorem 4). Importantly, the estimation error of

our method matches the best known error for tractable algorithms [50]. We also analyse the algorithm's convergence complexity and show its sublinear convergence and competitive iteration cost in large dimensions. In Section 5, we provide an encouraging simulation study, indicating that the proposed method has good empirical properties in terms of outliers detection and link prediction. Finally, we illustrate performances of our method on real data using the network of American political blogs and the "Les Misérables" characters network.

1.1 Example: "Les Misérables" characters network

Before introducing our general model, let us start with an illustration on an example."Les Misérables" characters network encodes interactions between characters of Victor Hugo's novel. The network was created by Donald Knuth, as part of the Stanford Graph Base [31]. It contains 77 nodes corresponding to characters of the novel, and 254 edges connecting two characters whenever they appear in the same chapter. The book itself spans around two decades of nineteenth century France and numerous characters. It is structured in five volumes, each one focused on a specific period and featuring handful of characters. One expects to observe communities in this network, corresponding roughly to the plots narrated in each volume: such structures are well captured by the classical Stochastic Block Model.

In the Stochastic Block Model (see, e.g., [24]), nodes are classified into k communities (for example corresponding to volumes of the book). Denote by $\mathcal{G} = (\mathcal{V}, \mathcal{E})$ the graph, where $\mathcal{V}$ is the set of nodes, and $\mathcal{E}$ the set of edges. For any $i \in \mathcal{V}$, denote by $c(i)$ its community assignment. Then, the probability that an edge connects two nodes only depends on their community assignments:

$$\mathbb{P}((i,j) \in \mathcal{E}) = \boldsymbol{Q}_{c(i)c(j)}. \tag{1}$$

In (1), $\boldsymbol{Q}$ denotes a $k \times k$ symmetric matrix of connection probabilities between communities. Usually, in the Stochastic Block Model, the community assignment is unknown and learned from data.

However, for "Les Misérables" character network, some of the characters behave differently, as their stories follow the entire novel. For instance, the main character, Jean Valjean, acts as a *hub* with 36 connections, well above the second most connected character Gavroche, with a degree of 22. Other characters, for instance, Cosette, do not necessarily have a large degree but are connected to characters across all the volumes, and thus also stand out from the communities structure. Nodes such as Cosette correspond to outliers with *mixed membership* profile. In Figure 1a, we display the communities assignment resulting from the classical SBM. Note that the node corresponding to Jean Valjean (large yellow node), is alone in its community. In addition, one of the clusters (in red) mainly contains some of the main characters of the novel (The Thénardier, Éponine, Javert).

To model simultaneously the community structure and the outlier profiles, we propose to decompose $\mathcal{V}$ into two set of nodes: the inliers $\mathcal{I}$ following the classical Stochastic Block Model structure and the outliers $\mathcal{O}$ for which we do not make any assumption on their connection pattern. As a result, the probability of connection between inliers is given, for any $(i,j) \in \mathcal{I}^2$, by

$$\mathbb{P}((i,j) \in \mathcal{E}) = \boldsymbol{L}^*_{ij},$$

where $\boldsymbol{L}^*$ is a symmetric matrix with entries in $[0,1]$ corresponding to classical SBM. On the other hand, for any outlier $i \in \mathcal{O}$ and for any node $j \in \mathcal{V}$ we set

$$\mathbb{P}((i,j) \in \mathcal{E}) = \left(\boldsymbol{S}^* + \boldsymbol{S}^{*\top}\right)_{ij},$$

with $\boldsymbol{S}^*$ an arbitrary matrix in $[0,1]^{n \times n}$. Our only assumption regarding the outliers is that their number is small compared to the size of the network, i.e., the matrix $\boldsymbol{S}^*$ is column-wise sparse. Note that the inlier and outlier sets are unknown a priori, and learned from the data. In Figure 1b, we display the communities assignment resulting from our model. The outlier nodes – which are selected automatically by our procedure – are indicated in red, and coincide with central characters of the novel. They correspond either to hubs (Jean Valjean, Myriel) or to nodes with mixed memberships (Cosette, Javert, Marius).

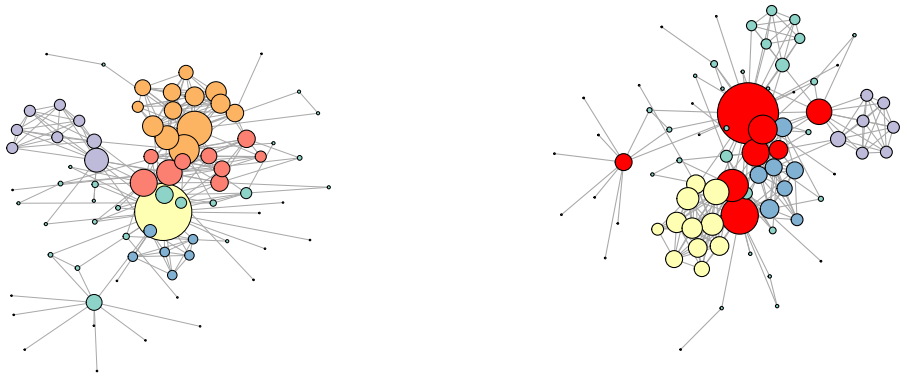

(a) SBM model with 6 communities (the number of communities is chosen to minimize the Integrated Completed Likelihood criterion).

(b) Proposed Stochastic Block Model with outliers. The detected outliers are colored in red, and classification is performed on the rest of the nodes.

Figure 1: Les Misérables characters network. The nodes are represented with size proportional to their degree, and colored according to their community assignment. On the left in Figure 1a, classification is performed according to the classical SBM model. On the right in Figure 1b, the detected outliers are indicated in red, and classification is performed on the rest of the nodes (inliers).

1.2 Organisation of the paper

The rest of the paper is organized as follows. First, in Section 1.3, we summarise notation used throughout this paper and, in Section 2, we introduce our model. Then, in Section 3, we present a computationally efficient algorithm for detecting outliers and estimating the connection probabilities between inliers. We also provide theoretical guarantees on the speed of convergence of this algorithm. In Section 4, we provide bounds on the error of the outliers detection and on the error of the estimation of the connection probabilities between inliers. In Section 5, we present numerical experiments which demonstrate the good empirical behaviour of our method, both in terms of outliers detection and in terms of prediction of the missing links. The proofs are relegated to the Appendix A.

1.3 Notations

The notation used in the paper is gathered in the following paragraph :

- We use bold notations for matrices and vectors : for any matrix $\boldsymbol{M}$, we denote by $\boldsymbol{M}_{ij}$ its entry on row i and column j. The vector corresponding to its i-th row is denoted by $\boldsymbol{M}_{i,\cdot}$, and the vector corresponding to its j-th column is denoted by $\boldsymbol{M}_{\cdot,j}$. The notation $\mathbf{0}$ denotes either a matrix or a vector with entries all equal to 0.

- We write $\odot$ to denote the entry-wise product for matrices or vectors. For any vector $\mathbf{v} \in \mathbb{R}^n$, we denote by $\|\mathbf{v}\|_2$ its Euclidean norm. For any two matrices $\boldsymbol{M}, \boldsymbol{N} \in \mathbb{R}^{n\times n}$, $\langle \boldsymbol{M} | \boldsymbol{N} \rangle \triangleq \sum_{ij} \boldsymbol{M}_{ij}\boldsymbol{N}_{ij}$ is the Frobenius scalar product between $\boldsymbol{M}$ and $\boldsymbol{N}$. For any matrix $\boldsymbol{M} \in \mathbb{R}^{n\times n}$, $\|\boldsymbol{M}\|_F$ is its Frobenius norm, $\|\boldsymbol{M}\|_*$ is its nuclear norm (the sum of its singular values), $\|\boldsymbol{M}\|_{\text{op}}$ is its operator norm (its largest singular value), and $\|\boldsymbol{M}\|_\infty \triangleq \max_{ij} |\boldsymbol{M}_{ij}|$ is the largest absolute value of its entries. Its column-wise 2,1-norm is denoted by $\|\boldsymbol{M}\|_{2,1} \triangleq \sum_j \sqrt{\sum_i \boldsymbol{M}_{ij}^2}$, and the column-wise 2,$\infty$-norm is denoted by $\|\boldsymbol{M}\|_{2,\infty} \triangleq \max_j \sqrt{\sum_i \boldsymbol{M}_{ij}^2}$. The weighed L_2-norm with respect to the sampling probability $\boldsymbol{\Pi}$ is written

$\|\boldsymbol{M}\|_{L_2(\boldsymbol{\Pi})}$. Finally, for any matrix $\boldsymbol{M}$ and any vector $\mathbf{v}$, we denote respectively by $(\boldsymbol{M})_+$ and $(\mathbf{v})_+$ the matrix and vector obtained by considering the positive part of their entries.

- For a matrix $\boldsymbol{M} \in \mathbb{R}^{n\times n}$, we denote by $\mathcal{P}_{\boldsymbol{M}}$ the projection defined as follows : for any matrix $\boldsymbol{A} \in \mathbb{R}^{n\times n}$, $\mathcal{P}^{\perp}_{\boldsymbol{M}}(\boldsymbol{A}) = \boldsymbol{A} - \mathcal{P}_{\boldsymbol{M}}(\boldsymbol{A})$, where $\mathcal{P}_{\boldsymbol{M}}(\boldsymbol{A}) = P^{\perp}_{U(\boldsymbol{M})}\boldsymbol{A}P^{\perp}_{V(\boldsymbol{M})}$, and $P^{\perp}_{U(\boldsymbol{M})}$ and $P^{\perp}_{V(\boldsymbol{M})}$ denote respectively the projection on the spaces orthogonal to the spaces spanned by the right and left singular vectors of $\boldsymbol{M}$.
- We denote by $[n]$ the set of integers from 1 to n, by $\mathcal{I}$ the set of inliers, and by $\mathcal{O}$ the set of outliers. The set of pairs of inliers is denoted $I \triangleq \mathcal{I}\times\mathcal{I}$, and its complement is denoted by $O \triangleq [n]\times[n]\setminus I$. For a set of indices $\mathcal{S}$ and a matrix $\boldsymbol{M} \in \mathcal{R}^{n\times n}$, we write $\boldsymbol{M}_{|\mathcal{S}} \triangleq \mathbb{1}_{\mathcal{S}} \odot \boldsymbol{M}$ where $\mathbb{1}_{\mathcal{S}}$ is the indicator matrix of the set $\mathcal{S}$. For any set $\mathcal{S}$, we denote by $|\mathcal{S}|$ its cardinality.

2 General model

We consider an undirected, unweighted graph with n nodes indexed from 1 to n. To encode the set of edges, we use the *adjacency matrix* of the graph, which we denote by $\boldsymbol{A}$. This matrix is defined as follows: set $\boldsymbol{A}_{ij} = 1$ if there exists an edge linking node i and node j, and $\boldsymbol{A}_{ij} = 0$ otherwise. Note that since the graph is undirected we have $\boldsymbol{A}_{ij} = \boldsymbol{A}_{ji}$. We assume there are no loops in the graph: no edge can connect a node to itself, and thus $\boldsymbol{A}_{ii} = 0$.

Probability of connection between inliers. For any pair of inliers $(i,j) \in \mathcal{I}^2$, $i < j$ we assume that $\boldsymbol{A}_{ij} \overset{ind.}{\sim} \text{Bernoulli}(\boldsymbol{L}^*_{ij})$, where $\boldsymbol{L}^*$ is a $n\times n$ symmetric matrix with entries in $[0,1]$. For inliers, we consider a more general model than the classical Stochastic Block Model assuming that $\boldsymbol{L}^*$ is low-rank with $\text{rank}(\boldsymbol{L}^*) = k$. This assumption is enough to model some interesting properties of the SBM, such as positive and negative homophily, and stochastic equivalence. Indeed, when $\text{rank}(\boldsymbol{L}^*) = k$, there exist a matrix $\boldsymbol{U} \in \mathbb{R}^{n\times k}$ and a diagonal matrix $\boldsymbol{\Lambda} \in \mathbb{R}^{k\times k}$ such that $\boldsymbol{L}^* = \boldsymbol{U}\boldsymbol{\Lambda}\boldsymbol{U}^\top$. The model can then be interpreted as follows: each row $\boldsymbol{U}_{i,\cdot}$ corresponds to a vector of k latent attributes describing the node i. If $\boldsymbol{\Lambda}_{aa} > 0$, two nodes sharing attributes of the same sign along the a-th coordinate will have a tendency to be more connected (everything else being equal), modelling positive homophily along this coordinate. If $\boldsymbol{\Lambda}_{aa} < 0$, they will tend to be less connected, modelling negative homophily. Note that two nodes with similar characteristics in the latent space will have similar stochastic behaviour (i.e. their probabilities of connection to other nodes will be given by similar vectors of probabilities). On the other hand, assuming that $\boldsymbol{L}^*$ is low-rank closely relates to the *latent eigenmodel*, described, for example, in [11]. In this model, the probability of connection of nodes i and j is given by $f(\boldsymbol{L}^*_{ij})$, where $\boldsymbol{L}^*$ is of rank k and f is a link function. Note that our algorithm can be extended to the latent eigenmodel by replacing $\boldsymbol{L}$ by $f(\boldsymbol{L})$ in the objective function (2).

Finally, most graphs encountered by practitioners are *sparse*, with a small average degree compared to the number of nodes. To account for the sparsity, we assume that the entries of $\boldsymbol{L}^*$ are bounded by ρ_n where ρ_n is a sequence of sparsity inducing parameters such that $\rho_n \to 0$. In particular, we have that the average degree of the graph grows as $\rho_n n$. In the rest of the paper we assume that $\rho_n \leq \frac{1}{2}$. This assumptions is only intended to clarify the exposition of our results, and can be easily removed.

Probability of connection of outlier nodes In our model we have no assumptions on the connectivity of outliers. In particular, we do not assume a block constant or a low rank structure. We set $\boldsymbol{L}^*_{ij} = 0$ for any pair of nodes (i,j) such that either $i \in \mathcal{O}$ or $j \in \mathcal{O}$, and we use matrix $\boldsymbol{S}^*$ to describe the outliers. For any inlier $j \in \mathcal{I}$, the j-th column of $\boldsymbol{S}^*$ is null. Therefore, the matrix $\boldsymbol{S}^*$ has at most $s = |\mathcal{O}|$ non-zero columns. For any outlier $j \in \mathcal{O}$, the j-th column of $\boldsymbol{S}^*$ describes the connectivity of j: for any $j \in \mathcal{O}$ and $i \in \mathcal{I}$, $\boldsymbol{A}_{ij} \sim \text{Bernoulli}(\boldsymbol{S}^*_{ij})$ and for any $(i,j) \in \mathcal{O}\times\mathcal{O}$, $\boldsymbol{A}_{ij} \sim \text{Bernoulli}(\boldsymbol{S}^*_{ij} + \boldsymbol{S}^*_{ji})$. We set $\boldsymbol{S}^*_{ii} = 0$ for any $i \in [n]$. With these notations, we have that

$$\mathbb{E}[\boldsymbol{A}] = \boldsymbol{L}^* - \text{diag}(\boldsymbol{L}^*) + \boldsymbol{S}^* + (\boldsymbol{S}^*)^\top.$$

To ensure that the graph remains sparse, we assume that $\|\boldsymbol{S}^*\|_\infty \leq \gamma_n$, where γ_n is a decreasing, sparsity inducing sequence. Note that we allow the outliers and inliers to have different sparsity levels: γ_n and ρ_n may be of different orders of magnitude.

In this model, the outliers may account for different types of behaviour of the nodes, such as hubs or mixed membership profiles. In practice, while most nodes may be assigned to a community and share a similar stochastic behaviour with members of their community, a fraction of the nodes may belong to two or more communities. Our model allows for such a behaviour by considering the nodes with mixed membership as outliers. Finally, while the SBM may describe accurately the behaviour of all the nodes, some communities may be too small to be estimated consistently, and induce a biais in the estimation of the connection probabilities of the remaining nodes. Here again, we can treat the nodes belonging to these communities as outliers. In all these cases, being able to detect nodes with singular behaviour provides valuable information on the network.

Note that this setting includes as particular case the Generalized Stochastic Block Model, introduced in [10]. In this model, the n nodes consist of $n - s$ inliers obeying the Stochastic Block Model (SBM), and s outliers, which are connected with other nodes in an arbitrary way.

Missing data pattern We say that we sample the pair (i, j) if we observe the presence or absence of the corresponding edge. We denote by $\boldsymbol{\Omega}$ the sampling matrix such that $\boldsymbol{\Omega}_{ij} = 1$ if the pair (i, j) is sampled, $\boldsymbol{\Omega}_{ij} = 0$ otherwise. The graph is unoriented and the sampling matrix is therefore symmetric; moreover we set $\mathrm{diag}(\boldsymbol{\Omega}) = \mathbf{0}$ since an observation of a entry on the diagonal of $\boldsymbol{A}$ does not carry any information. We assume that the entries $\{\boldsymbol{\Omega}_{ij}\}_{i<j}$ are independent random variables and that $\boldsymbol{\Omega}$ and $\boldsymbol{A}$ are independent. We denote by $\boldsymbol{\Pi} \in \mathbb{R}^{n\times n}$ the expectation of the random matrix $\boldsymbol{\Omega}$. Then, for any pair (i, j), $\boldsymbol{\Omega}_{ij} \sim \text{Bernoulli}(\boldsymbol{\Pi}_{ij})$. For any matrix $\boldsymbol{M} \in \mathbb{R}^{n\times n}$, we define

$$\|\boldsymbol{M}\|^2_{L_2(\boldsymbol{\Pi})} \triangleq \mathbb{E}\left[\|\Omega \odot \boldsymbol{M}\|_F^2\right].$$

This fairly general sampling scheme covers some of the settings encountered by practitioners. In particular, it covers the case of random dyad sampling (described, e.g., in [44]), where the probability of sampling any pair depends on the matrices $\boldsymbol{L}^*$ and $\boldsymbol{S}^*$ (and, if we consider the Stochastic Block Model, on the communities of the adjacent nodes).

3 Estimation procedure

In order to estimate the matrices $\boldsymbol{L}^*$ and $\boldsymbol{S}^*$, we consider the following objective function:

$$\mathcal{F}(\mathbf{S}, \boldsymbol{L}) \triangleq \frac{1}{2}\|\Omega \odot (\boldsymbol{A} - \boldsymbol{L} - \mathbf{S} - (\boldsymbol{S})^\top)\|_F^2 + \lambda_1\|\boldsymbol{L}\|_* + \lambda_2\|\boldsymbol{S}\|_{2,1}, \tag{2}$$

defined by a least squares data-fitting term penalized by a hybrid regularization term. On the one hand, the nuclear norm penalty $\|\boldsymbol{L}\|_*$ is a convex relaxation of the rank constraint, meant to induce low-rank solutions for $\boldsymbol{L}$. On the other hand, the term $\|\boldsymbol{S}\|_{2,1}$ is a relaxation of the constraint on the number of non-zero columns in $\boldsymbol{S}$, meant to induce column-wise sparse solutions for $\boldsymbol{S}$. Our estimators are defined as

$$\left(\widehat{\boldsymbol{S}}, \widehat{\boldsymbol{L}}\right) \in \underset{\boldsymbol{S}\in[0,1]^{n\times n}, \boldsymbol{L}\in[0,\rho_n]^{n\times n}_{sym}}{\arg\min} \mathcal{F}\left(\boldsymbol{S}, \boldsymbol{L}\right). \tag{3}$$

When information on the presence or absence of some edges is missing, the objective function may not have a unique minimizer. We propose to approximate our target parameters $(\widehat{\boldsymbol{S}}, \widehat{\boldsymbol{L}})$ by minimizing the objective (2) with an additional ridge penalization term, $\frac{\epsilon}{2}(\|\boldsymbol{L}\|_F^2 + \|\boldsymbol{S}\|_F^2)$, which ensures strong convexity of the objective function. While this additional penalty is not necessary to obtain convergence in terms of the objective value, it is required to obtain convergence of the parameters themselves. This additional penalty allows also to ensure approximate matching of the estimation and approximation errors, as detailed in our theoretical results. Note that, by choosing ϵ sufficiently small, $\mathcal{F}_\epsilon$ can be arbitrarily close to $\mathcal{F}$, but the choice of ϵ will impact the speed of convergence of our algorithm.

Furthermore, we assume for simplicity that the box constraints on $\boldsymbol{S}$ and $\boldsymbol{L}$ are always inactive. We make a final simplification by dropping the symmetry constraint on $\boldsymbol{L}$. Indeed, we will see later on that the low-rank matrix $\boldsymbol{L}$ remains symmetric throughout the algorithm, provided that it is intialized by a symmetric matrix. Thus, in the end, we (approximately) solve the following optimization problem:

$$\text{minimize} \quad \mathcal{F}_\epsilon(\boldsymbol{S}, \boldsymbol{L}) \triangleq \mathcal{F}(\boldsymbol{S}, \boldsymbol{L}) + \tfrac{\epsilon}{2}(\|\boldsymbol{L}\|_F^2 + \|\boldsymbol{S}\|_F^2). \tag{4}$$

Let us now describe the optimization procedure. First, we consider the augmented objective function:

$$\Phi_\epsilon(\boldsymbol{S},\boldsymbol{L},R) \triangleq \frac{1}{2}\|\Omega \odot (\boldsymbol{A}-\boldsymbol{L}-\boldsymbol{S}-(\boldsymbol{S})^\top)\|_F^2 + \lambda_1 R + \lambda_2\|\boldsymbol{S}\|_{2,1} + \frac{\epsilon}{2}(\|\boldsymbol{L}\|_F^2 + \|\boldsymbol{S}\|_F^2),$$

with $R \in \mathbb{R}_+$. Note that, if an optimal solution to (4) $(\hat{\boldsymbol{S}}_\epsilon, \hat{\boldsymbol{L}}_\epsilon)$ satisfies $\|\hat{\boldsymbol{L}}_\epsilon\|_* \leq \bar{R}$ for some $\bar{R} \geq 0$, then any optimal solution to the augmented problem

$$\begin{array}{ll} \text{minimize} & \Phi_\epsilon(\boldsymbol{S},\boldsymbol{L},R) \\ \text{such that} & \|\boldsymbol{L}\|_* \leq R \leq \bar{R} \end{array} \tag{5}$$

will also be optimal to (4) (we will show in appendix A.2 how the upper bound $\bar{R}$ can be chosen and tightened adaptively inside the algorithm). Thus, solving (5) we directly obtain the solution to our initial problem (4). Finally, our estimators are defined as the minimizers of the following augmented objective function:

$$\begin{array}{ll} (\hat{\boldsymbol{S}}_\epsilon, \hat{\boldsymbol{L}}_\epsilon, \tilde{R}) & \in \text{argmin } \Phi_\epsilon(\boldsymbol{S},\boldsymbol{L},R) \\ \text{such that} & \|L\|_* \leq R \leq \bar{R}. \end{array}$$

A natural option to solve problem (5) is the coordinate descent algorithm, where the parameters $(\boldsymbol{S},\boldsymbol{L},R)$ are updated alternatively along descent directions. To update $\boldsymbol{S}$, we apply the proximal gradient method. We use the conjugate gradient method (or Frank-Wolfe method [25], which relies on linear approximations of the objective function) to update $(\boldsymbol{L},R)$. Similar Mixed Coordinate Gradient Descent (MCGD) algorithms were considered in [37, 42, 16] to estimate sparse plus low-rank decompositions with hybrid penalty terms combining an ℓ_1 and a nuclear norm penalties. Here, we extend the procedure to handle the $\ell_{2,1}$ penalty as well. The details of the algorithm are described in Appendix A.2. The entire procedure is sketched in Algorithm 1, where we also define our final estimators $\left(\boldsymbol{L}^{(T)}, \boldsymbol{S}^{(T)}\right)$.

Algorithm 1 Mixed coordinate gradient descent (MCGD)

Initialization: $(\boldsymbol{L}^{(0)}, \boldsymbol{S}^{(0)}, R^{(0)}, t) \leftarrow (\boldsymbol{0}, \boldsymbol{0}, 0, 0)$
for $t = 1, \ldots, T$ **do**
  $t \leftarrow t+1$
  Compute the proximal update (6) to obtain $\mathbf{S}^{(t)}$.
  Compute the upper bound $\bar{R}^{(t)} = \lambda_1^{-1}\Phi_\epsilon(\boldsymbol{S}^{(t-1)}, \boldsymbol{L}^{(t-1)}, R^{(t-1)})$.
  Compute the direction $(\tilde{\boldsymbol{L}}^{(t)}, \tilde{R}^{(t)})$ using (9).
  Compute the Conjugate Gradient update (7), with step size β_t defined in (8) to obtain $(\boldsymbol{L}^{(t)}, R^{(t)})$.
end for
return $\left(\boldsymbol{L}^{(T)}, \mathbf{S}^{(T)}\right)$

Denote by $\boldsymbol{G}_L^{(t-1)} = -\Omega \odot (\boldsymbol{A}-\boldsymbol{L}^{(t-1)}-\boldsymbol{S}^{(t)}-(\boldsymbol{S}^{(t)})^\top) + \epsilon\boldsymbol{L}^{(t-1)}$ the gradient with respect to $\boldsymbol{L}$ of the quadratic part of the objective function, evaluated at $(\boldsymbol{S}^{(t)}, \boldsymbol{L}^{(t-1)})$ and by $\boldsymbol{G}_S^{(t-1)} = -2\Omega \odot (\boldsymbol{A}-\boldsymbol{L}^{(t-1)}-\boldsymbol{S}^{(t-1)}-(\boldsymbol{S}^{(t-1)})^\top) + \epsilon\boldsymbol{S}^{(t-1)}$ the gradient with respect to $\boldsymbol{S}$ of the quadratic part of the objective function, evaluated at $(\boldsymbol{S}^{(t-1)}, \boldsymbol{L}^{(t-1)})$. In Algorithm 1, the column-wise sparse component $\boldsymbol{S}$ is updated with a proximal gradient step:

$$\begin{array}{rl} \boldsymbol{S}^{(t)} & \in \text{argmin}\left(\eta\lambda_2\|\boldsymbol{S}\|_{2,1} + \frac{1}{2}\left\|\boldsymbol{S}-\boldsymbol{S}^{(t-1)}+\eta\boldsymbol{G}_S^{(t-1)}\right\|_F^2\right), \\ & = \mathsf{Tc}_{\eta\lambda_2}\left(\boldsymbol{S}^{(t-1)}-\eta\boldsymbol{G}_S^{(t-1)}\right), \end{array} \tag{6}$$

where $\mathsf{Tc}_{\eta\lambda_2}$ is the column-wise soft-thresholding operator such that for any $\mathbf{M} \in \mathbb{R}^{n\times n}$ and for any $\lambda > 0$, the j-th column of $\mathsf{Tc}_\lambda(\mathbf{M})$ is given by $(1-\lambda/\|\mathbf{M}_{\cdot,j}\|_2)_+\mathbf{M}_{\cdot,j}$. The step size η is constant and fixed in advance, and satisfies $\eta \leq 1/(2+\epsilon)$. The low-rank component given by $(\boldsymbol{L},R)$ is updated using a conjugate gradient step as follows:

$$\left(\boldsymbol{L}^{(t)}, R^{(t)}\right) = \left(\boldsymbol{L}^{(t-1)}, R^{(t-1)}\right) + \beta_t\left(\tilde{\boldsymbol{L}}^{(t)}-\boldsymbol{L}^{(t-1)}, \tilde{R}^{(t)}-R^{(t-1)}\right), \tag{7}$$

where $\beta_t \in [0,1]$ is a step size set to:

$$\beta_t = \min\left\{1, \frac{\langle \boldsymbol{L}^{(t-1)} - \tilde{\boldsymbol{L}}^{(t)}, \boldsymbol{G}_L^{(t-1)}\rangle + \lambda_1(R^{(t-1)} - \tilde{R}^{(t)})}{(1+\epsilon)\|\tilde{\boldsymbol{L}}^{(t)} - \boldsymbol{L}^{(t-1)}\|_F^2}\right\}. \tag{8}$$

The direction $(\tilde{\boldsymbol{L}}^{(t)}, \tilde{R}^{(t)})$ is defined by:

$$\begin{aligned}\left(\tilde{\boldsymbol{L}}^{(t)}, \tilde{R}^{(t)}\right) \in \quad & \operatorname{argmin}_{\mathbf{Z},R} \quad \langle \mathbf{Z}, \boldsymbol{G}_L^{(t-1)}\rangle + \lambda_1 R \\ & \text{such that} \quad \|\mathbf{Z}\|_* \leq R \leq \bar{R}^{(t)}.\end{aligned} \tag{9}$$

Note that, if the matrix $\boldsymbol{L}^{(t)}$ is symmetric, then the matrix $\boldsymbol{L}^{(t+1)}$ remains symmetric at iteration $t+1$. Indeed, the gradient $\boldsymbol{G}_L^{(t)}$ is defined in terms of the matrices $\boldsymbol{A}$, $\boldsymbol{\Omega}$, and $\boldsymbol{S}^{(t)} + (\boldsymbol{S}^{(t)})^\top$, all three symmetric matrices. Therefore, to obtain a symmetric estimator of $\boldsymbol{L}$, it suffices to initialize the algorithm with symmetric $\boldsymbol{L}^{(0)}$.

The Mixed Coordinate Gradient Descent algorithm described in Algorithm 1 converges sublinearly to the optimal solution of (5), as shown by the following result:

Theorem 1. *Let $\delta > 0$. After $T_\delta = \mathcal{O}(1/\delta)$ iterations, the iterate satisfies:*

$$\mathcal{F}_\epsilon(\boldsymbol{S}^{(T_\delta)}, \boldsymbol{L}^{(T_\delta)}) - \mathcal{F}_\epsilon(\hat{\boldsymbol{S}}_\epsilon, \hat{\boldsymbol{L}}_\epsilon) \leq \delta. \tag{10}$$

In addition, by strong convexity of $\mathcal{F}_\epsilon$,

$$\|\boldsymbol{S}^{(T_\delta)} - \hat{\boldsymbol{S}}_\epsilon\|_F^2 + \|\boldsymbol{L}^{(T_\delta)} - \hat{\boldsymbol{L}}_\epsilon\|_F^2 \leq \frac{2\delta}{\epsilon}. \tag{11}$$

In Appendix A.3 we provide a more detailed result, with an estimation of the constant in $\mathcal{O}(1/\delta)$.

4 Theoretical analysis of the estimator

In this section we provide theoretical analysis of our algorithm. First, we provide guarantees on the support recovery of the outliers. Next, we prove a non asymptotic bound on the risk of our estimator. We start by introducing assumptions on the missing values mechanism.

4.1 Assumption on the sampling scheme

Assumption 1. *There exist a strictly positive sequence μ_n such that for any $(i,j) \in I$, $\mu_n \leq \boldsymbol{\Pi}_{ij}$.*

Bounding the probabilities of observing any entry away from 0 is a usual assumption in the literature dealing with missing observations (different patterns for missing observations are discussed, e.g., in [29, 33, 38]). We denote by ν_n and $\tilde{\nu}_n$ two sequences such that for any $i \in I$, $\sum_{j\in\mathcal{I}} \boldsymbol{\Pi}_{ij} \leq \nu_n n$ and for any $i \in [n]$, $\sum_{j\in\mathcal{O}} \boldsymbol{\Pi}_{ij} \leq \tilde{\nu}_n s$. We always have $\nu_n \leq 1$ and $\tilde{\nu}_n \leq 1$. When ν_n and $\tilde{\nu}_n$ are decreasing sequences, we obtain better error rates by taking advantage of the fact that observations are distributed over different nodes in the network. Note that our estimators do not require the knowledge of the sequences μ_n and $\tilde{\nu}_n$. On the other hand, for the theoretical analysis we need an upper bound on $\nu_n\rho_n n$ (the average observed connectivity of inlier nodes), which can be estimated robustly.

Recall that we do not observe any entry on the diagonal of $\boldsymbol{A}$. Combined with Assumption 1, this implies that for any matrix $\boldsymbol{M} \in \mathbb{R}^{n\times n}$

$$\left\|\boldsymbol{M}_{|I}\right\|_F^2 \leq \frac{1}{\mu_n}\|\boldsymbol{M}\|_{L_2(\boldsymbol{\Pi})}^2 + n\|\boldsymbol{M}\|_\infty^2. \tag{12}$$

Moreover, since $|O| = 2ns + (s-1)(s-2)/2 \leq 3ns$, we find that

$$\left\|\boldsymbol{M}_{|O}\right\|_F^2 \leq 3ns\|\boldsymbol{M}\|_\infty^2. \tag{13}$$

Before stating the second assumption, recall that ρ_n and γ_n are two sparsity inducing sequences such that $\|\boldsymbol{L}^*\|_\infty \leq \rho_n$ and $\|\boldsymbol{S}^*\|_\infty \leq \gamma_n$. We assume that

Assumption 2. *$\nu_n\rho_n \geq \log(n)/n$ and $\tilde{\nu}_n\gamma_n \geq \log(n)/n$.*

Assumption 2 implies that the *observed* average node degree is not too small. Note that considering very sparse graphs, where the expectation of the probability of observing an edge is of order $\frac{1}{n}$, is of lesser interest since it has been shown in [14] that the trivial null estimator is minimax optimal in this setting. On the other hand, the sparsity threshold $\log(n)/n$ is known to correspond to phase transition phenomenons for recovering structural properties in the SBM [1]. We also need the following assumption on the "signal to noise ratio".

Assumption 3. *$\nu_n\rho_n n \geq \tilde{\nu}_n\gamma_n s$*

Here, edges connecting inliers to inliers can be seen as a "signal term", while edges connecting outliers to any other nodes can be seen as a "noise term". Now, recall that ρ_n bounds the probability of any inlier to be connected to any inlier, while γ_n bounds the probability of any inlier to be connected to any outlier. Then, Assumption 3 requires that we observe more connection between inliers than between inliers and outliers, or equivalently that the "signal" induced by the connections of the inliers be stronger than the "noise". When the sampling is uniform, that is each entry is observed with the same probability p, we have $\mu_n = \nu_n = \tilde{\nu}_n = p$ and Assumption 3 becomes $\rho_n n \geq \gamma_n s$.

4.2 Outlier detection

The $\|\cdot\|_{2,1}$-norm penalisation induces the column-wise sparsity of the estimator $\widehat{\boldsymbol{S}}$ (when appropriately calibrated, it allows only a small number of columns of $\widehat{\boldsymbol{S}}$ to be non-zero). Using this sparsity, we define the set of estimated outliers as

$$\widehat{\mathcal{O}} \triangleq \left\{ j \in [n] : \widehat{\boldsymbol{S}}_{\cdot,j} \neq \boldsymbol{0} \right\}. \tag{14}$$

The following lemma, proven in Appendix A.8.1, provides a characterization of this set:

Lemma 1. *For any $j \in [n]$, $\widehat{\boldsymbol{S}}_{\cdot,j} \neq \boldsymbol{0} \;\Leftrightarrow\; \left\| \boldsymbol{\Omega}_{\cdot,j} \odot \left(\boldsymbol{A}_{\cdot,j} - \widehat{\boldsymbol{L}}_{\cdot,j} - \widehat{\boldsymbol{S}}_{j,\cdot} \right)_+ \right\|_2 > \frac{\lambda_2}{2}$.*

Lemma 1 provides a lower bound on λ_2 that will prevent from erroneously reporting inliers as outliers by choosing λ_2 larger than the expected norm of columns corresponding to inliers. Note that for any inlier j, $\mathbb{E}[\|(\boldsymbol{\Omega} \odot (\boldsymbol{A}_{\cdot,j} - \boldsymbol{L}^*_{\cdot,j})_{|I})_+\|_2]$ is of the order $\sqrt{\nu_n\rho_n(n-s) + \tilde{\nu}_n\gamma_n s}$. If λ_2 falls below this threshold, some inliers are likely to be erroneously reported as outliers. Therefore, we choose $\lambda_2 \gtrsim \sqrt{\nu_n\rho_n(n-s) + \tilde{\nu}_n\gamma_n s}$. Under Assumption 3, this condition becomes $\lambda_2 \gtrsim \sqrt{\nu_n\rho_n n}$. With this choice of λ_2 we have the following results proven in Appendix A.4:

Theorem 2. *Let $\lambda_2 = 19\sqrt{\nu_n\rho_n n}$. Then, under Assumptions 1-3, there exists an absolute constants $c > 0$ such that with probability at least $1 - c/n$*

$$\widehat{\mathcal{O}} \cap \mathcal{I} = \emptyset. \tag{15}$$

One cannot hope further separate outliers from inliers without additional assumptions on how the first group differs from the second one. Here, we provide an intuition about our condition on the connectivity of outliers that is sufficient for outliers detection. According to Lemma 1, any outlier j will be reported as such if $\|(\boldsymbol{\Omega}_{\cdot,j} \odot (\boldsymbol{A}_{\cdot,j} - \widehat{\boldsymbol{L}}_{\cdot,j} - \widehat{\boldsymbol{S}}_{j,\cdot}))_+\|_2 > \lambda_2/2$. So, in order to detect an outlier j, the threshold λ_2 must be at least smaller than $\mathbb{E}[\|(\boldsymbol{\Omega}_{\cdot,j} \odot (\boldsymbol{A}_{\cdot,j} - \widehat{\boldsymbol{L}}_{\cdot,j} - \widehat{\boldsymbol{S}}_{j,\cdot}))_+\|_2]$. Recalling that $\widehat{\boldsymbol{L}}$ and $\widehat{\boldsymbol{S}}$ have nonnegative entries, we see that

$$\mathbb{E}\left[\left\| \left(\boldsymbol{\Omega}_{\cdot,j} \odot \left(\boldsymbol{A}_{\cdot,j} - \widehat{\boldsymbol{L}}_{\cdot,j} - \widehat{\boldsymbol{S}}_{j,\cdot} \right) \right)_+ \right\|_2 \right] \leq \mathbb{E}\left[\left\| (\boldsymbol{\Omega}_{\cdot,j} \odot (\boldsymbol{A}_{\cdot,j}))_+ \right\|_F \right] = \sqrt{\sum_{i \in \mathcal{I}} \boldsymbol{\Pi}_{ij} \boldsymbol{S}^*_{ij} + \sum_{i \in \mathcal{O}} \boldsymbol{\Pi}_{ij} (\boldsymbol{S}^*_{ij} + \boldsymbol{S}^*_{ij})}.$$

Thus, the condition $\sqrt{\nu_n\rho_n n} \lesssim \lambda_2 \lesssim \min_{j \in \mathcal{O}} \sqrt{\sum_{i \in \mathcal{I}} \boldsymbol{\Pi}_{ij} \boldsymbol{S}^*_{ij}}$ appears naturally when separating the inliers from the outliers. This condition is formalized in the following assumption:

Assumption 4. *$\min_{j \in \mathcal{O}} \sqrt{\sum_{i \in \mathcal{I}} \boldsymbol{\Pi}_{ij} \boldsymbol{S}^*_{ij}} > C\rho_n\nu_n n$ where C is an absolute constant defined in Section A.5.*

When the outliers represent only a small fraction of the nodes, we have that $|\mathcal{I}| \simeq n$. Then, Assumption 4 is met when outlier nodes have higher expected observed degree than inlier nodes. When the sampling probabilities are nearly uniform, this assumption essentially reads $\gamma_n \gtrsim \rho_n$; however it allows for more general settings, as long as the observed connections of the outliers are not too scarce. Under Assumption 4, we obtain the following results proven in Appendix A.5:

Theorem 3. *Let $\lambda_2 = 19\sqrt{\nu_n \rho_n n}$. Under Assumptions 1-4, there exists an absolute constant $c > 0$ such that $\mathcal{O} = \widehat{\mathcal{O}}$ with probability at least $1 - cs/n$.*

For both, Theorem 3 and Theorem 2 we actually show that the results hold with probabilities at least $1 - 8se^{-c_n n}$ and $1 - 6e^{-c_n n}$ respectively, where c_n is a sequence depending on ν_n and ρ_n such that $c_n \geq \log(n)/n$.

4.3 Estimation of the connections probabilities

In this section, we establish the non-asymptotic upper bound on the risk of our estimator. We denote the noise matrix $\boldsymbol{\Sigma} \triangleq \boldsymbol{A} - \mathbb{E}[\boldsymbol{A}]$. Let $\boldsymbol{\Gamma}$ be the random matrix defined as follows : for any (i, j), $\boldsymbol{\Gamma}_{ij} \triangleq \epsilon_{ij} \boldsymbol{\Omega}_{ij}$, where $\{\boldsymbol{\epsilon}_{ij}\}_{1 \leq i < j \leq n}$ is a Rademacher sequence. To clarify the exposition of our results, we introduce the following error terms

$$\Phi \triangleq n\rho_n^2 \left(\frac{\nu_n k}{\mu_n} + \nu_n s \right), \quad \Psi \triangleq 16 \tilde{\nu}_n \gamma_n \rho_n s n \quad \text{and} \quad \Xi \triangleq \frac{\sqrt{\nu_n n} \rho_n}{\lambda_1} + 1.$$

The following theorem, proven in Appendix A.6, provides the error bound for the risk of the estimator $\widehat{\boldsymbol{L}}$ that depends on the choice of the regularization parameter λ_1:

Theorem 4. *Assume that $\lambda_1 \geq 3 \left\| \boldsymbol{\Omega} \odot \boldsymbol{\Sigma}_{|I} \right\|_{op}$, and that $\lambda_2 = 19\sqrt{\nu_n \rho_n n}$. Then, under Assumptions 1-3, there exists absolute constants $C > 0$ and $c > 0$ such that with probability at least $1 - c/n$,*

$$\left\| \left(\widehat{\boldsymbol{L}} - \boldsymbol{L}^* \right)_{|I} \right\|^2_{L_2(\boldsymbol{\Pi})} \quad \leq \quad C \left(\frac{\lambda_1^2 k}{\mu_n} + \Phi + \Xi \Psi \right). \tag{16}$$

Next, we provide a choice for λ_1 such that the condition $\lambda_1 \geq 3 \left\| \boldsymbol{\Omega} \odot \boldsymbol{\Sigma}_{|I} \right\|_{op}$ holds with high probability. To do so, we must first obtain a high-probability bound on $\left\| \boldsymbol{\Omega} \odot \boldsymbol{\Sigma}_{|I} \right\|_{op}$. This is done in the following Lemma:

Lemma 2. $\mathbb{P}\left(\left\| \boldsymbol{\Omega} \odot \boldsymbol{\Sigma}_{|I} \right\|_{op} \geq 28\sqrt{\nu_n \rho_n n} \right) \leq e^{-\nu_n \rho_n n}$.

Using Lemma 2, we obtain the following corollary proven in Appendix A.7:

Corollary 1. *Choose $\lambda_1 = 84\sqrt{\nu_n \rho_n n}$ and $\lambda_2 = 19\sqrt{\nu_n \rho_n n}$. Then, under the conditions of Theorem 4, there exists absolute constants $C > 0$ and $c > 0$ such that with probability at least $1 - c/n$,*

$$\left\| \left(\widehat{\boldsymbol{L}} - \boldsymbol{L}^* \right)_{|I} \right\|^2_{L_2(\boldsymbol{\Pi})} \quad \leq \quad C \left(\frac{\nu_n}{\mu_n} \rho_n k n + (\nu_n \rho_n \vee \tilde{\nu}_n \gamma_n) \rho_n s n \right) \tag{17}$$

and

$$\left\| \left(\widehat{\boldsymbol{L}} - \boldsymbol{L}^* \right)_{|I} \right\|^2_{F} \quad \leq \quad \frac{C}{\mu_n} \left(\frac{\nu_n}{\mu_n} \rho_n k n + (\nu_n \rho_n \vee \tilde{\nu}_n \gamma_n) \rho_n s n \right). \tag{18}$$

We actually show that inequalities (16), (17) and (18) hold with probability at least $1 - 10e^{-c_n n}$, where c_n is a sequence depending on ν_n, $\tilde{\nu}_n$, ρ_n and γ_n such that $c_n \geq \log(n)/n$. Note that, by setting $2\delta/\epsilon = C/\mu_n \left(\nu_n \rho_n k n / \mu_n + (\nu_n \rho_n \vee \tilde{\nu}_n \gamma_n) \rho_n s n \right)$ in Theorem 1, we obtain approximate matching of the estimation and approximation errors after $\mathcal{O}\left(\mu_n / \epsilon \left(\nu_n \rho_n k n / \mu_n + (\nu_n \rho_n \vee \tilde{\nu}_n \gamma_n) \rho_n s n \right)^{-1} \right)$ iterations.

When $(\tilde{\nu}_n \gamma_n \vee \nu_n \rho_n)\, s \leq \nu_n k / \mu_n$, Corollary 1 implies that, with high probability, $\| (\widehat{\boldsymbol{L}} - \boldsymbol{L}^*)_{|I} \|^2_{L_2(\boldsymbol{\Pi})} \leq C \left(\nu_n / \mu_n \right) \rho_n k n$ which corresponds to the minimax optimal rate for low-rank matrix estimation problem.

Note that this condition allows for a growing number of outliers. For example, when the sampling is uniform, that is $\mu_n = \nu_n = \tilde{\nu}_n = p$, the number of outliers can grow as $k/(p(\rho_n \vee \gamma_n))$.

To the best of our knowledge, no results on robust estimation of the connection probabilities in the presence of outliers and missing observations have been established before. Previous rates of convergence for the problem of estimating the connection probabilities under the Stochastic Block Model with missing links have been established, for the uniform sampling scheme, in [14], and, for more general sampling schemes, in [17]. To compare our bound with these previous results, we consider the case of the uniform sampling and assume that the condition $(\tilde{\nu}_n\mu_n \vee \nu_n\rho_n)\, s \leq \nu_n k/\mu_n$ is met. In [14] and [17], the authors show that the risk of their estimators in $\|\cdot\|_{L_2(\mathbf{\Pi})}$-norm is of the order $\rho_n\left(\log(k)n + k^2\right)$, and that it is minimiax optimal. The rate provided by Corolary 1 is of the order $\rho_n kn$. So, for the relevant case $k \leq \sqrt{n}$, our method falls short of the minimax optimal rate for this problem by a factor $k/\log(k)$. Note that, estimators proposed in [14] and [17] have non-polynomial computational cost while our estimator can be used in practice. On the other hand, the authors of [50] propose a polynomial-time algorithm for estimating the probabilities of connections in the Stochastic Block Model under complete observation of the network. They show that the risk of their estimator for the connection probabilities is bounded by $C\rho_n kn$. Thus, our method matches the best known rate established for a polynomial time algorithm for the Stochastic Block Model while being robust to missing observations and outliers.

5 Numerical experiments

5.1 Outlier detection

In this section we start by illustrating the performance of our method in terms of outliers' detection. We consider two types of outliers: hubs and mixed membership profiles. We start by generating a graph containing $n = 200$ inlier nodes according to the Stochastic Block Model with three communities of approximately the same size. In each community, the probability of connection between nodes is equal to 0.5. The probability of connection between communities is equal to 0.2. Then, we generate s outlier nodes using the following two methods:

1. **Hubs**: outlier j connects to any other node i with probability π_{ij}, where we sample π_{ij} from a uniform distribution between π_{hub} and 1.

2. **Mixed menberships**: for any outlier j, we select at random two communities. For any other node i, if it belongs to one of the two communities, outlier j connects to i with probability π_{mix}. Otherwise, it connects to i with probability 0.2.

In each of these two situations, we consider an increasing number of outliers, as well as different values of the parameters π_{hub} and π_{mix}, which we use as proxies to quantify the signal (the larger are π_{hub} and π_{mix}, the easier is the detection problem). The results are presented in Tables 1 through 4. Tables 1 and 2 present the power and the false discovery rate (FDR) of hub detection for increasing π_{hub} and increasing number of outliers. In this setting, we are able to correctly select the outliers, even at the detection limit $\pi_{\mathsf{hub}} = 0.2$ where the outliers and inliers have approximately the same degree. Tables 3 and 4 present the power and FDR for outliers with mixed membership profiles, for increasing π_{mix} and increasing number of outliers. The results show that mixed membership nodes are harder to detect than hubs. For $\pi_{\mathsf{mix}} = 0.4$, where inliers and outliers have approximately the same degree, the power and FDR are of the order of 0.5. However, as π_{mix} increases, we recover the same behavior as for hubs.

5.2 Link prediction

We now evaluate the performance of our method in terms of prediction of the missing links. As before, we start by generating a network of size 200 using the Stochastic Block Model with three balanced communities. Then, we add two different types of outliers: hubs and nodes with mixed community membership. We set $\pi_{\mathsf{hub}} = 0.2$ and $\pi_{\mathsf{mix}} = 0.4$, corresponding to the detection limit where outliers have approximately the same degree as the inliers, and cannot be directly detected by inspecting the histogram of degrees. In both cases, we "remove" uniformly at random 20% of the entries in the adjacency matrix; we then use our

	$\pi_{\mathsf{hub}} = 0.2$	$\pi_{\mathsf{hub}} = 0.5$	$\pi_{\mathsf{hub}} = 0.8$
$s = 2$	0.97	0.98	0.97
$s = 5$	0.96	0.99	0.98
$s = 10$	0.91	0.91	0.91

Table 1: **Power** for **hubs** detection for increasing number of outliers (s) and increasing signal to noise ratio (π_{hub}), averaged across 100 replications.

	$\pi_{\mathsf{hub}} = 0.2$	$\pi_{\mathsf{hub}} = 0.5$	$\pi_{\mathsf{hub}} = 0.8$
$s = 2$	0.03	0.02	0.03
$s = 5$	0.03	0.01	0.1
$s = 10$	0.09	0.09	0.14

Table 2: **FDR** for **hubs** detection for increasing number of outliers (s) and increasing signal to noise ratio (π_{hub}), averaged across 100 replications.

	$\pi_{\mathsf{mix}} = 0.4$	$\pi_{\mathsf{mix}} = 0.6$	$\pi_{\mathsf{mix}} = 0.8$
$s = 2$	0.36	0.73	0.97
$s = 5$	0.45	0.84	0.94
$s = 10$	0.55	0.71	0.85

Table 3: **Power** for **mixed membership** detection for increasing number of outliers (s) and increasing signal to noise ratio (π_{mix}), averaged across 100 replications.

	$\pi_{\mathsf{mix}} = 0.4$	$\pi_{\mathsf{mix}} = 0.6$	$\pi_{\mathsf{mix}} = 0.8$
$s = 2$	0.64	0.26	0.07
$s = 5$	0.54	0.16	0.06
$s = 10$	0.45	0.28	0.15

Table 4: **FDR** for **mixed membership** detection for increasing number of outliers (s) and increasing signal to noise ratio (π_{mix}), averaged across 100 replications.

method to predict these missing links. We compare the prediction results with two competitors: the method implemented in the R [41] package `missSBM` [44, 45] which fits a Stochastic Block Model in the presence of missing links (but no outlier), and matrix completion as implemented in the R package `softImpute` [22]. We also include a comparison to link prediction using the average degree, as a baseline.

The results of link prediction are presented in Figure 2 for the hubs and in Figure 3 for the mixed membership, for an increasing number of outliers. We first note that our method is competitive in terms of link prediction, in all the situations simulated here. In particular, as the number of outliers increases (from left to right), the prediction error of `missSBM` and `softImpute` (which do not model outliers), increases. On the other hand, the prediction error of our algorithm is stable. We also note that, in the case of outliers with mixed memberships, although our method performs less accurately in terms of outliers detection (see Section 5.1), it still significantly improves over competitors in terms of link prediction, even in the "hard" regime $\pi_{\mathsf{mix}} = 0.4$.

5.3 Analysis of the political blogosphere data set

Finally, we show the performance of our algorithm on the network of political blogs, first analysed in [2]. This data set, collected before the 2004 American presidential election, records hyperlinks connecting political blogs to one another. These blogs have been labelled manually as either "liberal" or "conservative". In order to compare our algorithm with results obtained by benchmark methods for community detection on this dataset, we consider these labels as the true communities, and we express our error in terms of number of miss-classified nodes. Our method primarily aims at estimating probabilities of connection. We obtain estimates for the communities of the nodes by applying a standard clustering method on the rows of our estimator $\widehat{\boldsymbol{L}}^T$. More precisely, we estimate the communities of a node by taking the sign of the corresponding coordinate of the second eigenvector of $\widehat{\boldsymbol{L}}^T$.

We restrain our analysis by considering only the largest connected component of the graph, and forgetting the direction of the edges. Thus, we obtain a graph with $1,228$ nodes, $16,714$ edges and average degree 27. Note that the distribution of degrees is skewed to the right by the presence of highly connected nodes, and the median of the degrees is only 13. Following the results of Theorem 4, we choose penalization parameters for our algorithm of the form $\lambda_1 = C_1\sqrt{n\rho_n}$ and $\lambda_2 = C_2\sqrt{n\rho_n}$. The parameter $\sqrt{\rho_n n}$ is estimated by the square root of the average degree of the nodes. In order to tune the parameters C_1 and C_2, we ran our algorithm for a grid of values from 1 to 20. We found that the accuracy of our estimator for the communities detection does not decrease significantly for a rather large range of values of C_1 (C_1 ranges from 1 to 12), as long as C_2 is not too small.

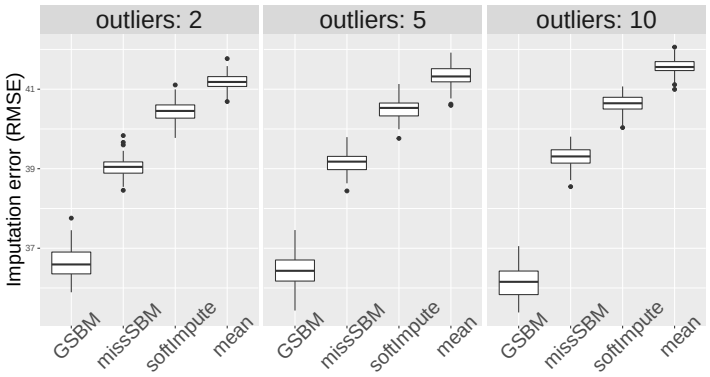

Figure 2: Link prediction error for stochastic block models with **hub outliers** with 200 inliers, 2 to 10 outliers, and 20% of **missing links**. Three prediction methods are compared: our generalized stochastic block model with outliers (GSBM), an SBM for incomplete data (missSBM R package) and a matrix completion method (R package softImpute). We include a comparison to a baseline (prediction with average degree). The experiment is performed for an increasing number of outliers (left: 2, middle: 5, right: 10). Results are averaged across 100 replications.

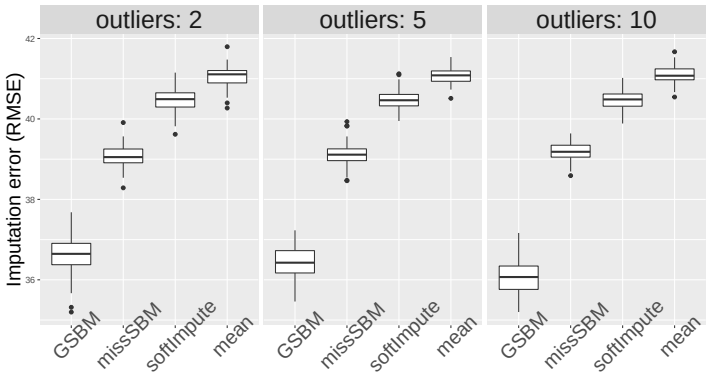

Figure 3: Link prediction error for stochastic block models with **mixed membership outliers** with 200 inliers, 2 to 10 outliers, and 20% of **missing links**. Three prediction methods are compared: our generalized stochastic block model with outliers (GSBM), an SBM for incomplete data (missSBM R package) and a matrix completion method (R package softImpute). We include a comparison to a baseline (prediction with average degree). The experiment is performed for an increasing number of outliers (left: 2, middle: 5, right: 10). Results are averaged across 100 replications.

We analyse the results obtained for $C_1 = 10$ and $C_2 = 5$. With this choice of parameters, our algorithm detects $s = 10$ outliers. Looking more carefully at the connecivity of these outliers, we see that they correspond to hubs, and that their degree, which is larger than 199, strongly departs from the degrees of the remaining nodes. In fact, most of them correspond to "news aggregation" websites, consisting mainly of links connecting to other sites (e.g. www.drudgereport.com, https://pjmedia.com/instapundit/), which explains their hub profile. Among the $n-s = 1212$ remaining nodes, which are considered as inliers, 84 nodes are missclassified. The number of missclassified nodes is comparable with the best-known methods that have been applied for this dataset. For example, the SCORE method developped in [26] obtains a missclassification error of 58 nodes. Benchmark methods such as convex relaxation of the maximum likelihood [10], profile likelihood methods for degree-corrected SBM [28], as well as modularity maximization [52, 39] obtain errors ranging from 59 to 68; however the tabu algorithm implemented to maximize these last two criterions is highly sensitive to its (random) initialization, and the average missclassifiaction error of these two methods based on 100 repetitions is of about 105 nodes, as it is shown in [26]. Thus, on this dataset our method leads to a classification error comparable with benchmark methods, while being primarily designed for estimating the connection probabilities and outliers detection.

References

[1] Abbe, E. (2018). Community detection and stochastic block models: Recent developments. Journal of Machine Learning Research, 18(177):1–86.

[2] Adamic, L. A. and Glance, N. (2005). The political blogosphere and the 2004 u.s. election: Divided they blog. In Proceedings of the 3rd International Workshop on Link Discovery, LinkKDD '05, pages 36–43, New York, NY, USA. ACM.

[3] Akoglu, L., Chandy, R., and Faloutsos, C. (2013). Opinion fraud detection in online reviews by network effects. International AAAI Conference on Web and Social Media.

[4] Bandeira, A. and van Handel, R. (2014). Sharp nonasymptotic bounds on the norm of random matrices with independent entries. The Annals of Probability, 44.

[5] Beck, A. and Tetruashvili, L. (2013). On the convergence of block coordinate descent type methods. SIAM Journal on Optimization, 23(4):2037–2060.

[6] Benyahia, O., Largeron, C., and Jeudy, B. (2017). Community detection in dynamic graphs with missing edges. In 2017 11th International Conference on Research Challenges in Information Science (RCIS), pages 372–381.

[7] Bleakley, K., Biau, G., and Vert, J.-P. (2007). Supervised reconstruction of biological networks with local models. Bioinformatics, 23(13):i57–i65.

[8] Boucheron, S., Lugosi, G., and Massart, P. (2013). Concentration Inequalities: A Nonasymptotic Theory of Independence. OUP Oxford.

[9] Boyd, S. and Vandenberghe, L. (2004). Convex Optimization. Cambridge University Press.

[10] Cai, T. T. and Li, X. (2015). Robust and computationally feasible community detection in the presence of arbitrary outlier nodes. Ann. Statist., 43(3):1027–1059.

[11] D. Hoff, P. (2007). Modeling homophily and stochastic equivalence in symmetric relational data. Advances in Neural Information Processing Systems 20 - Proceedings of the 2007 Conference, 20.

[12] Domingos, P. and Richardson, M. (2001). Mining the network value of customers. In Proceedings of the Seventh ACM SIGKDD International Conference on Knowledge Discovery and Data Mining, KDD '01, pages 57–66, New York, NY, USA. ACM.

[13] Dunne, J. A., Williams, R. J., and Martinez, N. D. (2002). Food-web structure and network theory: The role of connectance and size. Proceedings of the National Academy of Sciences of the United States of America, 99(20):12917–12922.

[14] Gao, C., Lu, Y., Ma, Z., and Zhou, H. H. (2016). Optimal estimation and completion of matrices with biclustering structures. J. Mach. Learn. Res., 17(1):5602–5630.

[15] Gao, C., Lu, Y., and Zhou, H. H. (2015). Rate-optimal graphon estimation. Ann. Statist., 43(6):2624–2652.

[16] Garber, D., Sabach, S., and Kaplan, A. (2018). Fast generalized conditional gradient method with applications to matrix recovery problems. arXiv e-prints, page arXiv:1802.05581.

[17] Gaucher, S. and Klopp, O. (2019). Maximum likelihood estimation of sparse networks with missing observations. Arxiv preprint, page arXiv:1902.10605.

[18] Giné, E. and Nickl, R. (2016). Mathematical foundations of infinite-dimensional statistical models. Cambridge Series in Statistical and Probabilistic Mathematics, [40]. Cambridge University Press, New York.

[19] Guimerà, R. and Sales-Pardo, M. (2009). Missing and spurious interactions and the reconstruction of complex networks. Proceedings of the National Academy of Sciences, 106(52):22073–22078.

[20] Gyöngyi, Z., Garcia-Molina, H., and Pedersen, J. (2004). Combating web spam with trustrank. In Proceedings of the Thirtieth International Conference on Very Large Data Bases - Volume 30, VLDB '04, pages 576–587. VLDB Endowment.

[21] Handcock, M. S. and Gile, K. J. (2010). Modeling social networks from sampled data. Ann. Appl. Stat., 4(1):5–25.

[22] Hastie, T., Mazumder, R., Lee, J. D., and Zadeh, R. (2015). Matrix completion and low-rank svd via fast alternating least squares. J. Mach. Learn. Res., 16(1):3367–3402.

[23] Hawkins, D. (1980). Identification of Outliers. Chapman and Hall.

[24] Holland, P. W., Laskey, K. B., and Leinhardt, S. (1983). Stochastic blockmodels: First steps. Social Networks, 5(2):109 – 137.

[25] Jaggi, M. (2013). Revisiting Frank-Wolfe: Projection-free sparse convex optimization. In Dasgupta, S. and McAllester, D., editors, Proceedings of the 30th International Conference on Machine Learning, volume 28 of Proceedings of Machine Learning Research, pages 427–435, Atlanta, Georgia, USA. PMLR.

[26] Jin, J. (2015). Fast community detection by score. Ann. Statist., 43(1):57–89.

[27] Karrer, B. and Newman, M. E. J. (2011a). Stochastic blockmodels and community structure in networks. Phys. Rev. E, 83:016107.

[28] Karrer, B. and Newman, M. E. J. (2011b). Stochastic blockmodels and community structure in networks. Phys. Rev. E, 83:016107.

[29] Klopp, O. (2014). Noisy low-rank matrix completion with general sampling distribution. Bernoulli, 20(1):282–303.

[30] Klopp, O., Tsybakov, A. B., and Verzelen, N. (2017). Oracle inequalities for network models and sparse graphon estimation. Ann. Statist., 45(1):316–354.

[31] Knuth, D. E. (1993). The Stanford GraphBase: A Platform for Combinatorial Computing. ACM, New York, NY, USA.

[32] Koltchinskii, V. (2011). Oracle Inequalities in Empirical Risk Minimization and Sparse Recovery Problems: École d'Été de Probabilités de Saint-Flour XXXVIII-2008. Lecture Notes in Mathematics. Springer Berlin Heidelberg.

[33] Koltchinskii, V., Lounici, K., and Tsybakov, A. B. (2011). Nuclear-norm penalization and optimal rates for noisy low-rank matrix completion. Ann. Statist., 39(5):2302–2329.

[34] Kossinets, G. (2006). Effects of missing data in social networks. Social Networks, 28(3):247 – 268.

[35] Lecué, G. and Lerasle, M. (2017). Robust machine learning by median-of-means : theory and practice. arXiv e-prints, page arXiv:1711.10306.

[36] Lomnitz, L. A. (1977). Networks of reciprocal exchange. In Lomnitz, L. A., editor, Networks and Marginality, pages 131 – 158. Academic Press.

[37] Mu, C., Zhang, Y., Wright, J., and Goldfarb, D. (2016). Scalable robust matrix recovery: Frank-wolfe meets proximal methods. ArXiv, abs/1403.7588.

[38] Negahban, S. and Wainwright, M. J. (2012). Restricted strong convexity and weighted matrix completion: Optimal bounds with noise. J. Mach. Learn. Res., 13:1665–1697.

[39] Newman, M. E. J. and Girvan, M. (2004). Finding and evaluating community structure in networks. Phys. Rev. E, 69:026113.

[40] Nolin, D. A. (2010). Food-sharing networks in lamalera, indonesia. Human Nature, 21(3):243–268.

[41] R Core Team (2019). R: A Language and Environment for Statistical Computing. R Foundation for Statistical Computing, Vienna, Austria.

[42] Robin, G., Wai, H.-T., Josse, J., Klopp, O., and Moulines, E. (2018). Low-rank interaction with sparse additive effects model for large data frames. In Proceedings of the 32Nd International Conference on Neural Information Processing Systems, NIPS'18, pages 5501–5511, USA. Curran Associates Inc.

[43] Sundar Mukherjee, S. and Chakrabarti, S. (2019). Graphon Estimation from Partially Observed Network Data. arXiv e-prints, page arXiv:1906.00494.

[44] Tabouy, T., Barbillon, P., and Chiquet, J. (2017). Variational Inference for Stochastic Block Models from Sampled Data. ArXiv e-prints.

[45] Tabouy, T., Barbillon, P., and Chiquet, J. (2019). misssbm: An r package for handling missing values in the stochastic block model.

[46] Thomas, M., Verzelen, N., Barbillon, P., Coomes, O., Caillon, S., Mckey, D., Elias, M., Garine, E., Raimond, C., Dounias, E., Jarvis, D., Wencelius, J., Leclerc, C., Labeyrie, V., pham hung, C., Hue, N., Sthapit, B., Rana, R., Barnaud, A., and Massol, F. (2015). A network-based method to detect patterns of local crop biodiversity: Validation at the species and infra-species levels. In Woodward, G. and Bohan, D. A., editors, Ecosystem Services, volume 53 of Advances in Ecological Research, pages 259 – 320. Academic Press.

[47] Tsai, C.-W., Lai, C.-F., Chao, H.-C., and Vasilakos, A. (2015). Big data analytics: A survey. Journal of Big Data, 2.

[48] Wang, Y., Chakrabarti, D., Wang, C., and Faloutsos, C. (2003). Epidemic spreading in real networks: an eigenvalue viewpoint. 22nd International Symposium on Reliable Distributed Systems, 2003. Proceedings., pages 25–34.

[49] Wu, Y.-J., Levina, E., and Zhu, J. (2018). Link prediction for egocentrically sampled networks. ArXiv, abs/1803.04084.

[50] Xu, J. (2018). Rates of convergence of spectral methods for graphon estimation. In Dy, J. and Krause, A., editors, Proceedings of the 35th International Conference on Machine Learning, volume 80 of Proceedings of Machine Learning Research, pages 5433–5442, Stockholmsmässan, Stockholm Sweden. PMLR.

[51] Yu, H., Braun, P., Yıldırım, M. A., Lemmens, I., Venkatesan, K., Sahalie, J., Hirozane-Kishikawa, T., Gebreab, F., Li, N., Simonis, N., Hao, T., Rual, J.-F., Dricot, A., Vazquez, A., Murray, R. R., Simon, C., Tardivo, L., Tam, S., Svrzikapa, N., Fan, C., de Smet, A.-S., Motyl, A., Hudson, M. E., Park, J., Xin, X., Cusick, M. E., Moore, T., Boone, C., Snyder, M., Roth, F. P., Barabási, A.-L., Tavernier, J., Hill, D. E., and Vidal, M. (2008). High-quality binary protein interaction map of the yeast interactome network. Science, 322(5898):104–110.

[52] Zhao, Y., Levina, E., and Zhu, J. (2012). Consistency of community detection in networks under degree-corrected stochastic block models. Ann. Statist., 40(4):2266–2292.

[53] Zhao, Y., Wu, Y.-J., Levina, E., and Zhu, J. (2017). Link prediction for partially observed networks. Journal of Computational and Graphical Statistics, 26(3):725–733.

A Proofs

The proofs are presented as follows. First, we recall in Section A.1 some results that will be used in our proofs. In Section A.2 we provide the details of the Algorithm 1. Section A.3 is devoted to the study of the convergence of our algorithm. Theorem 2 is proved in Section A.4, Theorem 3 is proved in Section A.5, while in Section A.6 we prove Theorem 4. Corollary 1 is proved in Sections A.7. Auxiliary Lemmas used throughout these sections are proved in Section A.8.

To ease notations, we denote henceforth by $\Delta \boldsymbol{S} = \boldsymbol{S}^* - \widehat{\boldsymbol{S}}$ and $\Delta \boldsymbol{L} = \boldsymbol{L}^* - \widehat{\boldsymbol{L}}$ the estimation errors of $\boldsymbol{S}^*$ and $\boldsymbol{L}^*$.

A.1 Tools

In our proofs, we will use Bernstein's inequality on different occasions. We state it here for the reader's convenience.

Theorem 5 (Bernstein's inequality)**.** *Let $X_1, ..., X_n$ be independent centered random variables. Assume that for any $i \in [n]$, $|X_i| \leq M$ almost surely, then*

$$\mathbb{P}\left(\left| \sum_{1 \leq i \leq n} X_i \right| \geq \sqrt{2t \sum_{1 \leq i \leq n} \mathbb{E}[X_i^2]} + \frac{2M}{3} t \right) \leq 2e^{-t} \tag{19}$$

We will also use Bousquet's theorem, as stated in [18], Theorem 3.3.16.

Theorem 6 (Bousquet)**.** *Let X_i, $i \in \mathbb{N}$ be independent $\mathcal{S}$-valued random variables, and let $\mathcal{F}$ be a countable class of functions $f = (f_1, ..., f_n) : \mathcal{S} \to [-1, 1]^n$ such that $\mathbb{E}[f_i(X_i)] = 0$ for any $f \in \mathcal{F}$ and $i \in [n]$. Set $Z = \sup_{f \in \mathcal{F}} \left| \sum_{1 \leq i \leq n} f_i(X_i) \right|$ and $v = \sup_{f \in \mathcal{F}} \sum_{1 \leq i \leq n} \mathbb{E}\left[f_i(X_i)^2 \right]$. Then, for any $x > 0$,*

$$\mathbb{P}\left(Z > \mathbb{E}[Z] + \frac{x}{3} + \sqrt{2x(2\mathbb{E}[Z] + v)} \right) \leq \exp(-x).$$

To bound the operator norm of random matrices with high probability, we use Corollary 3.6 in [4].

Proposition 1 (Bandeira, Van Handel, 2016)**.** *Let $\boldsymbol{X}$ be a $n \times n$ symmetric random matrix with $\boldsymbol{X}_{ij} = \xi_{ij} b_{ij}$, where $\{\xi_{ij}\}_{i \leq j}$ are independant symmetric random variables with unit variance, and $\{b_{ij}\}_{i \leq j}$ are fixed scalars. Let $\sigma \triangleq \max_i \sqrt{\sum_j b_{ij}^2}$, then for any $\alpha \geq 3$*

$$\mathbb{E}\left[\|\boldsymbol{X}\|_{op} \right] \leq e^{\frac{2}{3}} \left(2\sigma + 14\alpha \max_{ij} \left(\mathbb{E}\left[(\xi_{ij} b_{ij})^{2\alpha} \right] \right)^{\frac{1}{2\alpha}} \sqrt{\log(n)} \right).$$

The following high-probability bound on the spectral norm of a random matrix is based on Remark 3.13 in [4]. This remark provides a bound up to an unspecified absolute constant. In order to make this constant explicit, we follow the lines of the proof of this remark, and we combine Theorem 6.10 in [8], Proposition 1, and a symetrization argument (see, e.g., Corollary 3.3 in [4]) to obtain the following proposition.

Proposition 2. *Let $\boldsymbol{X}$ be an $n \times n$ symmetric matrix with $\boldsymbol{X}_{ij} = \xi_{ij} b_{ij}$, where $\{\xi_{ij}\}_{i \leq j}$ are independent centered random variables with unit variance, and $\{b_{ij}\}_{i \leq j}$ are fixed scalars. Then for every $t \geq 0$ and every $\alpha \geq 3$,*

$$\mathbb{P}\left(\|\boldsymbol{X}\|_{op} \geq 2e^{\frac{2}{3}} \left(2\sigma + 14\alpha \max_{ij} \left(\mathbb{E}\left[(\xi_{ij} b_{ij})^{2\alpha} \right] \right)^{\frac{1}{2\alpha}} \sqrt{\log(n)} \right) + t \right) \leq e^{-t^2 / 2\tilde{\sigma^*}^2}$$

where we have defined $\tilde{\sigma^*} \triangleq \max_{ij} |\boldsymbol{X}_{ij}|$ *and* $\sigma \triangleq \max_i \sqrt{\sum_j b_{ij}^2}$.

Proof. To prove the desired high-probability bound, we first bound the expectation of the spectral norm, using the same symmetrization trick as in Corollary 3.3 in [4]. Let $\boldsymbol{X}^{'}$ be an independent copy of the random matrix $\boldsymbol{X}$, and let $\boldsymbol{Y}$ be the symmetric matrix with random entries defined as $\boldsymbol{Y}_{ij} \triangleq \boldsymbol{X}_{ij} - \boldsymbol{X}^{'}_{ij}$ for any $(i,j) \in [n] \times [n]$. Note that, for any $(i,j) \in [n] \times [n]$, $i < j$, $\boldsymbol{Y}_{ij} = \sqrt{2} b_{ij} \times \left(\xi_{ij} - \xi^{'}_{ij}\right)/\sqrt{2}$, where $\boldsymbol{\xi}_{ij}$ are independent copies of ξ_{ij}, and $\left(\xi_{ij} - \xi^{'}_{ij}\right)/\sqrt{2}$ are symmetric random variable with unit variance. Applying Proposition 1, we find that

$$\mathbb{E}\left[\|\boldsymbol{Y}\|_{op}\right] \leq e^{\frac{2}{3}} \left(2\sigma_Y + 14\alpha \max_{ij} \left(\mathbb{E}\left[\left(\left(\xi_{ij} - \xi^{'}_{ij}\right) b_{ij}\right)^{2\alpha}\right]\right)^{\frac{1}{2\alpha}} \sqrt{\log(n)}\right)$$

with $\sigma_Y \triangleq \max_i \sqrt{\sum_j 2 b_{ij}^2} = \sqrt{2}\sigma$. Moreover for any $(i,j) \in [n] \times [n]$, $\left(\mathbb{E}\left[\left(\left(\xi_{ij} - \xi^{'}_{ij}\right) b_{ij}\right)^{2\alpha}\right]\right)^{\frac{1}{2\alpha}} \leq 2\left(\mathbb{E}\left[\left(\xi_{ij} b_{ij}\right)^{2\alpha}\right]\right)^{\frac{1}{2\alpha}}$. Recall that $\boldsymbol{X}$ is centered. Then, by Jensen inequality, $\mathbb{E}\left[\|\boldsymbol{X}\|_{op}\right] = \mathbb{E}\left[\|\boldsymbol{X} - \mathbb{E}[\boldsymbol{X}]\|_{op}\right] \leq \mathbb{E}\left[\left\|\boldsymbol{X} - \boldsymbol{X}^{'}\right\|_{op}\right] = \mathbb{E}\left[\|\boldsymbol{Y}\|_{op}\right]$. Hence,

$$\mathbb{E}\left[\|\boldsymbol{X}\|_{op}\right] \leq 2e^{\frac{2}{3}} \left(2\sigma + 14\alpha \max_{ij} \left(\mathbb{E}\left[\left(\xi_{ij} b_{ij}\right)^{2\alpha}\right]\right)^{\frac{1}{2\alpha}} \sqrt{\log(n)}\right). \tag{20}$$

Then, we use Talagrand's concentration inequality (see [8], Theorem 6.10) and find that for any $t > 0$,

$$\mathbb{P}\left[\|\boldsymbol{X}\|_{op} \geq \mathbb{E}\|\boldsymbol{X}\|_{op} + t\right] \leq e^{\frac{-t^2}{2\tilde{\sigma^*}}} \tag{21}$$

Combining equations (20) and (21) yields the desired result. □

A.2 Mixed coordinate gradient descent algorithm

Below, we describe the details of our algorithm. At iteration $t = 0$, we initialize the parameters $(\boldsymbol{S}^{(0)}, \boldsymbol{L}^{(0)}, R^{(0)})$; then, at iteration $t \geq 1$, we start by updating $\boldsymbol{S}$. Denote by $\boldsymbol{G}_S^{(t-1)} = -2\Omega \odot (\boldsymbol{A} - \boldsymbol{L}^{(t-1)} - \boldsymbol{S}^{(t-1)} - (\boldsymbol{S}^{(t-1)})^\top) + \epsilon \boldsymbol{S}^{(t-1)}$ the gradient with respect to $\boldsymbol{S}$ of the quadratic part of the objective function, evaluated at $(\boldsymbol{S}^{(t-1)}, \boldsymbol{L}^{(t-1)})$. The column-wise sparse component $\boldsymbol{S}$ is updated with a proximal gradient step:

$$\begin{aligned} \boldsymbol{S}^{(t)} &\in \operatorname{argmin} \left(\eta\lambda_2 \|\boldsymbol{S}\|_{2,1} + \tfrac{1}{2}\left\|\boldsymbol{S} - \boldsymbol{S}^{(t-1)} + \eta \boldsymbol{G}_S^{(t-1)}\right\|_F^2\right), \\ &= \mathsf{Tc}_{\eta\lambda_2}\left(\boldsymbol{S}^{(t-1)} - \eta \boldsymbol{G}_S^{(t-1)}\right), \end{aligned} \tag{22}$$

where $\mathsf{Tc}_{\eta\lambda_2}$ is the column-wise soft-thresholding operator such that for any $\mathbf{M} \in \mathbb{R}^{n \times n}$ and for any $\lambda > 0$, the j-th column of $\mathsf{Tc}_\lambda(\mathbf{M})$ is given by $(1 - \lambda/\|\mathbf{M}_{.,j}\|_2)_+ \mathbf{M}_{.,j}$. The step size η is constant and fixed in advance, and satisfies $\eta \leq 1/(2+\epsilon)$. Then, we compute the adaptive upper bound $\bar{R}^{(t)}$ as follows:

$$\bar{R}^{(t)} = \lambda_1^{-1} \Phi_\epsilon(\boldsymbol{S}^{(t)}, \boldsymbol{L}^{(t-1)}, R^{(t-1)}). \tag{23}$$

Note that, by definition:

$$\begin{aligned} \Phi_\epsilon(\boldsymbol{S}^{(t-1)}, \boldsymbol{L}^{(t-1)}, R^{(t-1)}) &\geq \Phi_\epsilon(\hat{\boldsymbol{S}}_\epsilon, \hat{\boldsymbol{L}}_\epsilon, \hat{R}) \\ &= \frac{1}{2}\|\Omega \odot (\boldsymbol{A} - \hat{\boldsymbol{L}}_\epsilon - \hat{\boldsymbol{S}}_\epsilon - (\hat{\boldsymbol{S}}_\epsilon)^\top)\|_F^2 + \lambda_1 \|\hat{\boldsymbol{L}}_\epsilon\|_* + \lambda_2 \|\hat{\boldsymbol{S}}_\epsilon\|_{2,1} \\ &\quad + \frac{\epsilon}{2}(\|\hat{\boldsymbol{L}}_\epsilon\|_F^2 + \|\hat{\boldsymbol{S}}_\epsilon\|_F^2) \\ &\geq \lambda_1 \|\hat{\boldsymbol{L}}_\epsilon\|_*, \end{aligned}$$

since every term in the objective function is non-negative. As a result, we obtain that

$$\|\hat{\boldsymbol{L}}_\epsilon\|_* \leq \lambda_1^{-1}\Phi_\epsilon(\boldsymbol{S}^{(t-1)}, \boldsymbol{L}^{(t-1)}, R^{(t-1)}),$$

and we get the upper bound (23). Finally, the low-rank component given by $(\boldsymbol{L}, R)$ is updated using a conjugate gradient step as follows:

$$\left(\boldsymbol{L}^{(t)}, R^{(t)}\right) = \left(\boldsymbol{L}^{(t-1)}, R^{(t-1)}\right) + \beta_t \left(\tilde{\boldsymbol{L}}^{(t)} - \boldsymbol{L}^{(t-1)}, \tilde{R}^{(t)} - R^{(t-1)}\right), \tag{24}$$

where $\beta_t \in [0,1]$ is a step size defined later on. Denote by $\boldsymbol{G}_L^{(t-1)} = -\Omega \odot (\boldsymbol{A} - \boldsymbol{L}^{(t-1)} - \boldsymbol{S}^{(t)} - (\boldsymbol{S}^{(t)})^\top) + \epsilon \boldsymbol{L}^{(t-1)}$ the gradient with respect to $\boldsymbol{L}$ of the quadratic part of the objective function, evaluated at $(\boldsymbol{S}^{(t)}, \boldsymbol{L}^{(t-1)})$. The direction $(\tilde{\boldsymbol{L}}^{(t)}, \tilde{R}^{(t)})$ is defined by:

$$\begin{array}{rl} \left(\tilde{\boldsymbol{L}}^{(t)}, \tilde{R}^{(t)}\right) \in & \operatorname{argmin}_{\mathbf{Z},R} \quad \langle \mathbf{Z}, \boldsymbol{G}_L^{(t-1)} \rangle + \lambda_1 R \\ & \text{such that} \quad \|\mathbf{Z}\|_* \leq R \leq \bar{R}^{(t)}. \end{array} \tag{25}$$

Let σ_1 be the largest singular value of the gradient matrix $\boldsymbol{G}_L^{(t-1)}$, and let u_1 and v_1 be the corresponding left and right singular vectors. Then, (25) admits the following closed-form solution:

$$\left(\tilde{\boldsymbol{L}}^{(t)}, \tilde{R}^{(t)}\right) = \begin{cases} (\mathbf{0}, 0) & \text{if } \lambda_1 \geq \sigma_1 \\ (-\bar{R}^{(t)} u_1 v_1^\top, \bar{R}^{(t)}) & \text{if } \lambda_1 < \sigma_1. \end{cases} \tag{26}$$

The step size β_t is set to:

$$\beta_t = \min\left\{1, \frac{\langle \boldsymbol{L}^{(t-1)} - \tilde{\boldsymbol{L}}^{(t)}, \boldsymbol{G}_L^{(t-1)} \rangle + \lambda_1 (R^{(t-1)} - \tilde{R}^{(t)})}{(1+\epsilon)\|\tilde{\boldsymbol{L}}^{(t)} - \boldsymbol{L}^{(t-1)}\|_F^2}\right\}. \tag{27}$$

We show in appendix A.3 that this choice of step size ensures that the objective function decreases at every iteration. The above steps are repeated iteratively until convergence, or for a predefined number of iterations. In practice, we stop the algorithm when the relative decrease of the objective falls below a predefined threshold (e.g., 10e-6).

A.3 Proof of Theorem 1

To prove Theorem 1, we proceed in three steps. First, we demonstrate that the objective function decreases after every update of $\boldsymbol{S}$ or $\boldsymbol{L}$. In a second step, we compute a lower bound on the amount by which the objective function decreases at each iteration. In a third step, we use this lower bound to demonstrate that the distance to the optimal solution at iteration $t \geq 1$, $\Delta^t = \Phi_\epsilon(\boldsymbol{S}^{(t)}, \boldsymbol{L}^{(t-1)}, R^{(t-1)}) - \Phi_\epsilon(\hat{\boldsymbol{S}}, \hat{\boldsymbol{L}}, \hat{R})$, decreases at a rate of the order of $1/t$.

Decrease of the objective between successive iterations: We start by showing that the proximal update for the $\mathbf{S}$ block yields a decrease of the objective. For $t \geq 1$, denote $Q^{(t-1)} = \lambda_2^{-1}\Phi_\epsilon(\mathbf{S}^{(t-1)}, \boldsymbol{L}^{(t-1)}, R^{(t-1)})$, and

$$g_S(\mathbf{S}^{(t-1)}, \boldsymbol{L}^{(t-1)}) = \langle \boldsymbol{G}_S(\boldsymbol{S}^{(t-1)}, \boldsymbol{L}^{(t-1)}), \mathbf{S}^{(t-1)} - \tilde{\mathbf{S}}^{(t-1)} \rangle + \lambda_2(\|\mathbf{S}^{(t-1)}\|_{2,1} - \|\tilde{\mathbf{S}}^{(t-1)}\|_{2,1}). \tag{28}$$

In (28), $\boldsymbol{G}_S(\boldsymbol{S}^{(t-1)}, \boldsymbol{L}^{(t-1)}) = -2\Omega \odot (\boldsymbol{A} - \boldsymbol{L}^{(t-1)} - \mathbf{S}^{(t-1)} - (\mathbf{S}^{(t-1)})^\top) + \epsilon \mathbf{S}^{(t-1)}$ is the gradient matrix with respect to $\mathbf{S}$ of the quadratic part of the objective function, evaluated at $(\mathbf{S}^{(t-1)}, \boldsymbol{L}^{(t-1)})$, and

$$\tilde{\mathbf{S}}^{(t-1)} = \arg\min_{\mathbf{S}} \quad \langle \boldsymbol{G}_S(\boldsymbol{S}^{(t-1)}, \boldsymbol{L}^{(t-1)}), \mathbf{S} \rangle + \lambda_2 \|\mathbf{S}\|_{2,1} \quad \text{s.t. } \|\mathbf{S}\|_{2,1} \leq Q^{(t-1)}.$$

Lemma 3. *For $t \geq 1$, the proximal update for the $\mathbf{S}$ block defined in (22) satisfies:*

$$\Phi_\epsilon(\mathbf{S}^{(t)}, \boldsymbol{L}^{(t-1)}, R^{(t-1)}) \leq \Phi_\epsilon(\mathbf{S}^{(t-1)}, \boldsymbol{L}^{(t-1)}, R^{(t-1)}) - \frac{\eta}{2} \frac{g_S^2(\mathbf{S}^{(t-1)}, \boldsymbol{L}^{(t-1)})^2}{(2Q^{(t-1)})}.$$

Proof. See Section A.8.3. □

We now prove a similar result, this time concerning the $(\boldsymbol{L}, R)$ block update. Recall that, for $t \geq 1$, $\bar{R}^{(t)} = \lambda_1^{-1}\Phi_\epsilon(\mathbf{S}^{(t)}, \boldsymbol{L}^{(t-1)}, R^{(t-1)})$.

$$g_L(\mathbf{S}^{(t)}, \boldsymbol{L}^{(t-1)}, R^{(t-1)}) = \langle \boldsymbol{G}_L(\boldsymbol{S}^{(t)}, \boldsymbol{L}^{(t-1)}), \boldsymbol{L}^{(t-1)} - \tilde{\boldsymbol{L}}^{(t-1)} \rangle + \lambda_1(R^{(t-1)} - \tilde{R}^{(t-1)}). \tag{29}$$

In (29), $\boldsymbol{G}_L(\boldsymbol{S}^{(t)}, \boldsymbol{L}^{(t-1)}) = -\Omega \odot (\boldsymbol{A} - \boldsymbol{L}^{(t-1)} - \mathbf{S}^{(t)} - (\mathbf{S}^{(t)})^\top) + \epsilon \boldsymbol{L}^{(t-1)}$ is the gradient matrix with respect to $\boldsymbol{L}$ of the quadratic part of the objective function, evaluated at $(\mathbf{S}^{(t)}, \boldsymbol{L}^{(t-1)})$. Recall that $M^{(t)} = \|\boldsymbol{G}_L(\boldsymbol{S}^{(t)}, \boldsymbol{L}^{(t-1)})\|_F$. We prove the following result, which ensures a decrease of the objective function after the conditional gradient update.

Lemma 4. *For $t \geq 1$, the conditional gradient update for the $(\boldsymbol{L}, R)$ block defined in (26) satisfies:*

$$\Phi_\epsilon(\mathbf{S}^{(t)}, \boldsymbol{L}^{(t)}, R^{(t)}) - \Phi_\epsilon(\mathbf{S}^{(t)}, \boldsymbol{L}^{(t-1)}, R^{(t-1)}) \leq -\frac{g_L^2(\mathbf{S}^{(t)}, \boldsymbol{L}^{(t-1)}, R^{(t-1)})}{\max\{2\bar{R}^{(t)}(\lambda_1 + M^{(t)}), 8(1+\epsilon)(\bar{R}^{(t)})^2\}}.$$

Moreover,

$$\Phi_\epsilon(\mathbf{S}^{(t)}, \boldsymbol{L}^{(t)}, R^{(t)}) - \Phi_\epsilon(\mathbf{S}^{(t)}, \boldsymbol{L}^{(t-1)}, R^{(t-1)}) \leq -\frac{(1+\epsilon)}{2}\|\boldsymbol{L}^{(t)} - \boldsymbol{L}^{(t-1)}\|_F^2. \tag{30}$$

Proof. See Section A.8.4. □

Lower bound on the decrement $\Phi_\epsilon(\boldsymbol{S}^{(t)}, \boldsymbol{L}^{(t-1)}, R^{(t-1)}) - \Phi_\epsilon(\boldsymbol{S}^{(t+1)}, \boldsymbol{L}^{(t)}, R^{(t)})$: Consider the function

$$g^t(Q^{(t)}, \bar{R}^{(t)}) \triangleq g_S(\boldsymbol{S}^{(t)}, \boldsymbol{L}^{(t-1)}) + g_L(\boldsymbol{S}^{(t)}, \boldsymbol{L}^{(t-1)}, \bar{R}^{(t-1)}).$$

In what follows, we compute upper and lower bounds on $g^t(Q^{(t)}, \bar{R}^{(t)})$. Note that $g^t(Q^{(t)}, \bar{R}^{(t)})$ depends on $(Q^{(t)}, \bar{R}^{(t)})$, because computing g_S and g_L involve solving constrained optimization problems, which depend on $Q^{(t)}$ and $\bar{R}^{(t)}$, respectively. By convexity of the quadratic term $\|\Omega \odot (\boldsymbol{A} - \boldsymbol{L} - \boldsymbol{S} - \boldsymbol{S}^\top)\|_F^2/2 + \epsilon/2(\|\boldsymbol{L}\|_F^2 + \|\boldsymbol{S}\|_F^2)$, we obtain that:

$$g^t(Q^{(t)}, \bar{R}^{(t)}) \geq \Phi_\epsilon(\boldsymbol{S}^{(t)}, \boldsymbol{L}^{(t-1)}, R^{(t-1)}) - \Phi_\epsilon(\tilde{\boldsymbol{S}}^{(t)}, \tilde{\boldsymbol{L}}^{(t-1)}, \tilde{R}^{(t-1)}).$$

Then, by definition of the minimizer $(\hat{\boldsymbol{S}}_\epsilon, \hat{\boldsymbol{L}}_\epsilon, \hat{R})$:

$$g^t(Q^{(t)}, \bar{R}^{(t)}) \geq \Phi_\epsilon(\boldsymbol{S}^{(t)}, \boldsymbol{L}^{(t-1)}, R^{(t-1)}) - \Phi_\epsilon(\hat{\boldsymbol{S}}_\epsilon, \hat{\boldsymbol{L}}_\epsilon, \hat{R}), \tag{31}$$

which gives the lower bound on $g^t(Q^{(t)}, \bar{R}^{(t)})$.

Let us now compute an upper bound for $g^t(Q^{(t)}, \bar{R}^{(t)})$. To do so, we start by upper bounding $g_S(\boldsymbol{S}^{(t)}, \boldsymbol{L}^{(t-1)})$ defined in (28). By definition,

$$\begin{aligned}
g_S(\mathbf{S}^{(t-1)}, \boldsymbol{L}^{(t-1)}) &= \max_{\|\boldsymbol{S}\|_{2,1} \leq Q^{(t)}} \{\langle \boldsymbol{G}_S(\boldsymbol{S}^{(t)}, \boldsymbol{L}^{(t-1)}), \boldsymbol{S}^{(t)} - \boldsymbol{S} \rangle + \lambda_2(\|\mathbf{S}^{(t)}\|_{2,1} - \|\boldsymbol{S}\|_{2,1})\} \\
&= \max_{\|\boldsymbol{S}\|_{2,1} \leq Q^{(t)}} \{\langle \boldsymbol{G}_S(\boldsymbol{S}^{(t)}, \boldsymbol{L}^{(t)}), \boldsymbol{S}^{(t)} - \boldsymbol{S} \rangle \\
&\quad + \langle \boldsymbol{G}_S(\boldsymbol{S}^{(t)}, \boldsymbol{L}^{(t-1)}) - \boldsymbol{G}_S(\boldsymbol{S}^{(t)}, \boldsymbol{L}^{(t)}), \boldsymbol{S}^{(t)} - \boldsymbol{S} \rangle + \lambda_2(\|\mathbf{S}^{(t)}\|_{2,1} - \|\boldsymbol{S}\|_{2,1})\} \\
&\leq \max_{\|\boldsymbol{S}\|_{2,1} \leq Q^{(t)}} \Big\{ \langle \boldsymbol{G}_S(\boldsymbol{S}^{(t)}, \boldsymbol{L}^{(t)}), \boldsymbol{S}^{(t)} - \boldsymbol{S} \rangle + \lambda_2(\|\mathbf{S}^{(t)}\|_{2,1} - \|\boldsymbol{S}\|_{2,1}) \\
&\quad + \|\boldsymbol{G}_S(\boldsymbol{S}^{(t)}, \boldsymbol{L}^{(t-1)}) - \boldsymbol{G}_S(\boldsymbol{S}^{(t)}, \boldsymbol{L}^{(t)})\|_F \|\boldsymbol{S}^{(t)} - \boldsymbol{S}\|_F \Big\}. \\
&\leq \underbrace{\langle \boldsymbol{G}_S(\boldsymbol{S}^{(t)}, \boldsymbol{L}^{(t)}), \boldsymbol{S}^{(t)} \rangle + \lambda_2 \|\mathbf{S}^{(t)}\|_{2,1} - \min_{\|\boldsymbol{S}\|_{2,1} \leq Q^{(t)}} \Big\{ \langle \boldsymbol{G}_S(\boldsymbol{S}^{(t)}, \boldsymbol{L}^{(t)}), \boldsymbol{S} \rangle + \lambda_2 \|\boldsymbol{S}\|_{2,1} \Big\}}_{I} \\
&\quad + \underbrace{\max_{\|\boldsymbol{S}\|_{2,1} \leq Q^{(t)}} \Big\{ \|\boldsymbol{G}_S(\boldsymbol{S}^{(t)}, \boldsymbol{L}^{(t-1)}) - \boldsymbol{G}_S(\boldsymbol{S}^{(t)}, \boldsymbol{L}^{(t)})\|_F \|\boldsymbol{S}^{(t)} - \boldsymbol{S}\|_F \Big\}}_{II}
\end{aligned}$$

On the one hand, by definition of $\tilde{\boldsymbol{S}}^{(t)}$ and $g_S(\boldsymbol{S}^{(t)}, \boldsymbol{L}^{(t)})$ (see (28) and (A.3)), we have:

$$I \leq g_S(\boldsymbol{S}^{(t)}, \boldsymbol{L}^{(t)}). \tag{32}$$

On the other hand, by definition of $Q^{(t)}$, $\|\boldsymbol{S}^{(t)}\|_{2,1} \leq Q^{(t)}$, which implies $\|\boldsymbol{S}^{(t)}\|_F \leq Q^{(t)}$; combined with $\|\boldsymbol{S}\|_F \leq Q^{(t)}$, we obtain that that $\|\boldsymbol{S}^{(t)} - \boldsymbol{S}\|_F \leq 2Q^{(t)}$. Note also that, as the gradient G_S is $(1+\epsilon)$-Lipschitz, we have $\|\boldsymbol{G}_S(\boldsymbol{S}^{(t)}, \boldsymbol{L}^{(t-1)}) - \boldsymbol{G}_S(\boldsymbol{S}^{(t)}, \boldsymbol{L}^{(t)})\|_F \leq (1+\epsilon)\|\boldsymbol{L}^{(t-1)} - \boldsymbol{L}^{(t)}\|_F$. Finally we obtain:

$$II \leq 2Q^{(t)}(1+\epsilon)\|\boldsymbol{L}^{(t-1)} - \boldsymbol{L}^{(t)}\|_F. \tag{33}$$

Combining (32) and (33), we finally obtain:

$$g_S(\mathbf{S}^{(t-1)}, \boldsymbol{L}^{(t-1)}) \leq g_S(\boldsymbol{S}^{(t)}, \boldsymbol{L}^{(t)}) + 2Q^{(t)}(1+\epsilon)\|\boldsymbol{L}^{(t-1)} - \boldsymbol{L}^{(t)}\|_F. \tag{34}$$

We now use (34) to derive our upper bound on $g^t(Q^{(t)}, \bar{R}^{(t)})$ as follows. Using Lemma 3 and Lemma 4, we obtain that:

$$\begin{aligned}
(g^{(t)}(Q^{(t)}, \bar{R}^{(t)}))^2 &\leq 2\Big\{g_L^2(\boldsymbol{S}^{(t)}, \boldsymbol{L}^{(t-1)}, R^{(t-1)}) + g_S^2(\boldsymbol{S}^{(t)}, \boldsymbol{L}^{(t)}) + 4(Q^{(t)})^2(1+\epsilon)^2\|\boldsymbol{L}^{(t-1)} - \boldsymbol{L}^{(t)}\|_F^2\Big\} \\
&\leq 2\Big\{(C_1^{(t)} + C_3^{(t)})(\Phi_\epsilon(\boldsymbol{S}^{(t)}, \boldsymbol{L}^{(t-1)}, R^{(t-1)}) - \Phi_\epsilon(\boldsymbol{S}^{(t)}, \boldsymbol{L}^{(t)}, R^{(t)})) \\
&\quad + C_2^{(t)}(\Phi_\epsilon(\boldsymbol{S}^{(t)}, \boldsymbol{L}^{(t)}, R^{(t)}) - \Phi_\epsilon(\boldsymbol{S}^{(t+1)}, \boldsymbol{L}^{(t)}, R^{(t)}))\Big\},
\end{aligned}$$

where

$$C_1^{(t)} = \max\{2\bar{R}^{(t)}(\lambda_1 + M^{(t)}), 8(1+\epsilon)(\bar{R}^{(t)})^2\}, \quad C_2^{(t)} = \frac{8(Q^{(t)})^2}{\eta}, \quad C_3^{(t)} = 8(1+\epsilon)(Q^{(t)})^2.$$

Define:

$$C^{(t)} = 2\max\{C_1^{(t)} + C_3^{(t)}, C_2^{(t)}\}. \tag{35}$$

We finally have the following lower bound:

$$(g^{(t)}(Q^{(t)}, \bar{R}^{(t)}))^2 \leq C^{(t)}(\Phi_\epsilon(\boldsymbol{S}^{(t)}, \boldsymbol{L}^{(t-1)}, R^{(t-1)}) - \Phi_\epsilon(\boldsymbol{S}^{(t+1)}, \boldsymbol{L}^{(t)}, R^{(t)})).$$

Convergence rate of order $1/t$: Recall that $\Delta^t := \Phi_\epsilon(\boldsymbol{S}^{(t)}, \boldsymbol{L}^{(t-1)}, R^{(t-1)}) - \Phi_\epsilon(\hat{\boldsymbol{S}}_\epsilon, \hat{\boldsymbol{L}}_\epsilon, \hat{R})$. Using the fact that

$$(g^{(t)}(Q^{(t)}, \bar{R}^{(t)}))^2 \geq (\Delta^t)^2,$$

proven in (31), we obtain that

$$\Delta^{t+1} \leq \Delta^t - \frac{1}{C^{(t)}}(\Delta^t)^2.$$

We use the following Lemma (see, e.g. [5, Lemma 3.5], [42, Lemma 8]).

Lemma 5. *Let $\{A_k\}_{k\geq 1}$ be a non-negative sequence satisfying:*

$$A_{k+1} \leq A_k - \gamma_k A_k^2, k \geq 1,$$

where $\gamma_k > 0$ for any $k \geq 1$. Then,

$$A_{k+1} \leq \frac{1}{\frac{1}{A_1} + \sum_{i=1}^k \gamma_i}.$$

Proof. See Section A.9 □

Lemma 5 yields that:

$$\Delta^{t+1} \leq \frac{1}{(\Delta^1)^{-1} + \sum_{i=1}^t \frac{1}{C^{(i)}}}.$$

noting that $\Delta^1 \leq \tilde{\Delta}^0 := \Phi_\epsilon(\boldsymbol{S}^{(0)}, \boldsymbol{L}^{(0)}, R^{(0)}) - \Phi_\epsilon(\hat{\boldsymbol{S}}_\epsilon, \hat{\boldsymbol{L}}, \hat{R})$, we have:

$$\Delta^{t+1} \leq \frac{1}{(\tilde{\Delta}^0)^{-1} + \sum_{i=1}^t \frac{1}{C^{(i)}}}. \tag{36}$$

Let us derive an upper bound on the time-varying constants $C^{(t)}$ defined in (35). We only need to bound $\bar{R}^{(t)}$, $M^{(t)}$ and $Q^{(t)}$. First note that, by Lemmas 3 and 4, $\bar{R}^{(t)} \leq \lambda_1^{-1}\Phi_\epsilon(\boldsymbol{S}^{(0)}, \boldsymbol{L}^{(0)}, R^{(0)})$, and $Q^{(t)} \leq \lambda_2^{-1}\Phi_\epsilon(\boldsymbol{S}^{(0)}, \boldsymbol{L}^{(0)}, R^{(0)})$. To bound $M^{(t)} = \|\boldsymbol{G}_L(\boldsymbol{S}^{(t)}, \boldsymbol{L}^{(t-1)})\|_F$, we start by noticing that the gradient $\boldsymbol{G}_L(\boldsymbol{S}^{(t)}, \boldsymbol{L}^{t-1})$ of the quadratic part of the objective with respect to $\boldsymbol{L}$ is bounded whenever $\boldsymbol{S}^{(t)}$ and $\boldsymbol{L}^{(t-1)}$ are bounded themselves. Since $\lambda_1\|\boldsymbol{L}^{(t-1)}\|_* + \lambda_2\|\boldsymbol{S}^{(t)}\|_{2,1} \leq \Phi_\epsilon(\boldsymbol{S}^{(t)}, \boldsymbol{L}^{(t-1)}, R^{(t-1)}) \leq \Phi_\epsilon(\boldsymbol{S}^{(0)}, \boldsymbol{L}^{(0)}, R^{(0)})$, the parameters $\boldsymbol{S}$ and $\boldsymbol{L}$ are indeed bounded, and we obtain that there exists $\bar{M} \geq 0$ such that $M^{(t)} \leq \bar{M}$ for any t. Define $\mathcal{F}_0 \triangleq \Phi_\epsilon(\boldsymbol{S}^{(0)}, \boldsymbol{L}^{(0)}, R^{(0)})$,

$$\bar{C}_1 = \max\{8\lambda_1^{-1}(1+\epsilon)\mathcal{F}_0^2, 2\lambda_1^{-1}\mathcal{F}_0(\lambda_1 + \bar{M})\}, \quad \bar{C}_2 = \frac{8\mathcal{F}_0^2}{\eta\lambda_2^2}, \quad \bar{C}_3 = 8\lambda_2^{-1}(1+\epsilon)\mathcal{F}_0^2,$$

and

$$\bar{C} \triangleq \max\left\{\bar{C}_1 + \bar{C}_3, \bar{C}_2\right\}.$$

Then, we obtain the following rate of convergence:

$$\Delta^{t+1} \leq \frac{1}{(\tilde{\Delta}^0)^{-1} + \sum_{i=1}^t \frac{1}{C^{(i)}}} \leq \frac{1}{(\tilde{\Delta}^0)^{-1} + t\bar{C}}. \tag{37}$$

Recall that $\Phi_\epsilon(\hat{\boldsymbol{S}}_\epsilon, \hat{\boldsymbol{L}}_\epsilon, \hat{R}) = \mathcal{F}(\hat{\boldsymbol{S}}_\epsilon, \hat{\boldsymbol{L}}_\epsilon)$ by equivalence of the two optimization problems (4) and (5). In addition, by definition, $\|L^{(t-1)}\|_* \leq R^{(t-1)}$, which gives $\mathcal{F}_\epsilon(\boldsymbol{S}^{(t)}, \boldsymbol{L}^{(t-1)}) \leq \Phi_\epsilon(\boldsymbol{S}^{(t)}, \boldsymbol{L}^{(t-1)}, R^{(t-1)})$. Thus, we obtain that $\mathcal{F}_\epsilon(\boldsymbol{S}^{(t)}, \boldsymbol{L}^{(t-1)}) - \mathcal{F}_\epsilon(\hat{\boldsymbol{S}}_\epsilon, \hat{\boldsymbol{L}}_\epsilon) \leq \Phi_\epsilon(\boldsymbol{S}^{(t)}, \boldsymbol{L}^{(t-1)}, R^{(t-1)}) - \Phi_\epsilon(\hat{\boldsymbol{S}}_\epsilon, \hat{\boldsymbol{L}}_\epsilon, \hat{R}) \leq \Delta^{t+1}$.
For $\delta > 0$, let T_δ be the integer number defined by:

$$T_\delta \triangleq \left\lfloor \bar{C}\left(\frac{1}{\delta} - \frac{1}{\mathcal{F}_0 - \mathcal{F}_\epsilon(\hat{\boldsymbol{S}}_\epsilon, \hat{\boldsymbol{L}}_\epsilon)}\right)\right\rfloor + 1.$$

Then, the T_δ-th iterate of the MCGD sequence satisfies:

$$\mathcal{F}_\epsilon(\boldsymbol{S}^{(T_\delta)}, \boldsymbol{L}^{(T_\delta)}) - \mathcal{F}_\epsilon(\hat{\boldsymbol{S}}_\epsilon, \hat{\boldsymbol{L}}_\epsilon) \leq \delta,$$

which proves sub-linear convergence of the MCGD iterates. Note that, by definition, $\mathcal{F}_0 - \mathcal{F}_\epsilon(\hat{\boldsymbol{S}}_\epsilon, \hat{\boldsymbol{L}}_\epsilon) \geq 0$, which implies that $T_\delta \leq \lfloor \bar{C}/\delta \rfloor + 1$. In addition, in the particular case where the initial point is set to $(\boldsymbol{S}^{(0)}, \boldsymbol{L}^{(0)}, R^{(0)}) = (\boldsymbol{0}, \boldsymbol{0}, 0)$, we can compute an upper bound on the constant $\bar{C}$, dependent on the dimensions of the problem. First, note that in this case, $\mathcal{F}_0 = \frac{1}{2}\|\Omega \odot \boldsymbol{A}\|_F^2$ is equal to the number of observed edges in the graph, denoted by E. Furthermore, by definition,

$$M^{(t)} = \|\boldsymbol{G}_L(\boldsymbol{S}^{(t)}, \boldsymbol{L}^{(t-1)})\|_F \leq \|\Omega \odot (\boldsymbol{A} - \boldsymbol{L}^{(t-1)} - \boldsymbol{S}^{(t)} - (\boldsymbol{S}^{(t)})^\top)\|_F + \|\epsilon\boldsymbol{L}^{(t-1)}\|_F.$$

Since, by Lemmas 3 and 4, the objective value decreases at every update of $\boldsymbol{L}$ and $\boldsymbol{S}$. As all the terms of the objective are positive, we have that $\|\Omega \odot (\boldsymbol{A} - \boldsymbol{L}^{(t-1)} - \boldsymbol{S}^{(t)} - (\boldsymbol{S}^{(t)})^\top)\|_F^2 \leq \mathcal{F}_0 = E$, and $\|\epsilon\boldsymbol{L}^{(t-1)}\|_F^2 \leq E$ as well. Thus, we obtain that, for any t, $M^{(t)} \leq 2\sqrt{E}$, which yields $\bar{M} \leq 2\sqrt{E}$. We then obtain that the constant $\bar{C}$ satisfies

$$\bar{C} \leq \bar{C}_0 \triangleq \max\left\{\frac{2E^2}{\eta\lambda_2^2}, 8(1+\epsilon)E^2\left(\frac{1}{\lambda_1} + \frac{1}{\lambda_2}\right) + \frac{2E^{3/2}}{\lambda_1} + 2E\right\}, \tag{38}$$

meaning that the number of iterations increases at most quadratically with the density of the graph. Note that, in practice, the convergence is much faster, and we observe that the algorithm converges after a few iterations.

A.4 Proof of Theorem 2

Recall that, by Lemma 1,

$$j \in \widehat{\mathcal{O}} \;\Leftrightarrow\; \left\| \boldsymbol{\Omega}_{\cdot,j} \odot \left(\boldsymbol{A}_{\cdot,j} - \widehat{\boldsymbol{L}}_{\cdot,j} - \widehat{\boldsymbol{S}}_{j,\cdot} \right)_+ \right\|_2 > \frac{\lambda_2}{4}.$$

In a first time, we show that with high probability, no inlier belongs to the set of estimated outliers. Consider $j \in \mathcal{I}$, then

$$\begin{aligned} \left\| \boldsymbol{\Omega}_{\cdot,j} \odot \left(\boldsymbol{A}_{\cdot,j} - \widehat{\boldsymbol{L}}_{\cdot,j} - \widehat{\boldsymbol{S}}_{j,\cdot} \right)_+ \right\|_2 &\leq \sqrt{\sum_{i \in \mathcal{I}} \left(\boldsymbol{\Omega}_{ij} \left(\boldsymbol{A}_{ij} - \widehat{\boldsymbol{L}}_{ij} - \widehat{\boldsymbol{S}}_{ji} \right)_+ \right)^2} + \sqrt{\sum_{i \in \mathcal{O}} \left(\boldsymbol{\Omega}_{ij} \left(\boldsymbol{A}_{ij} - \widehat{\boldsymbol{L}}_{ij} - \widehat{\boldsymbol{S}}_{ji} \right)_+ \right)^2} \\ &\leq \sqrt{\sum_{i \in \mathcal{I}} \left(\boldsymbol{\Omega}_{ij} \left(\boldsymbol{\Sigma}_{ij} + \Delta \boldsymbol{L}_{ij} - \widehat{\boldsymbol{S}}_{ji} \right)_+ \right)^2} + \sqrt{\sum_{i \in \mathcal{O}} \left(\boldsymbol{\Omega}_{ij} \boldsymbol{A}_{ij} \right)^2} \end{aligned}$$

where we have used that for $(i,j) \in \mathcal{I} \times \mathcal{I}$, $\boldsymbol{A}_{ij} = \boldsymbol{\Sigma}_{ij} + \boldsymbol{L}^*_{ij}$ and that $\widehat{\boldsymbol{L}}_{ij} \geq 0$ and $\widehat{\boldsymbol{S}}_{ij} \geq 0$. Therefore, we find that

$$\left\| \boldsymbol{\Omega}_{\cdot,j} \odot \left(\boldsymbol{A}_{\cdot,j} - \widehat{\boldsymbol{L}}_{\cdot,j} - \widehat{\boldsymbol{S}}_{j,\cdot} \right)_+ \right\|_2 \leq \sqrt{\sum_{i \in \mathcal{I}} \left(\boldsymbol{\Omega}_{ij} \boldsymbol{\Sigma}_{ij} \right)_+^2} + \sqrt{\sum_{i \in \mathcal{I}} \left(\boldsymbol{\Omega}_{ij} \Delta \boldsymbol{L}_{ij} \right)_+^2} + \sqrt{\sum_{i \in \mathcal{O}} \left(\boldsymbol{\Omega}_{ij} \boldsymbol{A}_{ij} \right)^2}.$$

Recalling that $\|\Delta \boldsymbol{L}\|_\infty \leq \rho_n$, we obtain

$$\max_{j \in \mathcal{I}} \left\{ \left\| \boldsymbol{\Omega}_{\cdot,j} \odot \left(\boldsymbol{A}_{\cdot,j} - \widehat{\boldsymbol{L}}_{\cdot,j} - \widehat{\boldsymbol{S}}_{j,\cdot} \right)_+ \right\|_2 \right\} \leq \left\| \boldsymbol{\Omega} \odot \boldsymbol{\Sigma}_{|I} \right\|_{2,\infty} + \rho_n \left\| \boldsymbol{\Omega}_{|I} \right\|_{2,\infty} + \left\| \boldsymbol{\Omega} \odot \boldsymbol{A}_{|\mathcal{O} \times \mathcal{I}} \right\|_{2,\infty}. \quad (39)$$

We bound $\left\| \boldsymbol{\Omega} \odot \boldsymbol{\Sigma}_{|I} \right\|_{2,\infty}$, $\rho_n \left\| \boldsymbol{\Omega}_{|I} \right\|_{2,\infty}$ and $\left\| \boldsymbol{\Omega} \odot \boldsymbol{A}_{|\mathcal{O} \times \mathcal{I}} \right\|_{2,\infty}$ using the following Lemma.

Lemma 6. *Under assumptions 1-3,*

$$\mathbb{P}\left(\left\| \boldsymbol{\Omega} \odot \boldsymbol{\Sigma}_{|I} \right\|_{2,\infty} \geq \sqrt{6 \nu_n \rho_n n} \right) \leq 2e^{-\nu_n \rho_n n} \quad (40)$$

$$\mathbb{P}\left(\left\| \boldsymbol{\Omega}_{|I} \right\|_{2,\infty} \geq 4\sqrt{\nu_n n} \right) \leq 2e^{-\nu_n n} \quad (41)$$

$$\mathbb{P}\left(\left\| \boldsymbol{\Omega} \odot \boldsymbol{A}_{|\mathcal{O} \times \mathcal{I}} \right\|_{2,\infty} \geq \sqrt{6 \nu_n \rho_n n} \right) \leq 2e^{-\nu_n \rho_n n}. \quad (42)$$

Proof. See Section A.8.5 □

Recall that $\lambda_2 = 19\sqrt{\nu_n \rho_n n}$. Combining Lemma 6, Lemma 2 and equation (39) yields that with probability larger than $1 - 6e^{-\nu_n \rho_n n}$,

$$\max_{j \in \mathcal{I}} \left\{ \left\| \boldsymbol{\Omega}_{\cdot,j} \odot \left(\boldsymbol{A}_{\cdot,j} - \widehat{\boldsymbol{L}}_{\cdot,j} - \widehat{\boldsymbol{S}}_{j,\cdot} \right)_+ \right\|_2 \right\} \leq 9\sqrt{\nu_n \rho_n n} < \frac{\lambda_2}{2}.$$

Using Lemma 1, we conclude that with probability at least $1 - 6e^{-\nu_n \rho_n n}$, $\widehat{\mathcal{O}} \cap \mathcal{I} = \emptyset$.

A.5 Proof of Theorem 3

Here, we prove that with high probability, all outliers are detected when $\min_{j \in \mathcal{O}} \sum_{i \in \mathcal{I}} \boldsymbol{\Pi}_{ij} \boldsymbol{S}^*_{ij} > C \rho_n \nu_n n$ for some absolute constant $C > 0$. For any $j \in [n]$, note that

$$\left\| \boldsymbol{\Omega}_{\cdot,j} \odot \left(\boldsymbol{A}_{\cdot,j} - \widehat{\boldsymbol{L}}_{\cdot,j} - \widehat{\boldsymbol{S}}_{j,\cdot} \right)_+ \right\|_2 \geq \sqrt{\sum_{i \in \mathcal{I}} \left(\boldsymbol{\Omega}_{ij} \left(\boldsymbol{A}_{ij} - \widehat{\boldsymbol{L}}_{ij} - \widehat{\boldsymbol{S}}_{ji} \right)_+ \right)^2}.$$

We have shown in Theorem 2 that with probability at least $1-6e^{-\nu_n\rho_n n}$, $\widehat{\boldsymbol{S}}_{ji}=0$ for any $i\in\mathcal{I}$ and any $j\in[n]$. When this equation holds, using the bound $\left\|\widehat{\boldsymbol{L}}\right\|_\infty \leq \rho_n$, we find that

$$\left\|\boldsymbol{\Omega}_{\cdot,j}\odot\left(\boldsymbol{A}_{\cdot,j}-\widehat{\boldsymbol{L}}_{\cdot,j}-\widehat{\boldsymbol{S}}_{j,\cdot}\right)_+\right\|_2 \quad\geq\quad \sqrt{\sum_{i\in\mathcal{I}}\left(\boldsymbol{\Omega}_{ij}\left(\boldsymbol{A}_{ij}-\rho_n\right)_+\right)^2}. \tag{43}$$

We use the following Lemma to obtain a lower bound on the right hand side of equation (43) when $j\in\mathcal{O}$.

Lemma 7. *Assume that* $\min_{j\in\mathcal{O}}\sum_{i\in\mathcal{I}}\boldsymbol{\Pi}_{ij}\boldsymbol{S}^*_{ij}\geq\nu_n\rho_n n$, *then*

$$\mathbb{P}\left(\min_{j\in\mathcal{O}}\sqrt{\sum_{i\in\mathcal{I}}\left(\boldsymbol{\Omega}_{ij}\left(\boldsymbol{A}_{ij}-\rho_n\right)_+\right)^2}\leq\frac{1}{4}\min_{j\in\mathcal{O}}\sqrt{\sum_{i\in\mathcal{I}}\boldsymbol{\Pi}_{ij}\boldsymbol{S}^*_{ij}}\right)\leq 2se^{-\frac{-\nu_n\rho_n n}{80}}.$$

Proof. See Section A.8.6. □

Combining this Lemma with equation (43), we see that with probability at least $1-2se^{-\frac{-\nu_n\rho_n n}{80}}-6e^{-\nu_n\rho_n n}$,

$$\left\|\boldsymbol{\Omega}_{\cdot,j}\odot\left(\boldsymbol{A}_{\cdot,j}-\widehat{\boldsymbol{L}}_{\cdot,j}-\widehat{\boldsymbol{S}}_{j,\cdot}\right)_+\right\|_2 \quad\geq\quad \frac{1}{4}\min_{j\in\mathcal{O}}\sqrt{\sum_{i\in\mathcal{I}}\boldsymbol{\Pi}_{ij}\boldsymbol{S}^*_{ij}}. \tag{44}$$

Recall that $\lambda_2=19\sqrt{\nu_n\rho_n n}$. When $\min_{j\in\mathcal{O}}\sum_{i\in\mathcal{I}}\boldsymbol{\Pi}_{ij}\boldsymbol{S}^*_{ij}>8\times 19\nu_n\rho_n n$, Lemma 7 and equation (44) imply that with probability larger than $1-2se^{-\frac{-\nu_n\rho_n n}{80}}-6e^{-\nu_n\rho_n n}$,

$$\left\|\boldsymbol{\Omega}_{\cdot,j}\odot\left(\boldsymbol{A}_{\cdot,j}-\widehat{\boldsymbol{L}}_{\cdot,j}-\widehat{\boldsymbol{S}}_{j,\cdot}\right)_+\right\|_2>\frac{\lambda_2}{2}.$$

Combining this result with Lemma 1, we find that with probability at least $1-2se^{-\frac{-\nu_n\rho_n n}{80}}-6e^{-\nu_n\gamma_n n}\geq 1-8se^{-\frac{-\nu_n\rho_n n}{80}}$, $\mathcal{O}\subset\widehat{\mathcal{O}}$. This concludes the proof of Theorem 3.

A.6 Proof of Theorem 4

To prove Theorem 4, we use the definition of $\widehat{\boldsymbol{L}}$, the separability of the $\|\cdot\|_*$-norm on orthogonal subspaces, and results on $\widehat{\boldsymbol{S}}$ proved in Theorem 3. Recall that $\Psi\triangleq 16\tilde{\nu}_n\gamma_n\rho_n sn$.

Lemma 8. *Assume that* $\lambda_1\geq 3\left\|\boldsymbol{\Omega}\odot\boldsymbol{\Sigma}_{|I}\right\|_{op}$, *and that* $\lambda_2=19\sqrt{\nu_n\rho_n n}$. *Then,*

$$\|\boldsymbol{\Omega}\odot\Delta\boldsymbol{L}\|_F^2 \quad\leq\quad \frac{\lambda_1}{3}\left(5\left\|\mathcal{P}_{\boldsymbol{L}^*}\left(\Delta\boldsymbol{L}\right)\right\|_*-\left\|\mathcal{P}^\perp_{\boldsymbol{L}^*}\left(\Delta\boldsymbol{L}\right)\right\|_*\right)+\Psi \tag{45}$$

$$\textit{and}\quad \|\Delta\boldsymbol{L}\|_* \quad\leq\quad 6\sqrt{k}\left\|\Delta\boldsymbol{L}_{|I}\right\|_F+6\sqrt{3ksn}\rho_n+\frac{3\Psi}{\lambda_1}. \tag{46}$$

hold simultaneously with equation (15) *with probability at least* $1-6e^{-\nu_n\rho_n n}-2e^{-\tilde{\nu}_n\gamma_n sn}$.

Proof. See Section A.8.7. □

Bounding the $\|\cdot\|_{L_2(\boldsymbol{\Pi})}$-norm of the error $\Delta\boldsymbol{L}$ by $\|\boldsymbol{\Omega}\odot\Delta\boldsymbol{L}\|_F^2$ is rather involved, and we use a peeling argument, combined with the bound on $\|\Delta\boldsymbol{L}\|_*$ obtained in equation (46) in Lemma 8. We recall that $\boldsymbol{\Gamma}$ is the random matrix defined as $\boldsymbol{\Gamma}_{ij}=\epsilon_{ij}\boldsymbol{\Omega}_{ij}$ for all $(i,j)\in[n]\times[n]$, where $\{\epsilon\}_{i\leq j}$ is a Rademacher sequence. Moreover, we introduce the following notation :

$$\beta\triangleq\mathbb{E}\left[\left\|\boldsymbol{\Gamma}_{|I}\right\|_{op}\right]\left(\frac{48^2\rho_n^2 k}{\mu_n}\mathbb{E}\left[\left\|\boldsymbol{\Gamma}_{|I}\right\|_{op}\right]+60\rho_n^2\sqrt{ksn}+\frac{32\Psi\rho_n}{\lambda_1}\right). \tag{47}$$

Lemma 9. *Assume that* $\lambda_1 \geq 3\left\|\boldsymbol{\Omega} \odot \boldsymbol{\Sigma}_{|I}\right\|_{op}$, *and that* $\lambda_2 = 19\sqrt{\nu_n \rho_n n}$. *Then, there exists an absolute constant* $C > 0$ *such that*

$$\left\|\Delta \boldsymbol{L}_{|I}\right\|_{L_2(\boldsymbol{\Pi})}^2 \leq C\left(\frac{\lambda_1^2 k}{\mu_n} + \nu_n \rho_n^2 sn + \frac{\nu_n \rho_n^2 kn}{\mu_n} + \Psi + \beta\right) \tag{48}$$

holds simultaneously with equations (15), (45) *and* (46) *with probability at least* $1 - 7e^{-\nu_n \rho_n n} - 2e^{-\tilde{\nu}_n \gamma_n sn}$.

Proof. See Section A.8.8. □

Finally, we bound β using the following lemma.

Lemma 10. $\mathbb{E}\left[\left\|\boldsymbol{\Gamma}_{|I}\right\|_{op}\right] \leq 84\sqrt{\nu_n n}$.

Lemma 10 implies that there exists some absolute constant $C > 0$ such that

$$\beta \quad \leq \quad C\sqrt{\nu_n n}\left(\frac{\rho_n^2 k}{\mu_n}\sqrt{\nu_n n} + \rho_n^2\sqrt{skn} + \frac{\Psi \rho_n}{\lambda_1}\right).$$

Proof. See Section A.8.9. □

Thus, there exists an absolute constant $C > 0$ such that when equation (48) holds,

$$\beta \quad \leq \quad C\left(\frac{\nu_n \rho_n^2 kn}{\mu_n} + \rho_n^2 n\sqrt{\nu_n sk} + \frac{\Psi\sqrt{\nu_n n}\rho_n}{\lambda_1}\right).$$

Combining Lemma 4 and Lemma 8-9, and noticing that $\sqrt{\nu_n sk} \leq \nu_n s + k$ and that $\frac{\nu_n}{\mu_n} \geq 1$, we find that there exists an absolute constant $C > 0$ such that with probability at least $1 - 7e^{-\nu_n \rho_n n} - 2e^{-\tilde{\nu}_n \gamma_n sn}$,

$$\begin{aligned}\left\|\Delta \boldsymbol{L}_{|I}\right\|_{L_2(\boldsymbol{\Pi})}^2 &\leq C\left(\frac{\lambda_1^2 k}{\mu_n} + \nu_n \rho_n^2 sn + \frac{\nu_n \rho_n^2 kn}{\mu_n} + \Psi + \frac{\nu_n \rho_n^2 kn}{\mu_n} + \rho_n^2 n\sqrt{\nu_n sk} + \frac{\Psi\sqrt{\nu_n n}\rho_n}{\lambda_1}\right) \\ &\leq C\left(\frac{\lambda_1^2 k}{\mu_n} + n\rho_n^2\left(\nu_n s + \frac{\nu_n k}{\mu_n}\right) + \Psi\left(\frac{\sqrt{\nu_n n}\rho_n}{\lambda_1} + 1\right)\right).\end{aligned}$$

Recall that $\Phi \triangleq n\rho_n^2\left(\frac{\nu_n k}{\mu_n} + \nu_n s\right)$, and that $\Xi \triangleq \frac{\sqrt{\nu_n n}\rho_n}{\lambda_1} + 1$. With these notations, we find that

$$\left\|\Delta \boldsymbol{L}_{|I}\right\|_{L_2(\boldsymbol{\Pi})}^2 \leq C\left(\frac{\lambda_1^2 k}{\mu_n} + \Phi + \Psi\Xi\right)$$

with probability at least $1 - 7e^{-\nu_n \rho_n n} - 2e^{-\tilde{\nu}_n \gamma_n sn}$. We conclude the proof of Theorem 4 by recalling that $\nu_n \rho_n n \geq \log(n)$ and $\tilde{\nu}_n \gamma_n n \geq \log(n)$.

A.7 Proof of Corollary 1

Lemma 2 allows us to choose λ_1 by bounding the noise terms $\left\|\boldsymbol{\Omega} \odot \boldsymbol{\Sigma}_{|I}\right\|_{op}$ with high probability. For the choice $\lambda_1 = 84\sqrt{\nu_n \rho_n n}$, we find that

$$\Xi \quad = \quad \left(1 + \frac{\sqrt{\nu_n \rho_n^2 n}}{84\sqrt{\nu_n \rho_n n}}\right) \leq 2.$$

Combining Lemma 2 with Theorem 4, we find that there exists an absolute constant $C > 0$ such that with probability at least $1 - 7e^{-\nu_n \rho_n n} - 3e^{-\tilde{\nu}_n \gamma_n ns}$,

$$\begin{aligned}\left\|\Delta \boldsymbol{L}_{|I}\right\|_{L_2(\boldsymbol{\Pi})}^2 &\leq C\left(\frac{\nu_n \rho_n kn}{\mu_n} + n\rho_n^2\left(\frac{\nu_n k}{\mu_n} + \nu_n s\right) + \nu_n \tilde{\nu}_n \rho_n \gamma_n sn\right) \\ &\leq C\left(\frac{\nu_n \rho_n kn}{\mu_n} + \rho_n(\nu_n \rho_n \vee \tilde{\nu}_n \gamma_n) sn\right).\end{aligned}$$

A.8 Proof of auxiliary Lemmas

A.8.1 Proof of Lemma 1

Recall that by definition of $\widehat{\boldsymbol{S}}$,

$$\widehat{\boldsymbol{S}} \in \underset{\boldsymbol{S}\in\mathbb{R}_+^{n\times n}}{\arg\min} \left\{ \frac{1}{2} \left\| \boldsymbol{\Omega} \odot \left(\boldsymbol{A} - \widehat{\boldsymbol{L}} - \boldsymbol{S} - \boldsymbol{S}^\top \right) \right\|_F^2 + \lambda_2 \|\boldsymbol{S}\|_{2,1} \right\} \tag{49}$$

Now, any subgradient of the objective function (49) at $\widehat{\boldsymbol{S}}$ is of the form

$$\nabla_{\boldsymbol{S}} \mathcal{F}\left(\widehat{\boldsymbol{S}}, \widehat{\boldsymbol{L}}\right) = 2\boldsymbol{\Omega} \odot \left(-\boldsymbol{A} + \widehat{\boldsymbol{L}} + \widehat{\boldsymbol{S}} + \widehat{\boldsymbol{S}}^\top \right) + \lambda_2 \boldsymbol{W}$$

where $\boldsymbol{W}$ is a subgradient of the $\|\cdot\|_{2,1}$-norm at $\widehat{\boldsymbol{S}}$. The matrix $\boldsymbol{W}$ obeys the following constraints :

- for any $j \in [n]$ such that the column $\widehat{\boldsymbol{S}}_{\cdot,j}$ is null, $\|\boldsymbol{W}_{\cdot,j}\|_2 \leq 1$;
- for any $j \in [n]$ such that $\widehat{\boldsymbol{S}}_{\cdot,j} \neq \boldsymbol{0}$, $\|\boldsymbol{W}_{\cdot,j}\|_2 = \frac{\widehat{\boldsymbol{S}}_{\cdot,j}}{\|\widehat{\boldsymbol{S}}_{\cdot,j}\|_2}$.

The Karush-Kuhn-Tucker conditions (see, e.g., [9], Section 5.5.3) imply that there exists $\boldsymbol{H} \in \mathbb{R}^{n\times n}$ and $\boldsymbol{W} \in \partial \|\cdot\|_{2,1}$ such that

$$2\boldsymbol{\Omega} \odot \left(-\boldsymbol{A} + \widehat{\boldsymbol{L}} + \widehat{\boldsymbol{S}} + \widehat{\boldsymbol{S}}^\top \right) + \lambda_2 \boldsymbol{W} - \boldsymbol{H} = \boldsymbol{0} \tag{50}$$

$$\boldsymbol{H}_{ij} \geq 0 \text{ for any } (i,j) \in [n] \times [n] \tag{51}$$

$$\boldsymbol{H} \odot \widehat{\boldsymbol{S}} = \boldsymbol{0} \tag{52}$$

First, we prove the implication $\widehat{\boldsymbol{S}}_{\cdot,j} = \boldsymbol{0} \Rightarrow \left\| \boldsymbol{\Omega} \odot \left(\boldsymbol{A}_{j,\cdot} - \widehat{\boldsymbol{L}}_{j,\cdot} - \widehat{\boldsymbol{S}}_{j,\cdot} \right)_+ \right\|_2 \leq \frac{\lambda_2}{2}$. To do so, assume that j is such that $\widehat{\boldsymbol{S}}_{\cdot,j} = \boldsymbol{0}$. Then, equation (50) implies that

$$\lambda_2 \boldsymbol{W}_{\cdot,j} = 2\boldsymbol{\Omega} \odot \left(\boldsymbol{A}_{\cdot,j} - \widehat{\boldsymbol{L}}_{\cdot,j} - \widehat{\boldsymbol{S}}_{j,\cdot} \right) + \boldsymbol{H}_{\cdot,j}.$$

Recall that $\|\boldsymbol{W}_{\cdot,j}\|_2 \leq 1$, and thus

$$\frac{2}{\lambda_2} \left\| \boldsymbol{\Omega}_{\cdot,j} \odot \left(\boldsymbol{A}_{\cdot,j} - \widehat{\boldsymbol{L}}_{\cdot,j} - \widehat{\boldsymbol{S}}_{j,\cdot} \right) + \frac{1}{2} \boldsymbol{H}_{\cdot,j} \right\|_2 \leq 1.$$

Moreover, by (51), $\boldsymbol{H}_{ij} \geq 0$. Therefore,

$$\begin{aligned} \frac{2}{\lambda_2} \left\| \boldsymbol{\Omega}_{\cdot,j} \odot \left(\boldsymbol{A}_{\cdot,j} - \widehat{\boldsymbol{L}}_{\cdot,j} - \widehat{\boldsymbol{S}}_{j,\cdot} \right)_+ \right\|_2 &\leq \frac{2}{\lambda_2} \left\| \left(\boldsymbol{\Omega}_{\cdot,j} \odot \left(\boldsymbol{A}_{\cdot,j} - \widehat{\boldsymbol{L}}_{\cdot,j} - \widehat{\boldsymbol{S}}_{j,\cdot} \right) + \frac{1}{2} \boldsymbol{H}_{\cdot,j} \right)_+ \right\|_2 \\ &\leq \frac{2}{\lambda_2} \left\| \boldsymbol{\Omega}_{\cdot,j} \odot \left(\boldsymbol{A}_{\cdot,j} - \widehat{\boldsymbol{L}}_{\cdot,j} - \widehat{\boldsymbol{S}}_{j,\cdot} \right) + \frac{1}{2} \boldsymbol{H}_{\cdot,j} \right\|_2 \leq 1. \end{aligned}$$

This concludes the proof of the first implication.

To prove the other implication, assume that j is such that $\widehat{\boldsymbol{S}}_{\cdot,j} \neq \boldsymbol{0}$. Then $\boldsymbol{W}_{\cdot,j} = \frac{\widehat{\boldsymbol{S}}_{\cdot,j}}{\|\widehat{\boldsymbol{S}}_{\cdot,j}\|_2}$, and equation (50) becomes

$$\left(2 + \frac{\lambda_2}{\left\| \widehat{\boldsymbol{S}}_{\cdot,j} \right\|_2} \right) \widehat{\boldsymbol{S}}_{\cdot,j} = 2\boldsymbol{\Omega}_{\cdot,j} \odot \left(\boldsymbol{A}_{\cdot,j} - \widehat{\boldsymbol{L}}_{\cdot,j} - \widehat{\boldsymbol{S}}_{j,\cdot} \right) + \boldsymbol{H}_{\cdot,j} + 2\left(1 - \boldsymbol{\Omega}_{\cdot,j}\right) \odot \widehat{\boldsymbol{S}}_{\cdot,j}.$$

First, assume that for some $i \in [n]$, $\boldsymbol{H}_{ij} \neq 0$. Then, equation (52) implies that $\widehat{\boldsymbol{S}}_{ij} = 0$, and so

$$\boldsymbol{\Omega}_{ij}\left(\boldsymbol{A}_{ij} - \widehat{\boldsymbol{L}}_{ij} - \widehat{\boldsymbol{S}}_{ji}\right) = -\boldsymbol{H}_{ij}/2 < 0.$$

On the other hand, assume that for $i \in [n]$, $\boldsymbol{H}_{ij} = 0$. Then, $\widehat{\boldsymbol{S}}_{ij} \geq 0$ implies that

$$\boldsymbol{\Omega}_{ij}\left(\boldsymbol{A}_{ij} - \widehat{\boldsymbol{L}}_{ij} - \widehat{\boldsymbol{S}}_{ji}\right) + (1 - \boldsymbol{\Omega}_{ij})\,\widehat{\boldsymbol{S}}_{ij} \geq 0$$

which implies that $\boldsymbol{\Omega}_{ij}\left(\boldsymbol{A}_{ij} - \widehat{\boldsymbol{L}}_{ij} - \widehat{\boldsymbol{S}}_{ji}\right) \geq 0$. This shows that for $j \in [n]$ such that $\widehat{\boldsymbol{S}}_{\cdot,j} \neq \boldsymbol{0}$,

$$\left(2 + \frac{\lambda_2}{\left\|\widehat{\boldsymbol{S}}_{\cdot,j}\right\|_2}\right)\widehat{\boldsymbol{S}}_{\cdot,j} = 2\boldsymbol{\Omega}_{\cdot,j} \odot \left(\boldsymbol{A}_{\cdot,j} - \widehat{\boldsymbol{L}}_{\cdot,j} - \widehat{\boldsymbol{S}}_{j,\cdot}\right)_+ + 2\,(1 - \boldsymbol{\Omega}_{\cdot,j}) \odot \widehat{\boldsymbol{S}}_{\cdot,j}. \tag{53}$$

Now, for all i such that $\boldsymbol{\Omega}_{ij} = 0$, equation (53) becomes $\left(2 + \frac{\lambda_2}{\left\|\widehat{\boldsymbol{S}}_{\cdot,j}\right\|_2}\right)\widehat{\boldsymbol{S}}_{ij} = 2\widehat{\boldsymbol{S}}_{ij}$, and thus $\widehat{\boldsymbol{S}}_{ij} = 0$. This remarks, combined with equation (53), implies that

$$\left(2 + \frac{\lambda_2}{\left\|\widehat{\boldsymbol{S}}_{\cdot,j}\right\|_2}\right)\widehat{\boldsymbol{S}}_{\cdot,j} = 2\boldsymbol{\Omega}_{\cdot,j} \odot \left(\boldsymbol{A}_{\cdot,j} - \widehat{\boldsymbol{L}}_{\cdot,j} - \widehat{\boldsymbol{S}}_{j,\cdot}\right)_+.$$

This implies in particular that

$$2\left\|\left(\boldsymbol{\Omega}_{\cdot,j} \odot \left(\boldsymbol{A}_{\cdot,j} - \widehat{\boldsymbol{L}}_{\cdot,j} - \widehat{\boldsymbol{S}}_{j,\cdot}\right)\right)_+\right\|_2 = 2\left\|\widehat{\boldsymbol{S}}_{\cdot,j}\right\|_2 + \lambda_2 > \lambda_2.$$

This concludes the proof of Lemma 1.

A.8.2 Proof of Lemma 2

Note that $\boldsymbol{\Omega} \odot \boldsymbol{\Sigma}_{|I}$ is a symmetric random matrix with independent centered entries. Moreover, for $(i,j) \in \mathcal{I}\times\mathcal{I}$, $(\boldsymbol{\Omega} \odot \boldsymbol{\Sigma})_{ij} = b_{ij}\xi_{ij}$, where we define $b_{ij} \triangleq \boldsymbol{\Pi}_{ij}\boldsymbol{L}^*_{ij}\left(1 - \boldsymbol{L}^*_{ij}\right)$ and $\xi_{ij} = \frac{\boldsymbol{\Omega}_{ij}\boldsymbol{\Sigma}_{ij}}{b_{ij}}$. With these notations, we see that $\max_{ij}\mathbb{E}\left[(\xi_{ij}b_{ij})^{2\alpha}\right]^{\frac{1}{2\alpha}} \leq 1$ and that $\max_i \sqrt{\sum_j b_{ij}^2} \leq \nu_n\rho_n n$. Applying Proposition 2 for $t = \sqrt{2\nu_n\rho_n n}$ and $\alpha = 3$, we find that

$$\mathbb{P}\left(\left\|(\boldsymbol{\Omega} \odot \boldsymbol{\Sigma})_{|I}\right\|_{op} \geq \sqrt{2}e^{\frac{2}{3}}\left(2\sqrt{\nu_n\rho_n n} + 42\sqrt{\log(n)}\right) + \sqrt{2\nu_n\rho_n n}\right) \leq e^{-\nu_n\rho_n n}.$$

We conclude the proof of Lemma 2 by recalling that $\log(n) \leq \nu_n\rho_n n$.

A.8.3 Proof of Lemma 3

First, using the 2-smoothness of the least-squares data fitting term and the ϵ-smoothness of the ridge regularization, we obtain that:

$$\begin{aligned}\mathcal{F}(\mathbf{S}^{(t)}, \boldsymbol{L}^{(t-1)}, R^{(t-1)}) \quad \leq \quad & \mathcal{F}(\mathbf{S}^{(t-1)}, \boldsymbol{L}^{(t-1)}, R^{(t-1)}) + \langle \boldsymbol{G}_S(\boldsymbol{S}^{(t-1)}, \boldsymbol{L}^{(t-1)}), \mathbf{S}^{(t)} - \mathbf{S}^{(t-1)}\rangle \\ & + \frac{2+\epsilon}{2}\|\mathbf{S}^{(t)} - \mathbf{S}^{(t-1)}\|_F^2 + \lambda_2(\|\mathbf{S}^{(t)}\|_{2,1} - \|\mathbf{S}^{(t-1)}\|_{2,1}).\end{aligned} \tag{54}$$

Then, by definition of the proximal operator, we have that:

$$\begin{aligned}\mathbf{S}^{(t)} \quad & \in \arg\min\left(\eta\lambda_2\|\mathbf{S}\|_{2,1} + \tfrac{1}{2}\|\mathbf{S} - \mathbf{S}^{(t-1)} - \eta\boldsymbol{G}_S(\boldsymbol{S}^{(t-1)}, \boldsymbol{L}^{(t-1)})\|_F^2\right) \\ & \in \arg\min\Big(\langle \boldsymbol{G}_S(\boldsymbol{S}^{(t-1)}, \boldsymbol{L}^{(t-1)}), \mathbf{S} - \mathbf{S}^{(t-1)}\rangle + \tfrac{1}{2\eta}\|\mathbf{S} - \mathbf{S}^{(t-1)}\|_F^2 \\ & \qquad + \lambda_2(\|\mathbf{S}\|_{2,1} - \|\mathbf{S}^{(t-1)}\|_{2,1})\Big).\end{aligned} \tag{55}$$

Combining (54), (55) and the fact that $\eta \leq 1/(2+\epsilon)$, we obtain that, for any $\mathbf{S} \in \mathbb{R}^{n\times n}$:

$$\begin{aligned}\mathcal{F}(\mathbf{S}^{(t)}, \boldsymbol{L}^{(t-1)}, R^{(t-1)}) \quad &\leq \quad \mathcal{F}(\mathbf{S}^{(t-1)}, \boldsymbol{L}^{(t-1)}, R^{(t-1)}) + \langle \boldsymbol{G}_S(\boldsymbol{S}^{(t-1)}, \boldsymbol{L}^{(t-1)}), \mathbf{S} - \mathbf{S}^{(t-1)}\rangle \\ &\quad + \frac{1}{2\eta}\|\mathbf{S} - \mathbf{S}^{(t-1)}\|_F^2 + \lambda_2(\|\mathbf{S}\|_{2,1} - \|\mathbf{S}^{(t-1)}\|_{2,1}).\end{aligned}$$

In particular, for matrices of the form $b\tilde{\boldsymbol{S}}^{(t-1)} + (1-b)\boldsymbol{S}^{(t-1)}$, $b \in \mathbb{R}$, we obtain:

$$\begin{aligned}\mathcal{F}(\mathbf{S}^{(t)}, \boldsymbol{L}^{(t-1)}, R^{(t-1)}) \quad &\leq \quad \mathcal{F}(\mathbf{S}^{(t-1)}, \boldsymbol{L}^{(t-1)}, R^{(t-1)}) + b\langle \boldsymbol{G}_S(\boldsymbol{S}^{(t-1)}, \boldsymbol{L}^{(t-1)}), \tilde{\mathbf{S}}^{(t-1)} - \mathbf{S}^{(t-1)}\rangle \\ &\quad + \frac{b^2}{2\eta}\|\tilde{\mathbf{S}}^{(t-1)} - \mathbf{S}^{(t-1)}\|_F^2 + \lambda_2(\|b\tilde{\mathbf{S}}^{(t-1)} + (1-b)\mathbf{S}^{(t-1)}\|_{2,1} - \|\mathbf{S}^{(t-1)}\|_{2,1}),\end{aligned}$$

and, using the triangular inequality:

$$\begin{aligned}\mathcal{F}(\mathbf{S}^{(t)}, \boldsymbol{L}^{(t-1)}, R^{(t-1)}) \quad &\leq \quad \mathcal{F}(\mathbf{S}^{(t-1)}, \boldsymbol{L}^{(t-1)}, R^{(t-1)}) + b\langle \boldsymbol{G}_S(\boldsymbol{S}^{(t-1)}, \boldsymbol{L}^{(t-1)}), \tilde{\mathbf{S}}^{(t-1)} - \mathbf{S}^{(t-1)}\rangle \\ &\quad + \frac{b^2}{2\eta}\|\tilde{\mathbf{S}}^{(t-1)} - \mathbf{S}^{(t-1)}\|_F^2 + b\lambda_2(\|\tilde{\mathbf{S}}^{(t-1)}\|_{2,1} - \|\mathbf{S}^{(t-1)}\|_{2,1}). \qquad (56)\end{aligned}$$

Finally, minimizing the right hand side of (56) with respect to b, we obtain the final result:

$$\mathcal{F}(\mathbf{S}^{(t)}, \boldsymbol{L}^{(t-1)}, R^{(t-1)}) - \mathcal{F}(\mathbf{S}^{(t-1)}, \boldsymbol{L}^{(t-1)}, R^{(t-1)}) \leq \frac{-\eta g_S(\mathbf{S}^{(t-1)}, \boldsymbol{L}^{(t-1)})^2}{(2Q^{(t-1)})^2},$$

where we have used that $\|\tilde{\mathbf{S}}^{(t-1)} - \mathbf{S}^{(t-1)}\|_F^2 \leq (2Q^{(t-1)})^2$.

A.8.4 Proof of Lemma 4

We first observe, using a Taylor expansion of the quadratic term of the objective function (the least-squares data fitting term plus the ridge regularization term), and (24) that:

$$\mathcal{F}(\mathbf{S}^{(t)}, \boldsymbol{L}^{(t)}, R^{(t)}) = \mathcal{F}(\mathbf{S}^{(t)}, \boldsymbol{L}^{(t-1)}, R^{(t-1)}) - \beta_t g_L(\mathbf{S}^{(t)}, \boldsymbol{L}^{(t-1)}, R^{(t-1)}) + \frac{\beta_t^2(1+\epsilon)}{2}\|\tilde{\boldsymbol{L}}^{(t)} - \boldsymbol{L}^{(t-1)}\|_F^2.$$

Now, recall that

$$\beta_t = \min\left\{1, \frac{\langle \boldsymbol{L}^{(t-1)} - \tilde{\boldsymbol{L}}^{(t)}, \boldsymbol{G}_L(\boldsymbol{S}^{(t)}, \boldsymbol{L}^{(t-1)})\rangle + \lambda_1(R^{(t-1)} - \tilde{R}^{(t)})}{(1+\epsilon)\|\tilde{\boldsymbol{L}}^{(t)} - \boldsymbol{L}^{(t-1)}\|_F^2}\right\},$$

with $(\tilde{\boldsymbol{L}}^{(t)}, \tilde{R}^{(t)})$ defined in (25), and g_L in (29).

Case 1: $\langle \boldsymbol{G}_L(\boldsymbol{S}^{(t)}, \boldsymbol{L}^{(t-1)}), \boldsymbol{L}^{(t-1)} - \tilde{\boldsymbol{L}}^{(t)}\rangle + \lambda_1(R^{(t-1)} - \tilde{R}^{(t)}) \geq (1+\epsilon)\|\tilde{\boldsymbol{L}}^{(t)} - \boldsymbol{L}^{(t-1)}\|_F^2$. Then, $\beta_t = 1$, and $g_L(\mathbf{S}^{(t)}, \boldsymbol{L}^{(t-1)}, R^{(t-1)}) \geq (1+\epsilon)\|\tilde{\boldsymbol{L}}^{(t)} - \boldsymbol{L}^{(t-1)}\|_F^2$. As a result, we observe:

$$\begin{aligned}\mathcal{F}(\mathbf{S}^{(t)}, \boldsymbol{L}^{(t)}, R^{(t)}) - \mathcal{F}(\mathbf{S}^{(t)}, \boldsymbol{L}^{(t-1)}, R^{(t-1)}) \quad &\leq \quad -\frac{1}{2}g_L(\mathbf{S}^{(t)}, \boldsymbol{L}^{(t-1)}, R^{(t-1)}) \\ &\leq \quad -\frac{1}{2}\frac{(g_L(\mathbf{S}^{(t)}, \boldsymbol{L}^{(t-1)}, R^{(t-1)}))^2}{g_L(\mathbf{S}^{(t)}, \boldsymbol{L}^{(t-1)}, R^{(t-1)})} \qquad (57) \\ &\leq \quad -\frac{1}{2}\frac{(g_L(\mathbf{S}^{(t)}, \boldsymbol{L}^{(t-1)}, R^{(t-1)}))^2}{\bar{R}^{(t)}(\lambda_1 + 2M^{(t)})},\end{aligned}$$

where, to obtain the last inequality, we have used that $M^{(t)} = \|\boldsymbol{G}_L(\boldsymbol{S}^{(t)}, \boldsymbol{L}^{(t-1)})\|_F \geq \|\boldsymbol{G}_L(\boldsymbol{S}^{(t)}, \boldsymbol{L}^{(t-1)})\|_{op}$, and the inequalities $R^{(t-1)} - \tilde{R}^{(t)} \leq \bar{R}^{(t)}$ and

$$\langle \boldsymbol{G}_L(\boldsymbol{S}^{(t)}, \boldsymbol{L}^{(t-1)}), \boldsymbol{L}^{(t-1)} - \tilde{\boldsymbol{L}}^{(t-1)}\rangle \leq 2M^{(t)}\bar{R}^{(t)}.$$

Case 2: $\langle \boldsymbol{G}_L(\boldsymbol{S}^{(t)}, \boldsymbol{L}^{(t-1)}), \boldsymbol{L}^{(t-1)} - \tilde{\boldsymbol{L}}^{(t)} \rangle + \lambda_1(R^{(t-1)} - \tilde{R}^{(t)}) < (1+\epsilon)\|\boldsymbol{L}^{(t-1)} - \tilde{\boldsymbol{L}}^{(t)}\|_F^2$. Then, $\beta_t = g_L(\mathbf{S}^{(t)}, \boldsymbol{L}^{(t-1)}, R^{(t-1)})/((1+\epsilon)\|\boldsymbol{L}^{(t-1)} - \tilde{\boldsymbol{L}}^{(t)}\|_F^2)$, and we obtain:

$$\begin{aligned}\mathcal{F}(\mathbf{S}^{(t)}, \boldsymbol{L}^{(t)}, R^{(t)}) - \mathcal{F}(\mathbf{S}^{(t)}, \boldsymbol{L}^{(t-1)}, R^{(t-1)}) &\leq -\frac{1}{2}\frac{(g_L(\mathbf{S}^{(t)}, \boldsymbol{L}^{(t-1)}, R^{(t-1)}))^2}{(1+\epsilon)\|\boldsymbol{L}^{(t-1)} - \tilde{\boldsymbol{L}}^{(t)}\|_F^2} \\ &\leq -\frac{1}{2}\frac{(g_L(\mathbf{S}^{(t)}, \boldsymbol{L}^{(t-1)}, R^{(t-1)}))^2}{(1+\epsilon)(2\bar{R}^{(t)})^2},\end{aligned}$$

where, to obtain the last inequality, we used that $\|\boldsymbol{L}^{(t-1)} - \tilde{\boldsymbol{L}}^{(t)}\|_F^2 \leq \|\boldsymbol{L}^{(t-1)} - \tilde{\boldsymbol{L}}^{(t)}\|_*^2 \leq (2\bar{R}^{(t)})^2$.

We finally prove (30) as follows. We start by noticing that $\|\tilde{\boldsymbol{L}}^{(t-1)} - \boldsymbol{L}^{(t-1)}\|_F^2 = \beta_t^2\|\boldsymbol{L}^{(t)} - \boldsymbol{L}^{(t-1)}\|_F^2$. If $\beta_t = 1$, then by definition of β_t:

$$g_L(\mathbf{S}^{(t)}, \boldsymbol{L}^{(t-1)}, R^{(t-1)}) \geq (1+\epsilon)\|\tilde{\boldsymbol{L}}^{(t-1)} - \boldsymbol{L}^{(t-1)}\|_F^2 = (1+\epsilon)\|\boldsymbol{L}^{(t)} - \boldsymbol{L}^{(t-1)}\|_F^2.$$

Inequality (57) then implies that:

$$\mathcal{F}(\mathbf{S}^{(t)}, \boldsymbol{L}^{(t)}, R^{(t)}) - \mathcal{F}(\mathbf{S}^{(t)}, \boldsymbol{L}^{(t-1)}, R^{(t-1)}) \leq -\frac{(1+\epsilon)}{2}\|\boldsymbol{L}^{(t)} - \boldsymbol{L}^{(t-1)}\|_F^2.$$

If $\beta_t = g_L(\mathbf{S}^{(t)}, \boldsymbol{L}^{(t-1)}, R^{(t-1)})/((1+\epsilon)\|\boldsymbol{L}^{(t-1)} - \tilde{\boldsymbol{L}}^{(t)}\|_F^2)$, then:

$$\begin{aligned}\|\tilde{\boldsymbol{L}}^{(t-1)} - \boldsymbol{L}^{(t-1)}\|_F^2 &= \beta_t^2\|\boldsymbol{L}^{(t)} - \boldsymbol{L}^{(t-1)}\|_F^2 = \frac{(g_L(\mathbf{S}^{(t)}, \boldsymbol{L}^{(t-1)}, R^{(t-1)}))^2}{(1+\epsilon)\|\tilde{\boldsymbol{L}}^{(t-1)} - \boldsymbol{L}^{(t-1)}\|_F^2} \\ &\leq \frac{2}{1+\epsilon}\left(\mathcal{F}(\mathbf{S}^{(t)}, \boldsymbol{L}^{(t-1)}, R^{(t-1)}) - \mathcal{F}(\mathbf{S}^{(t)}, \boldsymbol{L}^{(t)}, R^{(t)})\right),\end{aligned}$$

which proves the result.

A.8.5 Proof of Lemma 6

To prove equation (40) in Lemma 6, recall that for $j \in \mathcal{I}$, $\sum_{i\in\mathcal{I}} \mathbb{E}\left[\boldsymbol{\Omega}_{ij}\boldsymbol{\Sigma}_{ij}^2\right] \leq n\nu_n\rho_n$, that $\sum_{i\in\mathcal{I}} \mathbb{V}ar\left[\boldsymbol{\Omega}_{ij}\boldsymbol{\Sigma}_{ij}^2\right] \leq n\nu_n\rho_n$, and that $\|\boldsymbol{\Omega} \odot \boldsymbol{\Sigma} \odot \boldsymbol{\Sigma}\|_\infty \leq 1$. Applying Bernstein's inequality (19), we obtain that for any $j \in \mathcal{I}$ and $t > 0$,

$$\mathbb{P}\left(\sum_{i\in\mathcal{I}} \boldsymbol{\Omega}_{ij}\boldsymbol{\Sigma}_{ij}^2 \geq \nu_n\rho_n n + \sqrt{2t\nu_n\rho_n n} + \frac{3}{2}t\right) \leq 2e^{-t}$$

Choosing $t = 2\nu_n\rho_n n$, we find that

$$\begin{aligned}\mathbb{P}\left(\max_{j\in\mathcal{I}} \sqrt{\sum_{i\in\mathcal{I}} \boldsymbol{\Omega}_{ij}\boldsymbol{\Sigma}_{ij}^2} \geq \sqrt{6\nu_n\rho_n n}\right) &\leq 2ne^{-2\nu_n\rho_n n} \\ \mathbb{P}\left(\left\|\boldsymbol{\Omega} \odot \boldsymbol{\Sigma}_{|I}\right\|_{2,\infty} \geq \sqrt{6\nu_n\rho_n n}\right) &\leq 2e^{-\nu_n\rho_n n}\end{aligned}$$

where we have used the union bound and $\nu_n\gamma_n n \geq \log(n)$. This proves equation (40) in Lemma 2.

To prove equation (41) in Lemma 6, note that $\left\|\boldsymbol{\Omega}_{|I}\right\|_{2,\infty} \leq \left\|\boldsymbol{\Pi}_{|I} - \boldsymbol{\Omega}_{|I}\right\|_{2,\infty} + \left\|\boldsymbol{\Pi}_{|I}\right\|_{2,\infty}$ and $\left\|\boldsymbol{\Pi}_{|I}\right\|_{2,\infty} \leq \sqrt{\nu_n n}$. Moreover, for $j \in \mathcal{I}$, $\sum_{i\in\mathcal{I}} \mathbb{E}\left[\left(\boldsymbol{\Pi}_{ij} - \boldsymbol{\Omega}_{ij}\right)^2\right] \leq \nu_n n$, $\sum_{i\in\mathcal{I}} \mathbb{V}ar\left[\left(\boldsymbol{\Pi} - \boldsymbol{\Omega}_{ij}\right)^2\right] \leq \nu_n n$, and $\left\|\boldsymbol{\Pi}_{|I} - \boldsymbol{\Omega}_{|I}\right\|_\infty \leq 1$. We apply Bernstein's inequality and find that for any $j \in \mathcal{I}$ and $t > 0$,

$$\mathbb{P}\left(\sum_{i\in\mathcal{I}} \left(\boldsymbol{\Pi}_{ij} - \boldsymbol{\Omega}_{ij}\right)^2 \geq \nu_n n + \sqrt{2t\nu_n n} + \frac{3}{2}t\right) \leq 2e^{-t}$$

Choosing $t = 2\nu_n n$ and using an union bound, we find that

$$\begin{aligned}\mathbb{P}\left(\sup_{j\in\mathcal{I}}\sqrt{\sum_{i\in\mathcal{I}}\left(\mathbf{\Pi}_{ij}-\mathbf{\Omega}_{ij}\right)^2}\geq\sqrt{6\nu_n n}\right) &\leq 2ne^{-2n\nu_n}\\ \mathbb{P}\left(\left\|\mathbf{\Pi}_{|I}-\mathbf{\Omega}_{|I}\right\|_{2,\infty}\geq\sqrt{6\nu_n n}\right)&\leq 2e^{-\nu_n n}\end{aligned}$$

where we have used that $\nu_n n \geq \log(n)$. This proves equation (41).

To prove equation (42), recall that for $(i,j)\in\mathcal{O}\times\mathcal{I}$, $\mathbf{\Omega}_{ij}\boldsymbol{A}_{ij}\sim$Bernoulli$(\mathbf{\Pi}_{ij}\boldsymbol{S}^*_{ij})$, and that $\left\|\mathbf{\Pi}\odot\boldsymbol{S}^\top\right\|_\infty \leq \nu_n\gamma_n$. Then, applying Bernstein's inequality (19), we find that for any $j\in\mathcal{I}$ and any $t>0$,

$$\mathbb{P}\left(\sum_{i\in\mathcal{O}}\mathbf{\Omega}_{ij}\boldsymbol{A}_{ij}\geq s\nu_n\gamma_n+\sqrt{2ts\nu_n\gamma_n}+\frac{3t}{2}\right)\leq 2e^{-t}.$$

Choosing $t=2\nu_n\rho_n n$, we find that

$$\mathbb{P}\left(\sum_{i\in\mathcal{O}}\mathbf{\Omega}_{ij}\boldsymbol{A}_{ij}\geq s\nu_n\gamma_n+2\sqrt{\gamma_n\rho_n n s}\nu_n+3\nu_n\rho_n n\right)\leq 2e^{-t}.$$

Under Assumption 3, this implies

$$\mathbb{P}\left(\sum_{i\in\mathcal{O}}\mathbf{\Omega}_{ij}\boldsymbol{A}_{ij}\geq 6\nu_n\rho_n n\right)\leq 2e^{-2\nu_n\rho_n n}.$$

Using the union bound, and the bound $\nu_n\rho_n n\geq\log(n)$, we conclude that

$$\mathbb{P}\left(\max_{j\in\mathcal{I}}\sqrt{\sum_{i\in\mathcal{O}}\mathbf{\Omega}_{ij}\boldsymbol{A}_{ij}}\geq\sqrt{6\nu_n\rho_n nn}\right)\leq 2ne^{-2\nu_n\rho_n n}\leq 2e^{-\nu_n\rho_n n}.$$

This concludes the proof of Lemma 6.

A.8.6 Proof of Lemma 7

Recall that for $j\in\mathcal{O}$, $\left\{\left((\mathbf{\Omega}_{ij}\boldsymbol{A}_{ij}-\rho_n)_+\right)^2\right\}_{i\in\mathcal{I}}$ are independent random variables. Moreover, easy calculations yields that $\mathbb{E}\left[\left(\mathbf{\Omega}_{ij}\left(\boldsymbol{A}_{ij}-\rho_n\right)_+\right)^2\right]=\mathbf{\Pi}_{ij}\boldsymbol{S}^*_{ij}(1-\rho_n)^2$, and that $\mathbb{V}ar\left[\left(\mathbf{\Omega}_{ij}\left(\boldsymbol{A}_{ij}-\rho_n\right)_+\right)^2\right]\leq\mathbf{\Pi}_{ij}\boldsymbol{S}^*_{ij}(1-\rho_n)^2$. Applying Bernstein's inequality (19), we see that for any $t>0$,

$$\mathbb{P}\left(\left|\sum_{i\in\mathcal{I}}\mathbb{E}\left[\left(\mathbf{\Omega}_{ij}\left(\boldsymbol{A}_{ij}-\rho_n\right)_+\right)^2\right]-\sum_{i\in\mathcal{I}}\left(\mathbf{\Omega}_{ij}\left(\boldsymbol{A}_{ij}-\rho_n\right)_+\right)^2\right|\geq\sqrt{2t\sum_{i\in\mathcal{I}}\mathbf{\Pi}_{ij}\boldsymbol{S}^*_{ij}(1-\rho_n)^2}+\frac{3t}{2}\right)\leq 2e^{-t}.$$

Choosing $t=\frac{1}{80}\sum_{i\in\mathcal{I}}\mathbf{\Pi}_{ij}\boldsymbol{S}^*_{ij}(1-\rho_n)^2$, we find that

$$\mathbb{P}\left(\sum_{i\in\mathcal{I}}\left(\mathbf{\Omega}_{ij}\left(\boldsymbol{A}_{ij}-\rho_n\right)\right)_+^2\leq\sum_{i\in\mathcal{I}}\mathbf{\Pi}_{ij}\boldsymbol{S}^*_{ij}(1-\rho_n)^2-\frac{1}{2}\sum_{i\in\mathcal{I}}\mathbf{\Pi}_{ij}\boldsymbol{S}^*_{ij}(1-\rho_n)^2\right)\leq 2e^{-\frac{1}{80}\sum_{i\in\mathcal{I}}\mathbf{\Pi}_{ij}\boldsymbol{S}^*_{ij}(1-\rho_n)^2}.$$

When $\min_{j\in\mathcal{O}}\sum_{i\in\mathcal{I}}\mathbf{\Pi}_{ij}\boldsymbol{S}^*_{ij}(1-\rho_n)^2\geq\nu_n\rho_n n$ and $\rho_n\leq\frac{1}{2}$, this implies that

$$\mathbb{P}\left(\min_{j\in\mathcal{O}}\sqrt{\sum_{i\in\mathcal{I}}\left(\mathbf{\Omega}_{ij}\left(\boldsymbol{A}_{ij}-\rho_n\right)_+\right)^2}\leq\frac{1}{4}\min_{j\in\mathcal{O}}\sqrt{\sum_{i\in\mathcal{I}}\mathbf{\Pi}_{ij}\boldsymbol{S}^*_{ij}}\right)\leq 2se^{-\frac{-\nu_n\rho_n n}{80}}.$$

A.8.7 Proof of Lemma 8

Let $\partial \|\cdot\|_*$ and $\partial \|\cdot\|_{2,1}$ denote respectively the sub-differentials of $\|\cdot\|_*$ and $\|\cdot\|_{2,1}$ norms. Recall that $\left(\widehat{\boldsymbol{S}}, \widehat{\boldsymbol{L}}\right)$ minimizes $\mathcal{F}$. The standard optimality condition over a convex set states that for any admissible matrix $(\boldsymbol{S}, \boldsymbol{L})$, there exists $\widehat{\boldsymbol{V}} \in \partial \left\|\widehat{\boldsymbol{S}}\right\|_{2,1}$ and $\widehat{\boldsymbol{W}} \in \partial \left\|\widehat{\boldsymbol{L}}\right\|_*$ such that

$$\begin{aligned} -\left\langle \boldsymbol{\Omega} \odot \left(\boldsymbol{A} - \widehat{\boldsymbol{S}} - \widehat{\boldsymbol{S}}^\top - \widehat{\boldsymbol{L}}\right) \middle| \boldsymbol{S} - \widehat{\boldsymbol{S}} + \boldsymbol{S}^\top - \widehat{\boldsymbol{S}}^\top + \boldsymbol{L} - \widehat{\boldsymbol{L}} \right\rangle & \\ +\lambda_1 \left\langle \widehat{\boldsymbol{W}} \middle| \boldsymbol{L} - \widehat{\boldsymbol{L}} \right\rangle + \lambda_2 \left\langle \widehat{\boldsymbol{V}} \middle| \boldsymbol{S} - \widehat{\boldsymbol{S}} \right\rangle & \geq 0 \end{aligned} \tag{58}$$

Applying equation (58) for the admissible matrices $\left(\widehat{\boldsymbol{S}}, \boldsymbol{L}^*\right)$, we find that there exists $\widehat{\boldsymbol{W}} \in \partial \left\|\widehat{\boldsymbol{L}}\right\|_*$ such that

$$-\left\langle \boldsymbol{\Omega} \odot \left(\boldsymbol{A} - \widehat{\boldsymbol{S}} - \widehat{\boldsymbol{S}}^\top - \widehat{\boldsymbol{L}}\right) \middle| \Delta \boldsymbol{L} \right\rangle + \lambda_1 \left\langle \widehat{\boldsymbol{W}} \middle| \Delta \boldsymbol{L} \right\rangle \geq 0. \tag{59}$$

Recall that $\boldsymbol{\Sigma}_{|I} \triangleq \boldsymbol{A}_{|I} + \operatorname{diag}(\boldsymbol{L}^*) - \boldsymbol{L}^*$, that $\Delta \boldsymbol{L} \triangleq \boldsymbol{L}^* - \widehat{\boldsymbol{L}}$, and that $\boldsymbol{\Omega} \odot \operatorname{diag}(\boldsymbol{M}) = 0$ for any matrix $\boldsymbol{M}$. Thus, equation (59) becomes

$$-\left\langle \boldsymbol{\Omega} \odot \left(\boldsymbol{\Sigma}_I + \Delta \boldsymbol{L} + \boldsymbol{A}_{|O} - \widehat{\boldsymbol{S}} - \widehat{\boldsymbol{S}}^\top\right) \middle| \Delta \boldsymbol{L} \right\rangle + \lambda_1 \left\langle \widehat{\boldsymbol{W}} \middle| \Delta \boldsymbol{L} \right\rangle \geq 0. \tag{60}$$

Developing equation (60), we find that

$$\begin{aligned} -\left\langle \boldsymbol{\Omega} \odot \boldsymbol{\Sigma}_{|I} \middle| \Delta \boldsymbol{L} \right\rangle - \left\langle \boldsymbol{\Omega} \odot \Delta \boldsymbol{L} \middle| \Delta \boldsymbol{L} \right\rangle - \left\langle \boldsymbol{\Omega} \odot \left(\boldsymbol{A} - \widehat{\boldsymbol{S}} - \widehat{\boldsymbol{S}}^\top\right)_{|O} \middle| \Delta \boldsymbol{L} \right\rangle & \\ + \left\langle \boldsymbol{\Omega} \odot \left(\widehat{\boldsymbol{S}} + \widehat{\boldsymbol{S}}^\top\right)_{|I} \middle| \Delta \boldsymbol{L} \right\rangle + \lambda_1 \left\langle \widehat{\boldsymbol{W}} \middle| \Delta \boldsymbol{L} \right\rangle & \geq 0. \end{aligned}$$

We have proved in Theorem 3 that $\widehat{\boldsymbol{S}}_{|I} = \widehat{\boldsymbol{S}}_{|I}^\top = \boldsymbol{0}$ with probability at least $1 - 6e^{-\nu_n \rho_n n}$. Therefore, when equation (15) holds,

$$\|\boldsymbol{\Omega} \odot \Delta \boldsymbol{L}\|_F^2 \leq \left|\left\langle \boldsymbol{\Omega} \odot \boldsymbol{\Sigma}_{|I} \middle| \Delta \boldsymbol{L} \right\rangle\right| + \left|\left\langle \boldsymbol{\Omega} \odot \left(\boldsymbol{A} - \widehat{\boldsymbol{S}} - \widehat{\boldsymbol{S}}^\top\right)_{|O} \middle| \Delta \boldsymbol{L} \right\rangle\right| + \lambda_1 \left\langle \widehat{\boldsymbol{W}} \middle| \Delta \boldsymbol{L} \right\rangle.$$

Using the duality of the $\|\cdot\|_*$-norm and the $\|\cdot\|_{op}$-norm, we find that

$$\|\boldsymbol{\Omega} \odot \Delta \boldsymbol{L}\|_F^2 \leq \|\boldsymbol{\Omega} \odot \boldsymbol{\Sigma}_{|I}\|_{op} \|\Delta \boldsymbol{L}\|_* + \left|\left\langle \boldsymbol{\Omega} \odot \left(\boldsymbol{A} - \widehat{\boldsymbol{S}} - \widehat{\boldsymbol{S}}^\top\right)_{|O} \middle| \Delta \boldsymbol{L} \right\rangle\right| + \lambda_1 \left\langle \widehat{\boldsymbol{W}} \middle| \Delta \boldsymbol{L} \right\rangle.$$

Next, we bound the term $\left|\left\langle \boldsymbol{\Omega} \odot \left(\boldsymbol{A} - \widehat{\boldsymbol{S}} - \widehat{\boldsymbol{S}}^\top\right)_{|O} \middle| \Delta \boldsymbol{L} \right\rangle\right|$ using the following Lemma.

Lemma 11. *With probability at least* $1 - 2e^{-\tilde{\nu}_n \gamma_n s n}$,

$$\left|\left\langle \boldsymbol{\Omega} \odot \left(\boldsymbol{A} - \widehat{\boldsymbol{S}} - \widehat{\boldsymbol{S}}^\top\right)_{|O} \middle| \Delta \boldsymbol{L} \right\rangle\right| \leq 16 \tilde{\nu}_n \gamma_n \rho_n n s.$$

Proof. See Section A.8.10. □

Finally, we bound $\left\langle \widehat{\boldsymbol{W}} \middle| \Delta \boldsymbol{L} \right\rangle$. Note that by definition of the subgradient, $\left\langle \widehat{\boldsymbol{W}} \middle| \boldsymbol{L}^* - \widehat{\boldsymbol{L}} \right\rangle \leq \|\boldsymbol{L}^*\|_* - \left\|\widehat{\boldsymbol{L}}\right\|_*$. Using the separability of the spectral norm on orthogonal subspaces and the identity $\mathcal{P}_{\boldsymbol{L}^*}(\boldsymbol{L}^*) = \boldsymbol{L}^*$, we find that

$$\begin{aligned} \left\|\widehat{\boldsymbol{L}}\right\|_* &= \left\|\mathcal{P}_{\boldsymbol{L}^*}^\perp(\Delta \boldsymbol{L}) + \mathcal{P}_{\boldsymbol{L}^*}(\Delta \boldsymbol{L}) - \boldsymbol{L}^*\right\|_* \\ &= \left\|\mathcal{P}_{\boldsymbol{L}^*}^\perp(\Delta \boldsymbol{L})\right\|_* + \left\|\mathcal{P}_{\boldsymbol{L}^*}(\Delta \boldsymbol{L}) - \boldsymbol{L}^*\right\|_* \\ &\geq \left\|\mathcal{P}_{\boldsymbol{L}^*}^\perp(\Delta \boldsymbol{L})\right\|_* + \|\boldsymbol{L}^*\|_* - \left\|\mathcal{P}_{\boldsymbol{L}^*}(\Delta \boldsymbol{L})\right\|_*. \end{aligned}$$

Combining this result with Lemma 11, we find that with probability at least $1-6e^{-\nu_n\rho_n n}-2e^{-\tilde{\nu}_n\gamma_n sn}$,

$$\|\boldsymbol{\Omega}\odot\Delta\boldsymbol{L}\|_F^2 \;\leq\; \left\|\boldsymbol{\Omega}\odot\boldsymbol{\Sigma}_{|I}\right\|_{op}\left(\|\mathcal{P}_{\boldsymbol{L}^*}(\Delta\boldsymbol{L})\|_*+\left\|\mathcal{P}^{\perp}_{\boldsymbol{L}^*}(\Delta\boldsymbol{L})\right\|_*\right)+16\tilde{\nu}_n\gamma_n\rho_n sn+\lambda_1\left(\|\mathcal{P}_{\boldsymbol{L}^*}(\Delta\boldsymbol{L})\|_*-\left\|\mathcal{P}^{\perp}_{\boldsymbol{L}^*}(\Delta\boldsymbol{L})\right\|_*\right).$$

Recall that by definition, $\Psi\geq 16\tilde{\nu}_n\gamma_n\rho_n ns$. Thus, when $\lambda_1\geq 3\left\|\boldsymbol{\Omega}\odot\boldsymbol{\Sigma}_{|I}\right\|_{op}$,

$$\|\boldsymbol{\Omega}\odot\Delta\boldsymbol{L}\|_F^2 \;\leq\; \frac{\lambda_1}{3}\left(5\|\mathcal{P}_{\boldsymbol{L}^*}(\Delta\boldsymbol{L})\|_*-\left\|\mathcal{P}^{\perp}_{\boldsymbol{L}^*}(\Delta\boldsymbol{L})\right\|_*\right)+\Psi.$$

This proves equation (45) in Lemma 8. This result also implies that

$$\left\|\mathcal{P}^{\perp}_{\boldsymbol{L}^*}(\Delta\boldsymbol{L})\right\|_* \;\leq\; 5\|\mathcal{P}_{\boldsymbol{L}^*}(\Delta\boldsymbol{L})\|_*+\frac{3\Psi}{\lambda_1}.$$

Recall that $\boldsymbol{L}^*$ is of rank k and so $\mathcal{P}_{\boldsymbol{L}^*}(\Delta\boldsymbol{L})$ is of rank at most k. Therefore,

$$\begin{aligned}
\|\Delta\boldsymbol{L}\|_* &\leq 6\|\mathcal{P}_{\boldsymbol{L}^*}(\Delta\boldsymbol{L})\|_*+\frac{3\Psi}{\lambda_1}\leq 6\sqrt{k}\|\mathcal{P}_{\boldsymbol{L}^*}(\Delta\boldsymbol{L})\|_F+\frac{3\Psi}{\lambda_1}\\
&\leq 6\sqrt{k}\|\Delta\boldsymbol{L}\|_F+\frac{3\Psi}{\lambda_1}\leq 6\sqrt{k}\left\|\Delta\boldsymbol{L}_{|I}\right\|_F+6\sqrt{k(sn+s^2)}\rho_n+\frac{3\Psi}{\lambda_1}\\
&\leq 6\sqrt{k}\left\|\Delta\boldsymbol{L}_{|I}\right\|_F+6\sqrt{3ksn}\rho_n+\frac{3\Psi}{\lambda_1}.
\end{aligned}$$

where we have used that $\left\|\Delta\boldsymbol{L}_{|O}\right\|_F\leq\sqrt{|O|}\left\|\Delta\boldsymbol{L}_{|O}\right\|_\infty\leq\sqrt{s^2+2sn}\rho_n$. This completes the proof of Lemma 8.

A.8.8 Proof of Lemma 9

For ease of notations, let $\alpha=36^2\frac{\nu_n\rho_n^2 kn}{\mu_n}$. To prove Lemma 8, we consider the following two cases.

Case 1: $\left\|\Delta\boldsymbol{L}_{|I}\right\|^2_{L_2(\boldsymbol{\Pi})}\leq\alpha$. Then the result is immediate.

Case 2: $\left\|\Delta\boldsymbol{L}_{|I}\right\|^2_{L_2(\boldsymbol{\Pi})}>\alpha$. Let $r>0$ a constant to be specified later. We consider the following sets

$$\mathcal{S}^r=\left\{\boldsymbol{M}\in\mathbb{R}^{n\times n}_{sym}:\|\boldsymbol{M}\|_\infty\leq\rho_n,\left\|\boldsymbol{M}_{|I}\right\|^2_{L_2(\boldsymbol{\Pi})}\geq\alpha,\|\boldsymbol{M}\|_*\leq\sqrt{r}\left\|\boldsymbol{M}_{|I}\right\|_F+\sqrt{3rsn}\rho_n+\frac{3\Psi}{\lambda_1}\right\}.$$

Recall that the random noise matrix $\boldsymbol{\Gamma}$ is defined as follows: for any $(i,j)\in[n]\times[n]$, $i<j$, $\boldsymbol{\Gamma}_{ij}=\boldsymbol{\Gamma}_{ji}=\boldsymbol{\Omega}_{ij}\epsilon_{ij}$ where $(\epsilon_{ij})_{1\leq i<j\leq n}$ is a Rademacher sequence. Now, we define β_r as follows :

$$\beta_r\triangleq\mathbb{E}\left[\left\|\boldsymbol{\Gamma}_{|I}\right\|_{op}\right]\left(\frac{64r\rho_n^2}{\mu_n}\mathbb{E}\left[\left\|\boldsymbol{\Gamma}_{|I}\right\|_{op}\right]+15\sqrt{srn}\rho_n^2+\frac{32\Psi\rho_n}{\lambda_1}\right).$$

Lemma 12. *With probability larger than $1-e^{-\nu_n\rho_n n}$, simultaneously for any $\boldsymbol{M}\in\mathcal{S}^r$,*

$$\frac{1}{2}\|\boldsymbol{M}\|^2_{L_2(\boldsymbol{\Pi})}\leq\left\|\boldsymbol{\Omega}\odot\boldsymbol{M}_{|I}\right\|_F^2+\beta_r$$

Proof. See Section A.8.11. □

Recall that β was defined in equation (47), and note that $\beta=\beta_{36k}$. Then, equation (46) in Lemma 8 implies that $\Delta\boldsymbol{L}\in\mathcal{S}^{36k}$ with probability at least $1-6e^{-\nu_n\rho_n n}-2e^{-\tilde{\nu}_n\gamma_n sn}$. Combining equation (45) in Lemma 8 and Lemma 12, we find that with probability at least $1-7e^{-n\nu_n\rho_n}-2e^{-\tilde{\nu}_n\gamma_n sn}$,

$$\frac{1}{2}\left\|\Delta\boldsymbol{L}_{|I}\right\|^2_{L_2(\boldsymbol{\Pi})} \;\leq\; \frac{5\lambda_1}{3}\|\mathcal{P}_{\boldsymbol{L}^*}(\Delta\boldsymbol{L})\|_*+\Psi+\beta.$$

The matrix $\boldsymbol{L}^*$ is of rank at most k. Therefore,

$$\begin{aligned}
\left\|\Delta\boldsymbol{L}_{|I}\right\|^2_{L_2(\boldsymbol{\Pi})} &\leq \frac{10\lambda_1\sqrt{k}}{3}\|\Delta\boldsymbol{L}\|_F+2\Psi+2\beta\leq\frac{50\lambda_1^2 k}{9\mu_n}+\frac{\mu_n}{2}\|\Delta\boldsymbol{L}\|_F^2+\Psi+\beta\\
&\leq \frac{50\lambda_1^2 k}{9\mu_n}+\frac{\mu_n}{2}\left\|\Delta\boldsymbol{L}_{|I}\right\|_F^2+\frac{3}{2}\mu_n\rho_n^2 sn+\Psi+\beta
\end{aligned}$$

where we have used that $\left\|\Delta \boldsymbol{L}_{|O}\right\|_F^2 \leq 3\rho_n^2 ns$. Using equation (12), we find that

$$\left\|\Delta \boldsymbol{L}_{|I}\right\|_{L_2(\boldsymbol{\Pi})}^2 \quad \leq \quad \frac{1}{2}\left\|\Delta \boldsymbol{L}_{|I}\right\|_{L_2(\boldsymbol{\Pi})}^2 + \frac{\mu_n}{2}\rho_n^2 n + \frac{3}{2}\mu_n\rho_n^2 sn + \frac{50\lambda_1^2 k}{9\mu_n} + \Psi + \beta.$$

Thus

$$\left\|\Delta \boldsymbol{L}_{|I}\right\|_{L_2(\boldsymbol{\Pi})}^2 \quad \leq \quad 8\mu_n\rho_n^2 sn + \frac{100\lambda_1^2 k}{9\mu_n} + 2\Psi + 2\beta.$$

We conclude the proof of Lemma 9 by recalling that $\mu_n \leq \nu_n$.

A.8.9 Proof of Lemma 10

To prove Lemma 10, we use Proposition 1. For $(i,j) \in I$, set $b_{ij} = \sqrt{\boldsymbol{\Pi}_{ij}}$, and $\xi_{ij} = \frac{\epsilon_{ij}\boldsymbol{\Omega}_{ij}}{b_{ij}}$, and for $i \in \mathcal{I}$ set $b_{ii} = 0$. Note that for any $(i,j) \in \mathcal{I}$, $\boldsymbol{\Gamma}_{ij} = b_{ij}\xi_{ij}$, and that $\{\xi_{ij}\}_{i\leq j}$ is a sequence of independent symmetric random variables with unit variance. Moreover, for any $(i,j) \in I$, $|b_{ij}\xi_{ij}| \leq 1$, so for any $\alpha \geq 3$, $\left(\mathbb{E}\left[\left(\xi_{ij}b_{ij}\right)^{2\alpha}\right]\right)^{\frac{1}{2\alpha}} \leq 1$. Finally, note that for any $i \in \mathcal{I}$,

$$\sqrt{\sum_{j\in\mathcal{I}} b_{ij}^2} = \sqrt{\sum_{j\in\mathcal{I}} \boldsymbol{\Pi}_{ij}} \leq \sqrt{\nu_n n}.$$

Applying Proposition 1, we find that

$$\mathbb{E}\left[\left\|\boldsymbol{\Gamma}_{|I}\right\|_{op}\right] \leq e^{\frac{2}{3}}\left(\sqrt{\nu_n n} + 42\sqrt{\log(n)}\right)$$

We conclude this proof by recalling that $\nu_n n \geq \log(n)$.

A.8.10 Proof of Lemma 11

To prove Lemma 11, note that $\left\|\Delta \boldsymbol{L}\right\|_\infty \leq \rho_n$, and therefore

$$\left|\left\langle \boldsymbol{\Omega} \odot \left(\boldsymbol{A} - \widehat{\boldsymbol{S}} - \widehat{\boldsymbol{S}}^\top\right)_{|O} \middle| \Delta \boldsymbol{L} \right\rangle\right| \quad \leq \quad 2\rho_n \sum_{(i,j)\in O} \left|\boldsymbol{\Omega}_{ij}\left(\boldsymbol{A}_{ij} - \widehat{\boldsymbol{S}}_{ij} - \widehat{\boldsymbol{S}}_{ji}\right)\right|. \tag{61}$$

Recall that $\widehat{\boldsymbol{L}}$ and $\widehat{\boldsymbol{S}}$ have non-negative entries, and that $\widehat{\boldsymbol{L}}$ and $\boldsymbol{A}$ are symmetric. Therefore, equation (53) implies that $\left\{\widehat{\boldsymbol{S}}_{ij} = 0 \text{ or } \widehat{\boldsymbol{S}}_{ji} = 0\right\} \Rightarrow \boldsymbol{A}_{ij} = 0$, and that $\widehat{\boldsymbol{S}}_{ij} + \widehat{\boldsymbol{S}}_{ji} \leq \boldsymbol{A}_{ij}$. Thus, equation (61) implies

$$\left|\left\langle \boldsymbol{\Omega} \odot \left(\boldsymbol{A} - \widehat{\boldsymbol{S}} - \widehat{\boldsymbol{S}}^\top\right)_{|O} \middle| \Delta \boldsymbol{L} \right\rangle\right| \quad \leq \quad 2\rho_n \sum_{(i,j)\in O} \boldsymbol{\Omega}_{ij}\boldsymbol{A}_{ij}. \tag{62}$$

To conclude the proof of Lemma 11, we first prove the following result:

$$\mathbb{P}\left(\sum_{(i,j)\in O} \boldsymbol{\Omega}_{ij}\boldsymbol{A}_{ij} \geq 8\tilde{\nu}_n\gamma_n sn\right) \quad \leq \quad \exp(-\tilde{\nu}_n\gamma_n sn). \tag{63}$$

We use Bernstein's inequality to obtain equation (63). Note that $\{\boldsymbol{\Omega}_{ij}\boldsymbol{A}_{ij}\}_{(i,j)\in O, i<j}$ is a sequence of independent Bernoulli random variables such that for any $i \in [n]$, $\sum_{j\in\mathcal{O}} \mathbb{E}\left[\boldsymbol{\Omega}_{ij}\boldsymbol{A}_{ij}\right] \leq \tilde{\nu}_n\gamma_n s$, $\sum_{j\in\mathcal{O}} \mathbb{V}ar\left[\boldsymbol{\Omega}_{ij}\boldsymbol{A}_{ij}\right] \leq \tilde{\nu}_n\gamma_n s$, and $\left(\boldsymbol{\Omega}_{ij}\boldsymbol{A}_{ij} - \mathbb{E}\left[\boldsymbol{\Omega}_{ij}\boldsymbol{A}_{ij}\right]\right) \in [-1,1]$. Hence, applying Bernstein's inequality (19), we find that for any $t > 0$,

$$\mathbb{P}\left(\sum_{(i,j)\in O} \boldsymbol{\Omega}_{ij}\boldsymbol{A}_{ij} \geq 2\tilde{\nu}_n\gamma_n sn + \sqrt{2t \times \tilde{\nu}_n\gamma_n sn} + \frac{3t}{2}\right) \quad \leq \quad 2\exp(-t).$$

Choosing $t = 2\tilde{\nu}_n\gamma_n sn$, we obtain equation (63). We conclude the proof of Lemma 11 by combining equations (62) and (63).

A.8.11 Proof of Lemma 12

To prove Lemma 12, we show that the probability of the following "bad" event is small :

$$\mathcal{B} \triangleq \{\exists \boldsymbol{M} \in \mathcal{S}^r \text{ such that } \left| \left\| \boldsymbol{\Omega} \odot \boldsymbol{M}_{|I} \right\|_F^2 - \left\| \boldsymbol{M}_{|I} \right\|_{L_2(\boldsymbol{\Pi})}^2 \right| \geq \frac{1}{2} \left\| \boldsymbol{M}_{|I} \right\|_{L_2(\boldsymbol{\Pi})}^2 + \beta_r \}.$$

We use a standard peeling argument to control the probability of the event $\mathcal{B}$. For $T > \alpha$, define

$$\mathcal{S}(T) \triangleq \left\{ \boldsymbol{M} \in \mathcal{S}^r : \left\| \boldsymbol{M}_{|I} \right\|_{L_2(\boldsymbol{\Pi})}^2 \leq T \right\}, \; Z(T) = \sup_{\boldsymbol{M} \in \mathcal{S}(T)} \left| \left\| \boldsymbol{\Omega} \odot \boldsymbol{M}_{|I} \right\|_F^2 - \left\| \boldsymbol{M}_{|I} \right\|_{L_2(\boldsymbol{\Pi})}^2 \right|, \text{ and}$$

$$\mathcal{B}(T) \triangleq \left\{ \exists \boldsymbol{M} \in \mathcal{S}(T) : \left| \left\| \boldsymbol{\Omega} \odot \boldsymbol{M}_{|I} \right\|_F^2 - \left\| \boldsymbol{M}_{|I} \right\|_{L_2(\boldsymbol{\Pi})}^2 \right| \geq \frac{T}{4} + \beta_r \right\} = \left\{ Z(T) \geq \frac{T}{4} + \beta \right\}.$$

For $l \geq 1$, define also $\mathcal{S}_l \triangleq \left\{ \boldsymbol{M} \in \mathcal{S}^r : 2^{l-1}\alpha < \left\| \boldsymbol{M}_{|I} \right\|_{L_2(\boldsymbol{\Pi})}^2 \leq 2^l \alpha \right\} \subset \mathcal{S}\left(2^l \alpha\right)$ and

$$\begin{aligned} \mathcal{B}_l &\triangleq \left\{ \exists \boldsymbol{M} \in \mathcal{S}_l : \left| \left\| \boldsymbol{\Omega} \odot \boldsymbol{M}_{|I} \right\|_F^2 - \left\| \boldsymbol{M}_{|I} \right\|_{L_2(\boldsymbol{\Pi})}^2 \right| \geq \frac{\left\| \boldsymbol{M}_{|I} \right\|_{L_2(\boldsymbol{\Pi})}^2}{2} + \beta_r \right\} \\ &\subset \left\{ \exists \boldsymbol{M} \in \mathcal{S}_l : \left| \left\| \boldsymbol{\Omega} \odot \boldsymbol{M}_{|I} \right\|_F^2 - \left\| \boldsymbol{M}_{|I} \right\|_{L_2(\boldsymbol{\Pi})}^2 \right| \geq \frac{2^{l-1}}{2} \alpha + \beta_r \right\} \subset \mathcal{B}\left(2^l \alpha\right). \end{aligned}$$

Since $\mathcal{S}^r \subset \underset{l \geq 1}{\cup} \mathcal{S}_l$, it is easy to see that $\mathcal{B} \subset \underset{l \geq 1}{\cup} \mathcal{B}_l$. To control the probability of the events $\mathcal{B}_l$, it is enough to control the probability of the events $\mathcal{B}(T)$, which is done in the following lemma.

Lemma 13. *For any $T \geq \alpha$, we have $\mathbb{P}\left(\mathcal{B}(T)\right) \leq \exp(-\frac{T}{36^2 \rho_n})$.*

Proof. See Section A.8.12. □

We apply Lemma 13 to find

$$\begin{aligned} \mathbb{P}\left(\mathcal{B}\right) &\leq \sum_{l \geq 1} \mathbb{P}\left(\mathcal{B}_l\right) \leq \sum_{l \geq 1} \exp\left(-\frac{2^l \alpha}{36^2 \rho_n} \right) \\ &\leq \sum_{l \geq 1} \exp\left(-\frac{2l\alpha}{36^2 \rho_n} \alpha \right) = \frac{\exp\left(-\frac{2\alpha}{36^2 \rho_n}\right)}{1 - \exp\left(-\frac{2\alpha}{36^2 \rho_n}\right)} = \frac{\exp\left(-2\frac{\nu_n \rho_n k n}{\mu_n}\right)}{1 - \exp\left(-2\frac{\nu_n \rho_n k n}{\mu_n}\right)} \end{aligned}$$

Note that $\frac{\nu_n \rho_n k n}{\mu_n} \geq \nu_n \rho_n n \geq \log(n) \geq 1$, and so $\mathbb{P}\left[\mathcal{B}\right] \leq \frac{1}{2} \exp\left(-2\nu_n \rho_n n\right) \leq \exp\left(-\nu_n \rho_n n\right)$. This concludes the proof of Lemma 12.

A.8.12 Proof of Lemma 13

Recall that $Z(T) = 2 \sup_{\boldsymbol{M} \in \mathcal{S}(T)} \left| \sum_{(i,j) \in I} \boldsymbol{M}_{ij}^2 \left(\boldsymbol{\Omega}_{ij} - \boldsymbol{\Pi}_{ij} \right) \right|$, since all matrices in $\mathcal{S}$ are symmetric. In order to bound $Z(T)$, we begin by controlling the deviation of $Z(T)$ from its expectation. To do this, we apply Bousquet's Theorem 6 to the random variable $Z(T) = 2\rho_n \sup_{\boldsymbol{M} \in \mathcal{S}(T)} \left| \sum_{(i,j) \in I} f_{ij}^{\boldsymbol{M}}(\boldsymbol{\Omega}_{ij}) \right|$ where we set $f_{ij}^{\boldsymbol{M}}(\boldsymbol{\Omega}_{ij}) \triangleq \frac{(\boldsymbol{\Omega}_{ij} - \boldsymbol{\Pi}_{ij}) \boldsymbol{M}_{ij}^2}{\rho_n}$. The set of functions $\left\{ f_{ij}^{\boldsymbol{M}}, \boldsymbol{M} \in \mathcal{S}(T) \right\}$ is separable and we can apply Theorem 6 (see, e.g., [18], Section 2.1). Note that for any $(i,j) \in I$, $\mathbb{E}\left[f_{ij}^{\boldsymbol{M}}(\boldsymbol{\Omega}_{ij}) \right] = 0$, $\left| f_{ij}^{\boldsymbol{M}}(\boldsymbol{\Omega}_{ij}) \right| \leq 1$, $\mathbb{E}\left[\left(\boldsymbol{\Omega}_{ij} - \boldsymbol{\Pi}_{ij} \right)^2 \right] \leq \boldsymbol{\Pi}_{ij}$ and $\left\| \boldsymbol{M} \right\|_\infty \leq \rho_n$ so

$$v \triangleq 2 \sup_{\boldsymbol{M} \in \mathcal{S}(T)} \sum_{(i,j) \in I} \mathbb{E}\left[f_{ij}^{\boldsymbol{M}}(X_{ij})^2 \right] \leq 2 \sum_{(i,j) \in I} \boldsymbol{\Pi}_{ij} \frac{\boldsymbol{M}_{ij}^4}{\rho_n^2} \leq 2 \sup_{\boldsymbol{M} \in \mathcal{S}(T)} \sum_{(i,j) \in I} \boldsymbol{\Pi}_{ij} \boldsymbol{M}_{ij}^2 \leq T.$$

Theorem 6 implies that

$$\mathbb{P}\left(\frac{Z_T}{2\rho_n} > \frac{\mathbb{E}[Z_T]}{2\rho_n} + \frac{x}{3} + \sqrt{2x\left(\frac{2\mathbb{E}[Z_T]}{2\rho_n} + T\right)}\right) \leq \exp(-x)$$

$$\mathbb{P}\left(Z_T > \mathbb{E}[Z_T] + \frac{2\rho_n x}{3} + 2\rho_n x + 2\mathbb{E}[Z_T] + 2\rho_n\sqrt{2xT}\right) \leq \exp(-x)$$

where we used $2\sqrt{ab} \leq a+b$. Setting $x = \frac{T}{36^2\rho_n}$ and noticing that $\rho_n \leq 1$ leads to

$$\mathbb{P}\left(Z_T > 2\mathbb{E}[Z_T] + \frac{T}{8}\right) \leq \exp(-\frac{T}{36^2\rho_n}). \tag{64}$$

In a second time, in order to bound $\mathbb{E}[Z_T]$, we apply a standard symetrization argument (see, e.g., [32], Theorem 2.1). We obtain that

$$\mathbb{E}[Z(T)] \leq 4\mathbb{E}\left[\sup_{\boldsymbol{M}\in\mathcal{S}(T)}\left|\sum_{(i,j)\in I}\epsilon_{ij}\boldsymbol{M}_{ij}^2\boldsymbol{\Omega}_{ij}\right|\right] \tag{65}$$

where $(\epsilon_{ij})_{1\leq i<j\leq n}$ is a Rademacher sequence. For $i<j$, define $\phi_{ij} : x \to \frac{x^2}{2\rho_n}$. Recall that for any (i,j), $\boldsymbol{\Omega}_{ij} \in \{0,1\}$, and so $\boldsymbol{\Omega}_{ij} = \boldsymbol{\Omega}_{ij}^2$. With these notations, equation (65) becomes

$$\mathbb{E}[Z(T)] \leq 8\rho_n\mathbb{E}\left[\sup_{\boldsymbol{M}\in\mathcal{S}(T)}\left|\sum_{i<j}\epsilon_{ij}\phi_{ij}\left(\boldsymbol{\Omega}_{ij}\boldsymbol{M}_{ij}\right)\right|\right].$$

We note that for $\boldsymbol{M} \in \mathcal{S}(T)$, $\|\boldsymbol{M}\|_\infty \leq \rho_n$. Therefore, the functions ϕ_{ij} are 1-Lipschitz functions on $[-\rho_n, \rho_n]$ vanishing at 0. We apply Talagrand's contraction principle (see, e.g., Theorem 2.2 in [32]) and find that

$$\mathbb{E}[Z(T)] \leq 16\rho_n\mathbb{E}\left[\sup_{\boldsymbol{M}\in\mathcal{S}(T)}\left|\sum_{(i,j)\in I}\epsilon_{ij}\boldsymbol{M}_{ij}\boldsymbol{\Omega}_{ij}\right|\right] = 8\rho_n\mathbb{E}\left[\sup_{\boldsymbol{M}\in\mathcal{S}(T)}\left|\left\langle\boldsymbol{M}\middle|\boldsymbol{\Gamma}_{|I}\right\rangle\right|\right]$$

where for any (i,j), $\boldsymbol{\Gamma}_{ij} = \epsilon_{ij}\boldsymbol{\Omega}_{ij}$. By the duality of the $\|\cdot\|_*$-norm and $\|\cdot\|_{op}$-norm, and by definition of $\mathcal{S}^r$, we find that

$$\begin{aligned}\mathbb{E}[Z(T)] &\leq 8\rho_n \sup_{\boldsymbol{M}\in\mathcal{S}(T)}\|\boldsymbol{M}\|_*\,\mathbb{E}\left[\left\|\boldsymbol{\Gamma}_{|I}\right\|_{op}\right] \\ &\leq 8\rho_n\left(\sqrt{r}\sup_{\boldsymbol{M}\in\mathcal{S}(T)}\left\|\boldsymbol{M}_{|I}\right\|_F + \sqrt{3rsn}\rho_n + \frac{3\Psi}{\lambda_1}\right)\mathbb{E}\left[\left\|\boldsymbol{\Gamma}_{|I}\right\|_{op}\right].\end{aligned}$$

Using equation (12), we find that

$$\begin{aligned}\mathbb{E}[Z(T)] &\leq 8\rho_n\left(\sqrt{r}\left(\frac{1}{\sqrt{\mu_n}}\sup_{\boldsymbol{M}\in\mathcal{S}(T)}\left\|\boldsymbol{M}_{|I}\right\|_{L_2(\boldsymbol{\Pi})} + \sqrt{n}\rho_n\right) + \sqrt{3rsn}\rho_n + \frac{3\Psi}{\lambda_1}\right)\mathbb{E}\left[\left\|\boldsymbol{\Gamma}_{|I}\right\|_{op}\right] \\ &\leq \left(\frac{8\rho_n\sqrt{r}}{\sqrt{\mu_n}}\sup_{\boldsymbol{M}\in\mathcal{S}(T)}\left\|\boldsymbol{M}_{|I}\right\|_{L_2(\boldsymbol{\Pi})} + 8\sqrt{nr}\rho_n^2 + 8\sqrt{3srn}\rho_n^2 + \frac{32\Psi\rho_n}{\lambda_1}\right)\mathbb{E}\left[\left\|\boldsymbol{\Gamma}_{|I}\right\|_{op}\right].\end{aligned}$$

Using the definition of $\mathcal{S}(T)$, we find that

$$\begin{aligned}\mathbb{E}[Z(T)] &\leq \left(\frac{8\rho_n\sqrt{rT}}{\sqrt{\mu_n}} + 8\sqrt{rn}\rho_n^2 + 8\sqrt{3srn}\rho_n^2 + \frac{32\Psi\rho_n}{\lambda_1}\right)\mathbb{E}\left[\left\|\boldsymbol{\Gamma}_{|I}\right\|_{op}\right] \\ &\leq \frac{T}{16} + \mathbb{E}\left[\left\|\boldsymbol{\Gamma}_{|I}\right\|_{op}\right]\left(\frac{64r\rho_n^2}{\mu_n}\mathbb{E}\left[\left\|\boldsymbol{\Gamma}_{|I}\right\|_{op}\right] + 15\sqrt{srn}\rho_n^2 + \frac{32\Psi\rho_n}{\lambda_1}\right) \\ &= \frac{T}{16} + \beta^r.\end{aligned} \tag{66}$$

Combining equation (64) and equation (66) yields the desired result.

A.9 Proof of Lemma 5

Consider the following chain of inequality:

$$\frac{1}{A_{k+1}} - \frac{1}{A_k} = \frac{A_k - A_{k+1}}{A_k A_{k+1}} \geq \gamma_k \frac{A_k}{A_{k+1}} \geq \gamma_k,$$

since $A_{k+1} \leq A_k$. Thus, we obtain

$$\frac{1}{A_{k+1}} - \frac{1}{A_1} = \sum_{i=1}^{k} \left(\frac{1}{A_{i+1}} - \frac{1}{A_i} \right) \geq \sum_{i=1}^{k} \gamma_i,$$

which gives the result after reshuffling the terms.